Prediction of Seismic Collapse Risk in Steel Moment Framed Structures by Metaheuristic Algorithm

Fooad Karimi Ghaleh Jough

Submitted to the
Institute of Graduate Studies and Research
in partial fulfillment of the requirements for the degree of

Doctor of Philosophy
in
Civil Engineering

Eastern Mediterranean University
January 2016
Gazimağusa, North Cyprus

Approval of the Institute of Graduate Studies and Research

Prof. Dr. Cem Tanova
Acting Director

I certify that this thesis satisfies the requirements as a thesis for the degree of Master of Science in Civil Engineering.

Prof. Dr. Özgür Eren
Chair, Department of Civil Engineering

We certify that we have read this thesis and that in our opinion it is fully adequate in scope and quality as a thesis for the degree of Doctor of Philosophy in Civil Engineering.

Assoc. Prof. Dr. Serhan Sensoy
Supervisor

Examining Committee

1. Prof. Dr. Ayşe Daloğlu
2. Prof. Dr. Semih Küçükarslan
3. Prof. Dr. M. Semih Yücemen
4. Assoc. Prof. Dr. Serhan Şensoy
5. Asst. Prof. Dr. Giray Özay

ABSTRACT

Depending on the many aspects of seismic performance evaluation procedures, different collapse performance levels may be obtained. Fragility curves in different limit states are the most important tools for evaluating the performance of structures marred by varying degrees of damage. These curves are also vital in determining the decision making variables as specified by the procedure developed by researchers of Pacific Earthquake Engineering Research Center. These curves play a significant role in the determination and management of consequences of earthquakes. The present thesis is mainly focused on the fragility curve for the sidesway collapse limit state. One important issue in deriving fragility curves is how uncertainties are blended and incorporated into the model under seismic conditions. The fragility curve for sidesway collapse limit state is influenced by different uncertainty sources including, aleatory, epistemic (modelling) and cognitive uncertainties. In this study, incremental dynamic analysis is applied to consider aleatory uncertainty, while strong ground motion selected by K-Means algorithm, which is used for proper selection of record to record uncertainty and reduction of time cost instead of random selection. Analytical equations of Response Surface Method are obtained through incremental dynamic analysis results by Cuckoo algorithm which predicts mean and standard deviation of collapse fragility curve. Takagi-Sugeno-Kang model is used for material quality by response surface coefficient. Finally collapse fragility curves with various sources of uncertainty are derived through large number of material quality values and meta variable inferred by Takagi-Sugeno-Kang fuzzy model based on response surface method coefficients.

On the other hand, the optimized fuzzy method is used to compile the fragility curves by considering epistemic and aleatory uncertainties for the model under collapse conditions at 2% interstory drift ratio and sidesway collapse. In proposed method, model parameters are fuzzy values and the Fuzzy C-means based on particle swarm optimization is used to estimate mean and standard deviation to derive the fragility curve (these two being fuzzy values themselves). The Fuzzy C-means based on particle swarm optimization algorithm is trained using scenarios compiled via the incremental dynamic analysis method. Results obtained from the full Monte Carlo method were used for comparison and verification. According to the comparison of results, it is observed that the proposed method is very efficient and decreasing computational run time compared with the full Monte Carlo method.

Keywords: Modelling uncertainty, Cognitive uncertainty, TSK model, Cuckoo algorithm, FCM-PSO.

ÖZ

Performans değerlendirme yöntemlerinin farklılıkları neticesinde elde edilen göçme durumu performans seviyelerinde de farklılıklar olmaktadır. Hasar görebilirlik eğrileri, farklı performans seviyelerinde, yapıların performans seviyelerinin belirlenmesinde önemli bir yöntem olarak kullanılmaktadır. Hasar görebilirlik eğrileri özellikle "Pasifik Deprem Mühendisliği Araştırma Merkesi" çalışmalarında da karar alma mekanizmasının bir parçası olarak hazırlanan raporlarda önemli bir yöntem olarak kullanılmıştır. Bu eğriler deprem öncesi ve sonrası deprem yönetimi çalışmalarında önemli verilerin elde edilmesinde rol oynamıştır. Bu çalışmada özellikle hasar görebilirlik eğrileri, yanal deplasmana bağlı göçme durumu performans seviyesinde, çalışılmıştır. Bununla birlikte hasar görebilirlik eğrilerinin oluşturulmasında yapı modelinin ve deprem tehlikesinin içerdiği belirsizliklerin sonuçlara nasıl entegre edildiği önem kazanmaktadır. Göçme performans seviyesi hasargörebilirlik eğrileri *deprem tehlikesine bağlı, modele bağlı* ve *malzeme ve işcilik kalitesine* bağlı belirsizlikler olarak düşünülmelidir. Bu çalışmada, artımsal dinamik analiz yöntemi kayıttan kayıda belirsizliğinin etkisini belirlemek maksadı ile kullanılmış olup özellikle deprem kayıtlarının seçiminde K-ortalamaları algoritması entegre edilmiştir. Böylelikle uygun deprem kayıtlarının seçilmesinde K-ortalamaları algoritması rastgele seçime kıyasla daha etkili bir yöntem olarak sunulmuştur. Tepki Yüzeyi Yöntemi için analitik denklemler artımsal dinamik analiz eğrilerinin Cuckoo algoritması kullanılarak standart sapma ve ortalama değerleri heaplanması ile göçme hasargörebilirlik eğrileri elde edilmiştir. Takagi-Sugeno-Kang bulanık mantık modeli malzeme kalitesine bağlı belirsizliğin entegre edilmesi maksadı ile kullanılmıştır. Bu bağlamda göçme hasargörebilirlik eğrileri birçok belirsizliğin de dikkate alınması ve

birçok malzeme ve/veya işcilik kalitesinin Takagi-Sugeno-Kang bulanık mantık modelinin Tepki Yüzeyi Yöntemi ile entegre edilmesi sonucunda elde edilmiştir. Diğer yandan, optimize edilen bulanık mantık yönteminin "deprem tehlikesine bağlı" ve "modellemeye bağlı" belirsizlikleride içerecek şekilde uygulanması ve %2 göreli kat ötelenmesinin göçme sınır değeri olarak belirlenmesi ile hasargörebilirlik eğrileri elde edilmiştir. Önerilen yöntemde, model parametreleri bulanık mantık değerleri olarak elde edilmiş ve FCM-PSO algoritması kullanılarak ortalama ve standart sapma değerleri belirlenerek göçme hasar görebilirlik eğrileri çizilmiştir. FCM-PSO algoritması artımsal dinamik analiz yöntemi ile elde edilen eğriler kullanılarak eğitilmiş ve senaryolar oluşturulmuştur. Tüm sonuçlar tam Monte-Carlo yöntemindeki sonuçlarla karşılaştırılmıştır. Önerilen yöntemin, Monte-Carlo yöntemi ile elde edilen sonuçlarla uyumlu olduğu ve daha az bir hesap hacmi gerktirdiği görülmüştür

Anahtar Kelimeler: Modelleme belirsizlikleri, Malzeme ve İşcilik belirsizlikleri, TSK modeli, Cuckoo Algoritması, FCM-PSO

ACKNOWLEDGMENT

Foremost, I would like to express my sincere appreciation to my advisor Assoc. Prof. Dr. Serhan Şensoy for his extreme support of my PhD study and for forcing me sometimes kicking and screaming to concentrate on my work and to overcome my stress and being my ideal in academic life. I would like to thank to all the members of the Civil Engineering Department in Eastern Mediterranean University.

I owe my wife a great appreciation for her patience and fortitude during this period. Also I would like to thank my family especially my grandmother for her prayers and great motivation.

TABLE OF CONTENTS

ABSTRACT iii

ÖZ v

ACKNOWLEDGMENT vii

LIST OF TABLES xi

LIST OF FIGURES xii

LIST OF ABBREVIATION xvii

1 INTRODUCTION 1

1.1 Earthquake Engineering by Performance-Based Approach 1

1.2 Guidelines for Performance-Based Seismic Design of Structures 2

1.3 New Insight to Performance-Based Guidelines 4

1.4 Pacific Earthquake Engineering Research Center Approach 6

1.5 Fragility Curves and Structure's Collapse Limit State 9

1.6 Determining the Structures' Collapse Fragility Curve in the Form of Incremental Dynamic Analysis 11

1.7 Available Methods to Consider Uncertainties in Construction of Collapse Fragility Curves 17

1.7.1 First-Order Second-Moment Method (FOSM) 18

1.7.2 Mean Estimation Method 20

1.7.3 Confidence Interval Method 21

1.7.4 Monte Carlo Method Based on Response Surface 23

1.8 Literature Review on Fragility Analysis Considering Uncertainties through ANN 24

1.9 Objectives and Statement of the Problem 26

1.10 Thesis Structure and Limitation 29
2 FRAGILITY CURVES IN SIDESWAY COLLAPSE LIMIT STATE 32
2.1 Introduction 32
2.2 Appropriate Parameters of Seismic Demand and Intensity 34
2.3 Hysteresis Models with Considering Strength and Stiffness Degradation 35
2.4 Ibarra-Krawinkler Backbone Model 38
2.5 Physical Interpretation of Parameters in Ibarra-Krawinkler Model 45
2.6 Calibration of Moment-Rotation Model by Experimental Results 48
2.6.1 Loading History and Comparison of Experimental and Analytical Results 52
2.7 Monte Carlo Method 54
2.8 Appropriate Strong Ground Motions for Collapse Determination 55
2.9 Sensitivity of Collapse Fragility Curve to Modeling Parameters 56
2.10 Summary 57
3 THE EFFECT OF COGNITIVE UNCERTAINTY 59
3.1 Introduction 59
3.2 Combination of Sources of Uncertainties 62
3.3 Record to Record (Aleatory) Uncertainty 63
3.3.1 Lloyd's algorithm (K-means algorithm) 65
3.4 Modelling Uncertainty (Epistemic Uncertainty) 66
3.4.1 Cuckoo optimization algorithm 67
3.5 Theory of Inference in a Fuzzy Expert System (Cognitive Uncertainty) 68
3.6 Consideration of Various Uncertainties on Sample Study Structures 70
3.6.1 Design of Structure 70
3.6.2 Numerical Tests 76

3.6.3 Sensitivity Analysis 81
3.7 Summary 93
4 INTERVAL ANALYSIS BY FCM-PSO APPROACH 95
4.1 Introduction 95
4.2 Basic Concepts of Hyperspectral Clustering 99
4.2.1 Particle Swarm Optimization (PSO) 99
4.2.2 Fuzzy C-means Algorithm Based on PSO 100
4.3 Research Methodology 102
4.4 Sample Study 105
4.4.1 Structural Model 105
4.4.2 Interval Based on FCM-PSO 108
4.4.3 Full Monte Carlo method 117
4.5 Summary 121
5 CONCLUSIONS AND RECOMMENDATIONS 122
5.1 Summary 122
5.2 Conclusions 124
5.3 Recommendations 124
REFERENCES 126
APPENDIX 140
Appendix A: Theory of Fuzzy Inference System 141
Appendix B: Selected 100 Natural Earthquakes Based on Site Specification 148

LIST OF TABLES

Table 2.1: Applying various models to consider cyclic deterioration mode..... 37

Table 2.2: Some experimental results in beam calibration 50

Table 2.3: The various connection types in beam calibration..... 51

Table 3.1: The design properties for 5 and 10 story buildings..... 72

Table 3.2: The modelling parameters for beam and column for uncertainty analysis74

Table 3.3: The suit of 40 ground motion records..... 79

Table 3.4: The variation interval of collapse fragility curve by uncertainty analysis 91

Table 3.5: Probability of collapse and mean annual frequency with considering various uncertainties 91

Table 4.1: Variation epistemic uncertainty with different level of membership function 116

Table 4.2: The effect of epistemic uncertainty on mean and SD according the different approaches..... 119

LIST OF FIGURES

Figure 1.1: Performance objective in SEOAC 4

Figure 1.2: The procedure of decision variables and uncertainties in PEER approach 7

Figure 1.3: The probability distribution of engineering demand parameter and capacity of structure accordance with EDP-Based method 14

Figure 1.4: The probability distribution of engineering demand parameter and capacity of structure according to IM-Based method 16

Figure 1.5: Considering mean estimation method to consider epistemic uncertainty 21

Figure 1.6: Considering confidence interval method to consider epistemic uncertainty 23

Figure 2.1: Various stiffness and strength degradation in ISO loading 36

Figure 2.2: Moment-rotation backbone curve of Ibarra-Krawinkler model 39

Figure 2.3: Bi-linear model 40

Figure 2.4: Peak-oriented model 40

Figure 2.5: Pinching model 41

Figure 2.6: Primary strength deterioration model 43

Figure 2.7: Post-capping strength deterioration model 43

Figure 2.8: Unloading stiffness deterioration mode 44

Figure 2.9: Reloading stiffness deterioration mode 45

Figure 2.10: Plastic deformations of connections 46

Figure 2.11: Panel, joint and node 46

Figure 2.12: SDOF model for validating of the software result 49

Figure 2.13: Modified Ibarra-Krawinkler model for compatibility of experimental results and the proposed model 53

Figure 2.14: The history of cyclic displacement applied the sample structure 53

Figure 2.15: Moment-rotation diagram in the proposed method 54

Figure 2.16: Collapse fragility curve obtained by the Monte Carlo simulation approach 55

Figure 3.1: Uncertainty analysis of the system fragility curve by RSM and TSK method 61

Figure 3.2: The pseudo code representation of Cuckoo algorithm 68

Figure 3.3: Fuzzy expert systems perform fuzzy reasoning 69

Figure 3.4: The Plan of sample structures 71

Figure 3.5: Elevations view of samples 72

Figure 3.6: Backbone curve of moment rotation model based on modified Ibarra-Medina-Krawinkler 73

Figure 3.7: Effects of cyclic deterioration modelling on M-θ backbone curves 74

Figure 3.8: M2-WO panel zone 75

Figure 3.9: K-means sampling in the three-dimensional space 77

Figure 3.10: (a) The validation of selection of the ground motion based on the K-means, (b) fragility curve based on the various number of records 78

Figure 3.11: IDA curves for 5-story building, a) good quality b) average quality c) low quality 80

Figure 3.12: Tornado diagram from sensitivity analysis for 5-story building (a) good quality (b) average quality (c) Low quality, Histogram demonstrating the outcome of 33 sensitivity analysis for (d) good quality (e) average and low quality 82

Figure 3.13: Best value of CO algorithm 83

Figure 3.14: Statistical value for regression analysis of RSM 84

Figure 3.15: Response surface curves for collapse limit state for each quality level of 5-story sample structure 85

Figure 3.16: The structure of TSK system 86

Figure 3.17: Seismic hazard curve 87

Figure 3.18: Collapse fragilities obtained for (a) 5-story building with modelling and MQ quality (b) 5-story with various quality (c) 10-story with modelling and MQ quality (d) 10-story with various quality 89

Figure 3.19: Fragility curve for collapse safety, considering modelling and material quality uncertainty for (a) 5-story building in 84% confidence (b)10-story in 84% (c) 5-story in 95% (d) 10-story in 95% 90

Figure 3.20: Effect of confidence level on of MAF with considering comprehensive sources of uncertainty (a) 5-story building (b) 10-story building 92

Figure 4.1: Proposed approach flowchart for incorporating epistemic uncertainty associated with fuzzy randomness 98

Figure 4.2: Flowchart of the optimization of fragility curve by FCM-PSO method 101

Figure 4.3: α-section definition of fuzzy parameter of X 101

Figure 4.4: 3D view of sample structure. 105

Figure 4.5: The analytical model of three-story, three-bay moment resisting frame 106

Figure 4.6: Subassembly model in OpenSees software 106

Figure 4.7: Tree diagram for pre-assumed values of epistemic 109

Figure 4.8: Proposed FCM-PSO approach to predict mean and standard deviation 109

Figure 4.9: Sample collapse fragility curves for 81 cases 110

Figure 4.10: Median of sample IDA curves (β) a) BD=1,CD=1,BS=0,CS=0 b) BD=0,CD=0,BS=1,CS=1 c) BD=0,CD=0,BS=0,BS=0 d) BD=-1,CD=-1,BS=-1,CS=-1 111

Figure 4.11: Comparison of mean values based on IDA versus estimated mean of fragility curve 112

Figure 4.12: Comparison of SD values based on IDA versus estimated SD of fragility curve 113

Figure 4.13: The membership function of mean and SD of fragility curve in interval analysis 115

Figure 4.14: Collapse fragility curve for different interval of meta variable 116

Figure 4.15: Structural response fragilities representing the collapse limit state and the 2% interstory drift (IDR) limit state 120

LIST OF ABBREVIATIONS

ATC	American Technology Council
NERHP	National Earthquake Hazard Reduction Program
FEMA	Federal Emergency Management Agency
SEOAC	Structural Engineers Association of California
PEER	Pacific Earthquake Engineering Research
IM	Intensity Measure
EDP	Engineering Demand Parameter
DM	Damage Measure
DV	Decision Variable
IDA	Incremental Dynamic Analysis
FOSM	First Order-Second Moment
MAF	Mean Annual Frequency
LHS	Latin Hypercube Sampling
ANN	Artificial Neural Network
RTR	Record To Record
FIS	Fuzzy Inference System
CO	Cuckoo Optimization
FCM	Fuzzy C-Means
PSO	Particle Swarm Optimization
MIDR	Maximum Inter-story Drift Ratio
BS	Beam Strength
BD	Beam Ductility
CS	Column Strength

CD	Column Ductility
MQ	Material Quality
RSM	Response Surface Method
TSK	Takagi-Sugeno-Kang
CAV	Cumulative Absolute Velocity
I_A	Arias Intensity
I_C	Characteristic Intensity
GA	Genetic Algorithm
ELR	Egg Laying Radius
KB	knowledge-based
SD	Standard Deviation
COC	Center of Cluster
MPE	Maximum Probable Earthquake
MCE	Maximum Considerable Earthquake
RMSE	Root Mean Square Error
MSE	Mean Square Error

Chapter 1

INTRODUCTION

1.1 Earthquake Engineering by Performance-Based Approach

The occurrence of ample earthquakes resulting in large economic losses as in the 1994 Northridge (17-26 billion dollars), 1989 Loma Prieta (11 billiondollars) and San Fernando (2.7 billion dollars) earthquakes [1], the seismic assessment approaches, bearing criteria for direct or indirect economic losses and fatality due to earthquakes, have been recently highlighted. For this reason, earthquake engineers and scientists have developed a performance-based earthquake engineering method for buildings and bridges to guarantee more reliable approaches in determining the structures' seismic performance [1]. Considering the limits of the first generation of performance-based guidelines and the necessity of explicit inclusion of existing uncertainties, the researchers of Pacific Earthquake Engineering Research Center (PEER) have provided a framework for performance-based earthquake engineering [2]. The proposed procedure includes integration of data and models related with seismic hazard, structure's seismic response and earthquake's damage and loss. By combining these data, the fundamental result reveals the probable consequences of different earthquake scenarios, Mean Annual Frequency (MAF) of seismic damages and fatalities and indirect damages due to the lack of exploitation. Determining these parameters as reliable criteria as well as the management of the results of earthquakes will form a common language among different interested groups with different approaches. Every existing step in this method is influenced by different uncertainty sources. These

uncertainties involved in the damages caused by earthquakes are considered aleatory and epistemic uncertainties. This thesis is aimed at providing the written procedures regarding the involvement of different uncertainty sources in the fragility curve of the collapse limit state. Considering the fact that the final result of the proposed approach is determined by combining the uncertainties related to each aforementioned section, then the involvement of different uncertainties will highly be effective.

In this chapter, the proposed method, by Pacific Research Center for the assessment of structure's seismic performance, and the importance of vulnerability curves, especially the collapse fragility curve are explained. Further, the incremental dynamic analysis is introduced and the collapse fragility curve is determined using the former analysis. Various methods for the determination and combination of different uncertainty sources presented in the fragility curve are provided. Finally, this chapter seeks to describe the proposed method and the structure of the thesis and its limitations.

1.2 Guidelines for Performance-Based Seismic Design of Structures

Performance-based earthquake engineering began in the early 21st century after the introduction of the UBC 1927 regulations [1]. The performance-based goals of this guideline dictate that buildings should tolerate those motions caused by earthquake without collapsing or risking the lives of their inhabitants [1]. Procedural requirements for damage control for important interior equipment of buildings were added to the performance-based criteria in 70s. Modern procedures of performance-based design and structure's assessment against earthquake (e.g. ICC 2000 and ASCE-2006) [3, 4] introduced some requirements to provide certain performances (life safety, immediate occupancy and collapse prevention) at a certain level of the seismic risk of the earthquake.

More comprehensive reports for structures' performance-based design have been published ever since [5]. The first of these classifications has been Vision 2000 [6], aiming at achieving predictable levels of performance for structures in their different seismic levels. In this procedure, earthquakes with different intensities including frequent intensity (50% probability over 30 years), occasional intensity, rare intensity (10% probability over 50 years) and very rare intensity (10% probability over 100 years) have been defined. Moreover, the structures' performance levels have also been classified as operational, fully operational, life safety and collapse prevention. These performance-based levels have been defined according to the damages occurred to the building's structural and non-structural elements. Based on the land usage and building's significance level, Vision 2000 considers such relations between the expected performance and the earthquake's intensity, as shown in Figure 1.1, as performance goals [5].

Following the previous studies in this field, the American Technology Council (ATC) [7] published a report regarding the seismic assessment and rehabilitation of concrete buildings in 1996. In line with the National Earthquake Hazard Reduction Program (NEHRP), in 1997, the Federal Emergency Management Agency (FEMA) published reports as FEMA 273 [8] and FEMA 274 [9]. These reports, on the reformation of the existing buildings, were prepared by the Building Seismic Safety Council and they led to the codification of FEMA356 [10].

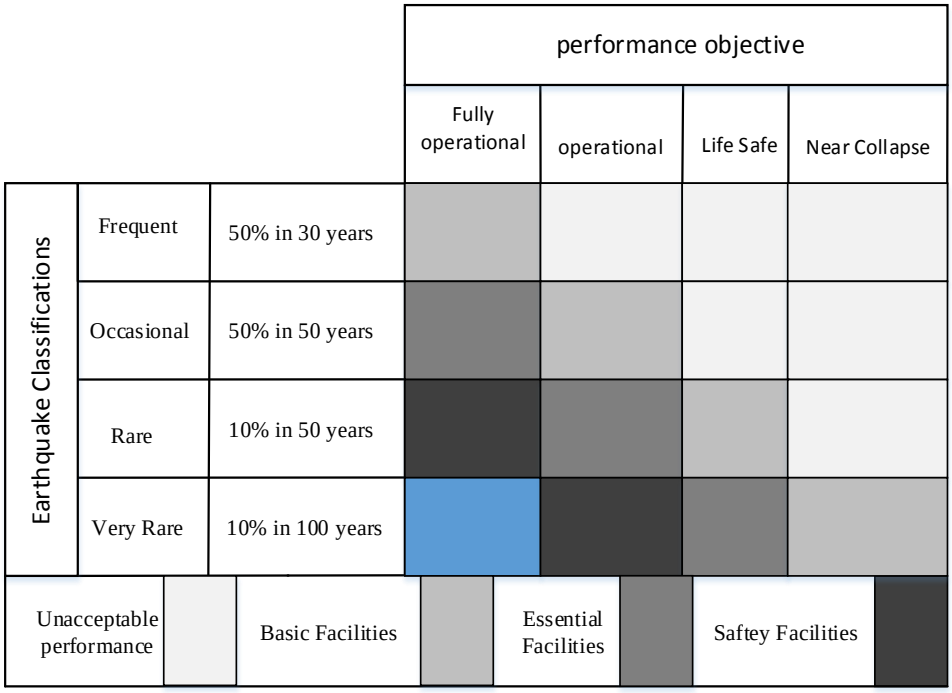

Figure 1.1: Performance objective in SEOAC[1] [6]

The purpose of this codification was the functional development and establishment of FEMA 273[8] as an obligatory guideline. Like Vision 2000 [6], this report also defined different performance goals for buildings based on their land use. Each goal then included the building's desirable performance in a risk level of earthquake (which is similar to those risk levels in Vision 2000). It is assumed that a building's target performance for a certain risk level of earthquake is defined by the user and designer. In this report, the structure is designed based on assumed details to yield a desirable performance which was defined for structural and non-structural elements.

1.3 New Insight to Performance-Based Guidelines

Despite the increasing progress in structures' performance-based design and assessment reports, against earthquakes, over the past years, there are still limitations that make the usage of performance-based term (based on the effect of earthquakes on

[1] Structural Engineers Association of California

structures) suspicious. Lack of any comprehensive approach for selecting strong ground motions proportionate to different seismic levels for dynamic analysis of structures, using performance-based criteria of building's forming elements. Lack of a common discussion among the individuals involved in construction projects and earthquake risk management (like owners, beneficiaries, policyholders and engineers) for expressing the desired and expected performance of structures are among these limitations too.

In addition to the limitations mentioned, the reliability range of achieving the desired performance, life and financial losses (with this assumption that the expected performance is met) and their related uncertainties, have not yet been determined. Lack of any codified method and the required data for determining the vulnerability of the buildings' components, lack of any definition for damage states of buildings' components and related uncertainties are also amongst the other limitations presented above. It seems that researchers have a long way ahead of them for providing real performance-based guidelines.

Achieving enough data, the development of more accurate analytic models and of different methods for determining and involving uncertainties in predicting the structures' seismic performance and expressing their outcomes in a common and simple language for all the beneficiaries involved in construction projects are also amongst those issues that need to be resolved.

For this purpose, the researchers of the Pacific Earthquake Engineering Research Center (PEER) have considered a comprehensive plan to determine the structures'

seismic performance based on decision variables common to all beneficiaries and involvement of existing uncertainties.

1.4 Pacific Earthquake Engineering Research Center Approach

Determination and assessment method of structures' seismic performance with a probabilistic approach is a multi-dimensional program in the Pacific Earthquake Engineering Research Center, which focuses on the development of a codified method in determining the structures' seismic performance considering different uncertainty sources. This program aimed at providing a more comprehensive approach than the first generation of performance guidelines in determining the structures' seismic performance and using non-deterministic ingredient for the involvement of different uncertainty sources in the buildings' seismic performance. Decision variables which are considered as expressive criteria of buildings' performance against earthquake in this approach are presented in the form of parameters of direct economic loss caused by lack of timely exploitation and fatality due to earthquake. In order to determine these parameters, PEER approach divide the problem into seismic hazard analysis, structure's response analysis in different seismic hazard levels, structure's damage analysis in different levels of its responses and damage analysis in different damage levels.

Determining each section contains some uncertainties regarding the combination which in PEER approach results in probability distribution of decision variables. This probability distribution will be considered as a criterion for decision making, evaluating, strengthening and designing buildings against earthquakes. The existing elements of the proposed method is shown in Figure 1.2[11].

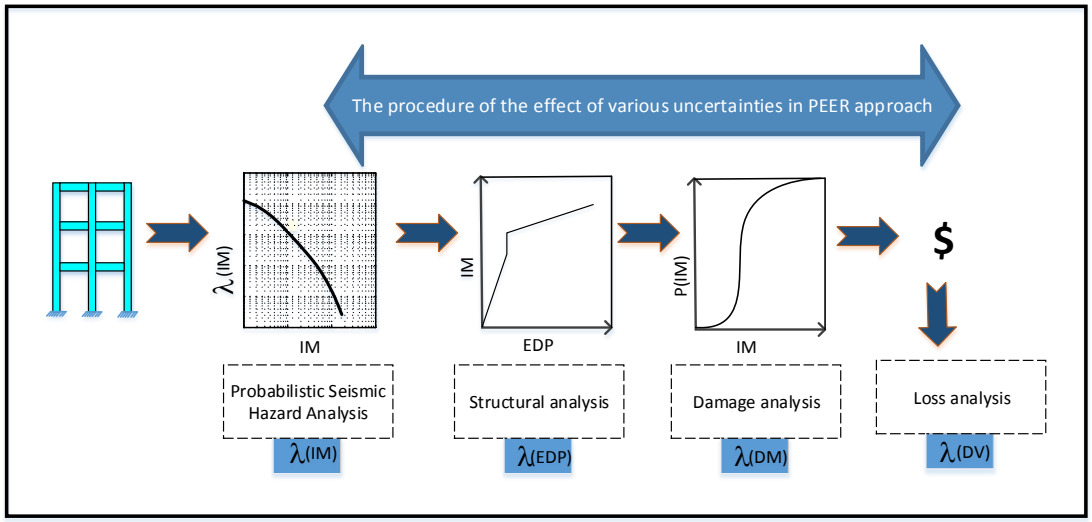

Figure 1.2: The procedure of decision variables and uncertainties in PEER approach

These parameters are defined as follows:

Intensity Measure (IM): it is a scalar parameter or a vector specifying a characteristic of strong ground motions caused by earthquakes. They generally use the first mode of spectral acceleration (S_a (T_1)) as an IM parameter to enable the determination of the structure's response for different intensities [12-15]. Employing other scalar parameters other than the first mode spectral acceleration and vector parameters as IM has been studied by many researchers [16-18].

Engineering Demand Parameter (EDP): specifies a parameter of a structure's response that is determined in different seismic intensities. This parameter should be selected in a way that its relation with the variable of the final decision can be justified. Usually for determining the damage to structural and non-structural components, inter-story drift (story drift) and acceleration parameters of the building's stories are respectively used as an engineering demand parameter. The probability distribution of this parameter in different seismic intensities is determined using such methods as a

building's incremental dynamic analysis, non-liner static analysis or simple dynamic analysis.

Damage Measure (DM): by applying a certain level of EDP to building in the given IM, it specifies the level of damage in different components of the building. Determining this parameter for different elements of a building includes the determination of different limit states in components as well as their fragility curves in different limit states. Those different damage limit states and fragility curves of a building's components are obtained using analytic, experimental and synthetic methods as well as expert opinion [19].

Decision variable (DV): It is a decision-making parameter about the philosophy of designing new structures, reinforcement, replacement of old structures, risk management of earthquakes and so forth. Decision variables of the PEER approach are defined as direct economic loss caused by lack of "on time" exploitation and life damage due to earthquakes. Enough data about the values of decision variables and their change in different levels of a building's damage should be available to use the PEER approach equation (1-1) [11].

$$\lambda(DV) = \iiint G(DV|DM)dG(DM|EDP) \times dG(EDP|IM)d\lambda(IM) \qquad (1\text{-}1)$$

Where, λ (IM) is the mean annual frequency of an earthquake intensity measure (e.g. maximum ground acceleration, spectral acceleration of first mode, etc.), G (EDP|IM) is the complementary cumulative probability distribution for a simple demand parameter (e.g. structure's maximum displacement, inter-story drift, story's acceleration, etc.). In case a degree of intensity measure is applied, G(DM|EDP) is the

complementary cumulative probability distribution for a structure's damage parameter (e.g. collapse damage state, collapse state based on the life safety performance) in case a degree of demand is applied and G(DV|DM) is the complementary cumulative distribution for a decision parameter (e.g. direct and indirect loss and life damage) in case a degree of damage is applied in the structure. By using the law of total probabilities and considering such parameters as an intensity measure, structure's demand and damage and decision variable as random variables, the uncertainty level related to decision-making variable will be determined by using the equation (1-1).

Given the fact that the proposed procedure attempts to directly include uncertainties in every step of determining the seismic hazard, building seismic response, damage and losses, different uncertainty sources and their combination and determination methods for achieving a comprehensive probability distribution for the final decision variables is of utmost importance. Therefore, determining buildings' seismic performance, fragility curve for the collapse limit state and involvement and synthesis of the existing uncertainties are the main concentration of this study. The collapse vulnerability curve and its determination method as well as the existing uncertainties will be discussed next.

1.5 Fragility Curves and Structure's Collapse Limit State

One important part used in the assessment of a structure’s seismic performance in the PEER approach is the building's fragility curve for different limit states. The first step for determination of fragility curves of forming components is to determine their related limit states. They are defined as the limit states of a building's forming components and the general limit states of the building. By using the fragility curves of a building's forming components and summing the damages of each part, one can

determine the possible and total structural damage. On the other hand, it is possible that the limit states are defined on the level of a building's overall performance (e.g. the limit state of immediate occupancy, life safety, collapse prevention and collapse). The building's vulnerability or fragility, either in the form of fractional or overall performance, is defined as the probability of achieving or exceeding a certain limit state, assuming the exposure of a system to an extent of engineering demand parameter. This relation can be generally presented in the following form:

$$P(DM|EDP) = P[Demand > Capacity|EDP = edp_i] \quad (1\text{-}2)$$

P (DM|EDP) indicates the probability of the extent of the damage in case a degree of engineering demand is applied. In order to determine this probability, the probability of applied demand exceeding the existing capacity should be specified first. Such fragility relations can be determined using analytical, experimental and expert opinions[19].

An important limit state, studied in this thesis, is the sideway collapse limit state. Lateral collapse is defined as the total instability of a building's system due to lateral displacements of a building under intense ground motions and second-degree impacts of P-Δ, to the extent, that emergent mechanism cause the whole structure instability and collapse. Reports of the damages caused by many earthquakes indicate that one of the most important factors affecting the direct economic and life losses is the building's lateral collapse [20, 21]. Many researchers have recently focused on the collapse limit state of structures [22-24]. In addition, preventing such limit states has become important in many existing regulations on performance- and force-based design against earthquakes, which are generally aimed at life safety performances in case of

strong earthquakes [10, 25, 26]. Factors leading to changes in a building's collapse capacity are divided into two factors: aleatory and epistemic uncertainties. Accordingly, aleatory uncertainty consists of factors that posses random features or according to our current knowledge and data, cannot be accurately predicted. The best example for such uncertainty is an earthquake's intensity and frequency. Given the limited information about the mechanism of an earthquake occurrence, fault movements and tensions and their slip resistance, it is not possible to accurately predict the occurrence of an earthquake. Therefore, by considering the occurrence of an earthquake as an aleatory variable and using an appropriate probability model based on the passed earthquakes in a region, the probability of an earthquake-occurrence with certain magnitude can be estimated. Moreover, intense ground motions in a region due to earthquakes can be considered as an aleatory uncertainty factor. On the other hand, epistemic uncertainties are those parts of factors that cause change in the collapse capacity of structures of which a predictive model can be designed based on the existing data. The deviation of the expected values from the actual values is indicative of an epistemic uncertainty. The effects of these uncertainty factors can be reduced by collecting more data or using a more appropriate analytical model. Parameters of a structure's modeling, building construction quality and analytic models in predicting a building's real behavior can be included as epistemic uncertainties [27].

1.6 Determining the Structures' Collapse Fragility Curve in the Form of Incremental Dynamic Analysis

Incremental dynamic analysis (IDA) is a parametric analysis during which the structure is analyzed under earthquake records with different scales. IDA curves show the structure's response parameter towards the intensity measure of earthquakes. The concept of incremental dynamic analysis has been explained in a study by Cornell and

Vamvatsikos [28]. Moreover, this method is used for the estimation of a structure's collapse in (FEMA, 2000)[29] report. While using incremental dynamic analysis for determining the fragility curve of a particular limit state, appropriate seismicity records of the region are selected. After selecting an appropriate parameter for measuring intensity, the selected records are scaled based on increasing scale ratios. Then, the appropriate engineering demand parameter under different records with different coefficients will be determined by using the dynamic analysis of the target structure model under the effect of scaled records. Plotted curves in the IM-EDP page indicate any changes in a structure's response towards different intensity measures. It shows that incremental dynamic analysis can be employed for determining the collapse fragility curve from different points of views. Probability distribution of a structure's lateral collapse capacity, which specifies the probability of reaching the collapse limit state in structures, can be obtained through an incremental dynamic analysis. Thus, the collapse probability distribution makes them possible to be used in the framework of the PEER probability approach for obtaining the probability distribution of the decision-making parameter. The collapse fragility curve can be determined using IDA diagrams in two ways, from an IM-based or EDP-based perspective. In both cases, the collapse fragility curve is obtained by comparing a structure's demand towards earthquake and the current capacity of the structure. Accordingly, the collapse limit state occurs when the applied demand of the structure exceeds its collapse capacity. Considering the probabilistic analysis of the demand and capacity parameters, the probability of reaching at the collapse limit state is presented in the form of the "collapse fragility curve". The difference between these two perspectives is the variable used in the form of demand and capacity probability framework [24].

According to the EDP-based approach, the structure reaches to the collapse limit state when generated Engineering Demand Parameter, due to application of earthquake record with the IM intensity, exceeds the structure's capacity (EDP). The Engineering Demand Parameter can be selected as the displacement (inter-story drift) or force (axial force of columns) parameters. Thus, the probability distribution of the Engineering Demand Parameter of a structure is obtained through the probability distribution of its capacity in the form of Engineering Demand Parameter and the probability of Applied Engineering Demand going beyond a structure's capacity. The equation for determining the collapse fragility curve, based on the Engineering Demand Parameter method, is as follows:

$$P(Collapse)|IM = im_i) = \sum_{edp_i} P\,(EDP_d > EDP_c|EDP_c = edp_c, IM = im_i).P(EDP_c = edp_{c_i}) \quad (1\text{-}3)$$

Where, P (EDPd>EDPc | EDPc = edpci, IM=imi) specifies the probability of Applied Engineering Demand (EDPd), exceeds the structure's collapse capacity in the form of Engineering Demand Parameter (EDPc). Each random value of the capacity (edpci) and intensity measures (imi) should be calculated in the above equation. Moreover, the expression P (EDPc = edpci) specifies the probability that the structure's capacity is equal to the random capacity of edpci.

In order to determine fore- mentioned probabilities (equation (1-3)), the probability distributions of the engineering demand and a structure's collapse capacity should be determined in the engineering demand format.

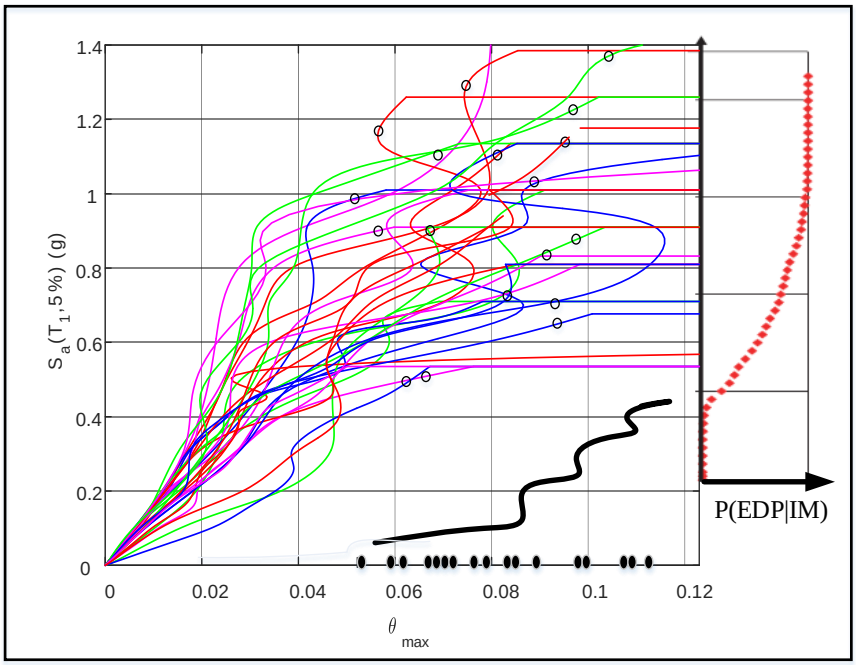

Figure 1.3: The probability distribution of engineering demand parameter and capacity of structure accordance with EDP-Based method

Several methods exist for the determination of these two probability distributions. They are divided into determining methods of mean and the standard deviation of collapse fragility curve based on the narrow-band analysis, multiple narrow-band analysis, cloud analysis, scaled cloud analysis and incremental dynamic analysis. Determining the collapse fragility curve using an incremental dynamic analysis is considered as the most accurate method for determining the probability curves of the engineering demand and a structure's capacity parameters for different limit states. On the other hand, more analyses and calculation time, are needed for the preparation of the IDA curves in comparison with the other proposed approaches [30]. This procedure, based on the engineering demand parameter in accordance with the equation (1-3), is shown in Figure 1.3. It samples the two IMs of P (EDP|IM) probability distribution. Additionally, the dots representing the collapse are identified as empty black circles on the IDA curves (SAC/FEMA method is used for defining the collapse limit state according to the condition that the curve slope is less than 20%

of the initial slope of the IDA curve, meaning the structure has reached the collapse limit state). Empty black circles on the EDP axis (shown with solid black circles) indicate the probability distribution of P (EDP_c). The collapse probability distribution for different IMs is determined by the equation (1-3) and is shown with dots in the right part of Figure 1.3.

The IM-based approach is another perspective for the determination of the collapse probability distribution. It is based on the direct usage of the intensity measure parameter in determining the collapse fragility curve which was introduced by Ibarra et al, [30]. In this method, the random variable is defined as the collapse capacity in the form of intensity measure (IM_c). The collapse capacity is the extent of the intense ground motion under the influence of a building undergoing a dynamic instability. Therefore, determining the probability curve related with IM_c is made possible by the incremental dynamic analysis. For this purpose, the IM_c values for a class of intense ground motions, related with the region's seismicity, are determined by using the incremental dynamic analysis. The probability distribution fitted to IM_c values specifies the collapse fragility curve in this present method. The fragility curve is determined by using the following equation:

$$P(Collapse|IM = im_i) = P\left(im_i > IM_{collapse}\right) \qquad (1\text{-}4)$$

In this approach, a dot on the IDA curve is identified as the representative spot for the collapse limit state.

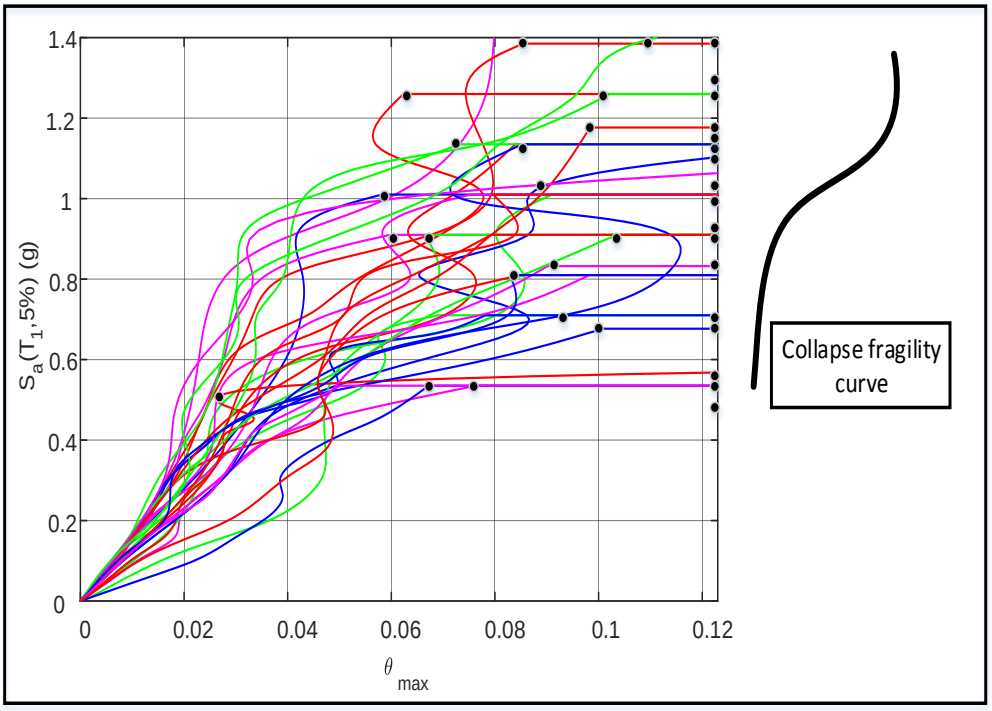

Figure 1.4: The probability distribution of engineering demand parameter and capacity of structure according to IM-Based method

A structure's dynamic analysis, using the existing algorithms, is not possible in intensity more than the intensity measure of that dot.

In other words, the last intensity measure related to the last dot on the IDA curve, where a structure's convergence in dynamic analysis is achieved, will be considered as the collapse intensity. Determining the collapse fragility curve in this approach is shown in Figure 1.4. The last dot on the IDA curve is shown with black circle points in Figure 1.4. These dots on the intensity measure axis and the fitness of probability curve on the above dots indicate the collapse fragility curve in the present approach.

Using the EDP-based approach for determining the collapse fragility curve in a certain intensity measure shows higher collapse probability than the IM-based approach. This is due to the definition of collapse capacity in the form of Engineering Demand Parameter. After passing the point where the IDA slope curve is less than 20% of the initial slope, the structure still has capacity. Unlike the EDP-based approach, this

capacity is taken into account in the IM-based approach. Given this limitation and also the fact that determining a dot representative of collapse on the IDA curve requires the engineering demand parameter caused by the strong non-linear effects of a structure's elements (with low-intensity measure, engineering demand parameter is highly increased), the present thesis applies the IM-based approach for determining the collapse fragility curve.

1.7 Available Methods to Consider Uncertainties in Construction of Collapse Fragility Curves

Two sources of uncertainty are involved in determining a structure’s collapse fragility curve; an uncertainty source due to the random parameters and another uncertainty source due to the lack of data and limited knowledge about the used model. Since the existing probability approaches are used for the determination and synthesis of these two uncertainty sources for the structure's collapse fragility curve in the following chapters, this section explains the first order-second moment, mean estimation, confidence interval and Monte Carlo methods based on the response level.

In the present study, uncertainties caused by strong ground motions observed for the specific site are considered as the random parameter of collapse fragility curve. This is itself divided into the uncertainty of intensity measure parameter and its occurrence in the site, uncertainties of frequency content of the observed record in the region, endurance time of the observed record, the earthquake's source mechanism, etc. The probabilistic seismic hazard analysis of an earthquake (which indicates the mean annual frequency based on different values of IM) is usually used for the first class of this uncertainty. For the second uncertainty class, records of different earthquakes in

the form of incremental dynamic analysis method are used to determine the collapse fragility curves.

Epistemic and cognitive uncertainties, investigated in the present study, are uncertainties of those parameters that have been used in this model for determining the structure's seismic response against earthquake. In the case of steel moment resistant buildings, this type of uncertainties are related to the moment-rotation of a structure's connections and their parameters. The uncertainty caused by a construction quality and its effect on the collapse fragility curve is also highlighted in the present study which will be presented in the form of fuzzy-random methods, neural networks and a fuzzy inference system. Finally, the synthesis methods of aleatory and epistemic uncertainties in the form of mean estimation, confidence interval and Monte Carlo simulation methods based on response level, which are compared with the other proposed approaches, will be explained further in this thesis.

1.7.1 First-Order Second-Moment Method (FOSM)

When analyzing the reliability of structures, First-Order and Second-Moment methods are used to estimate their reliability index and damage probability. In developing any structures' collapse fragility curves, this approach is similarly employed for the estimation of their collapse fragility parameters (mean and standard deviation). The general relation between the First-Order Second-Moment method is obtained based on the first two terms of Taylor series of collapse fragility curve's mean value function. Accordingly, if Y is the function of random parameters Q_1, Q_2,….. Q_n, its mean and standard deviation values are obtained through the Taylor series around the mean value function of these parameters with uncertainty. The simple state of these series is when its linear section, meaning the first two terms (first order) and its two first moments

(mean and standard deviation) are used. Therefore, mean and standard deviation values of variable Y can be obtained by the following equation:

$$Y = g(Q_1, Q_2, \dots, Q_n)$$

$$\mu_Y \approx g(\mu_{Q1}, \mu_{Q2}, \dots \mu_{Qn}) + \frac{1}{2}\sum_{i=1}^{n}\sum_{j=1}^{n}(\frac{\partial^2 g}{\partial q_i \partial q_j})\rho_{qi,qj}\,\sigma_{qi}\,\sigma_{qj} \qquad (1\text{-}1)$$

$$\beta_Y^2 \approx \sum_{i=1}^{n}\sum_{j=1}^{n}(\frac{\partial g}{\partial q_i})(\frac{\partial g}{\partial q_j})\rho_{qi,qj}\,\sigma_{qi}\,\sigma_{qj}$$

Where, derivatives of g function based on q_i and q_j, are determined in mean values of Q_i and Q_j parameters and $\rho_{qi,qj}$ is the correlation coefficient between q_i و q_j parameters and β_{qi} and β_{qj} values of standard deviation of Q_i and Q_j.

Since the mean value function is not based on the uncertainty parameters of a certain function, the mean values of fragility curve are produced around the mean values of random parameters in order to calculate g derivatives. The first order derivatives of the mean function based on random parameters are determined using one-side or two-side derivatives (shown by equations (1-2) and (1-3))

$$\frac{\partial g}{\partial Q} = \frac{g(\mu_Q) - g(\mu_Q \pm n\beta_Q)}{\pm n\beta_Q} \qquad (1\text{-}2)$$

$$\frac{\partial g}{\partial Q} = \frac{g(\mu_Q - n\sigma_Q) - g(\mu_Q + n\beta_Q)}{2n\beta_Q} \qquad (1\text{-}3)$$

The mean value of fragility curve is determined in the produced values on one side of the random parameters' mean value ($+n\beta$ or $-n\beta$) in the equation (1-2). However in

equation (1-3), the mean value of the fragility curve should be determined on both sides of ($+n\beta$) and ($-n\beta$).

Many scientists have used the first-order, the second-moment approach for considering the effects of epistemic uncertainties on the collapse fragility curves [31].

1.7.2 Mean Estimation Method

Mean estimation method is an approach for combining the epistemic and aleatory uncertainty parameters. In this method, the mean value of the fragility curve will not change by involving epistemic uncertainty parameters. It is assumed that uncertainties caused by epistemic parameters influence the standard deviation value.

Accordingly in this method, the standard deviation value of the collapse fragility curve can be determined through the following equation, considering both aleatory and epistemic uncertainty sources:

$$\beta_T^2 = \beta_{Aleatory}^2 + \beta_{Epistemic}^2 \qquad (1\text{-}4)$$

Where, $\beta^2_{\text{Aleatory}}$ indicates the variance of the fragility curve caused by aleatory uncertainties (when all epistemic uncertainties have a mean value and the collapse fragility curve have been obtained) the $\beta^2_{\text{Epistemic}}$ indicates the variance due to epistemic uncertainties (which have been gained using FOSM method). Mean estimation method keeps the mean value constant and increases the standard deviation of the collapse fragility curve (Figure 1.5). This approach is limited in the sense that the uncertainties caused by the lack of knowledge only affect the standard deviation of the collapse fragility curve.

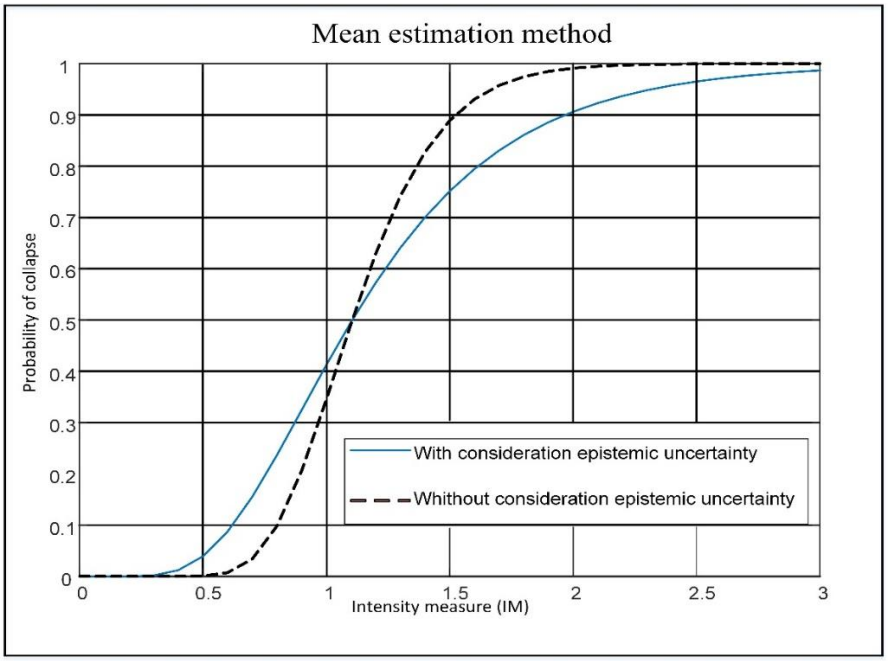

Figure 1.5: Considering mean estimation method to consider epistemic uncertainty

1.7.3 Confidence Interval Method

Another approach for the synthesis of epistemic uncertainties and aleatory parameters is the confidence interval method in which it is assumed that epistemic uncertainty changes the mean value of the collapse fragility curve. Accordingly, the probability distribution is considered on the mean value of the fragility curve obtained from aleatory uncertainties (when all parameters have mean value). In this distribution, the mean value will not change and the standard deviation is obtained through FOSM method. Moreover, epistemic uncertainties of this distribution will not influence the standard deviation of the collapse fragility curve.

The final collapse fragility curve for different percentages of confidence interval is gained by the displacement of the initial curve over the considered probability distribution for mean value. Figure 1.6 shows how this method is used for the involvement of epistemic uncertainties in the collapse fragility curve and final probability distribution.

Cornell et al. [32] and Ellingwood et al.[33] employed this approach in their research. Since the obtained collapse fragility curve for different confidence intervals is displaced only by considering the effects of the aleatory uncertainties, the present method cannot involve the effects of epistemic uncertainties on the standard deviation of fragility curve. In addition, the resulting fragility curve affected by both aleatory and epistemic uncertainties in this approach highly depends on the selected confidence level.

For instance, the collapse probability in 50% confidence level (not including epistemic uncertainties) for spectral acceleration $S_a(T_1)$ = 1g is near zero, while it is increased to more than 0.4 for 90% confidence level. This shows high dependency of the final response to the selected confidence interval. Moreover, aleatory and epistemic sources of uncertainty should be completely separated in the present method, while in many problems they are separated based on expert opinion.

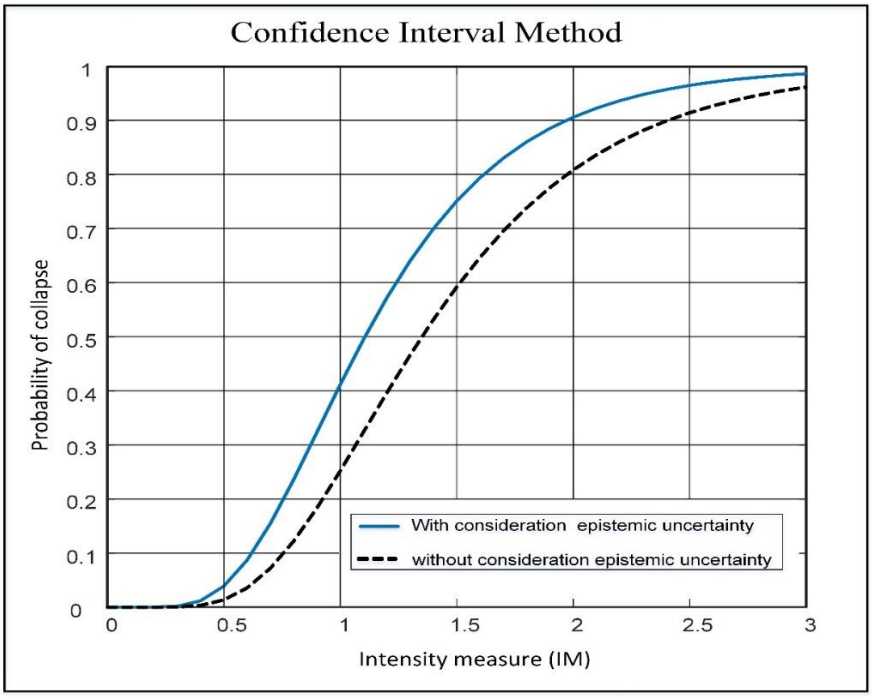

Figure 1.6: Considering confidence interval method to consider epistemic uncertainty

1.7.4 Monte Carlo Method Based on Response Surface

The third method for the involvement of epistemic uncertainties is by using Monte Carlo simulation method. It is basically used in the field of structural reliability in which effective variables on their demand and capacity are expressed in the form of probability distributions. In this approach, the structure reliability is calculated by simulating ample amount of aleatory variables and applying problem-solving for each simulated value [34]. Since the number of simulations is very high, using this method is time consuming and system response lacks time and cost efficiency. Similarly, in determining the collapse fragility curve when aleatory variables are chosen, the time and cost of problem-solving increases accordingly. Therefore, estimation methods, like response surface [35] and sampling, based on the Latin Hypercube Sampling (LHS) algorithm [36] have been used in the reliability problems for reducing the calculation time.

The Monte Carlo method is combined with the response surface method for the determination of collapse fragility of concrete buildings in a study conducted by Liel et al. [22]. Modeling variables are considered in the form of such aleatory parameters as strength and ductility of beams, columns and connections in the former research. Then the mean and standard deviation functions of the probability distribution of the sample frames are determined by simulating a limited number of modeling variables and then estimated with the second-order functions. Constant coefficients required in this estimation are determined using nonlinear regression analysis based on the least squares errors. Thereafter, the obtained functions are considered as a criterion in determining the mean value and standard deviation of the collapse fragility curve and used in simulations (with high number of modeling variables) instead of the dynamic analysis of the sample frame from the obtained second-order function.

The Monte Carlo method is well known for its accuracy and efficiency in determining and affecting epistemic uncertainties in the collapse fragility curve. It further suggests that epistemic uncertainties affect both the mean values and standard deviation of the collapse fragility curve. While Monte Carlo method does not have the limitation of the two former methods, using a specific function for determining the mean value and standard deviation of the collapse fragility curve instead of a structure's dynamic analysis causes this method to be approximate in its determination of the final collapse fragility curve.

1.8 Literature Review on Fragility Analysis Considering Uncertainties through ANN

Artificial Neural Network (ANN) is applied for generating fragility analysis in previous relevant studies. Lagaros and Fragiadakis [37] used artificial neural network

for quick assessment of the exceedance probabilities for each damage state for a particular seismic zone. Papadrakakis et al. [38] suggested Monte Carlo method which is updated by the neural network for the sensitivity approach and also they established fragility analysis for different damage states of concrete dams. They suggested that input data exist on ANN consist of record variables and resultant outcome data are regarded as the pseudo spectral Acceleration (Sa) associated with different damage states. Cardaliaguet and Euvrand [39] applied an ANN algorithm to estimate a function and its derivatives in control theory. Li [40] indicated that any multivariate performance and its existing derivatives could be coincidentally estimated by a radial basis ANN while the presumption on the performance are relevantly gentle. Chapman and Crossland [41] showed an example of ANN application for prediction of the failure probability of pipe work under different working situations. Whereas effectiveness of the neural network approach is demonstrated to estimate the fragility analysis of a damage state other than collapse (e.g. moderate damage, extensive damage) by Mitropoulo and Papadrakakis [38] while the main target of this paper is to show the effectiveness of the neural network approach in deriving collapse fragility curves, epistemic uncertainties effects are equally considered in this study.

Reliability analysis of the SMR frame is affected by particular parameters. Effects of each particular parameters e.g., material quality [42], irregular story [43], and building height [44] are considered to achieve fragility curves by many researchers. Rajeev and Tesfamariam [45] both considered interactions among the parameters such as irregularities (weak story, irregular story, vertical discontinuities etc.,) and material quality to develop fragility curves. Liel et al. [24] presented the effect of modelling uncertainty in collapse limit state in comparison with the other limit states, such as, immediate occupancy and life safety in fragility curves.

Lignos [23] incorporated Record To Record (RTR) variability and modelling uncertainties through the incremental dynamic analysis on deriving fragility curves. Fuzzy logic is used for risk analysis, safety evaluation and structural analysis to consider the impact of modelling uncertainty ([45, 46]).

The use of random-fuzzy method for incorporating epistemic uncertainties in a model is discussed by Moller and Beer [46]. In their method, parameters with aleatory uncertainties are considered as random variables with probability distributions while parameters with epistemic uncertainties are taken as fuzzy numbers.

Firstly in this study, K-means an algorithm is applied to select ground motion properly and cuckoo searching algorithm is used to consider the epistemic uncertainty. Fuzzy inference system trained by Sugeno type model is used to derive the response surface coefficient of different material quality to consider cognitive uncertainty. Finally fuzzy cluster method based on the particle swarm optimization is applied to predict the mean and the standard deviation of the collapse fragility curve in the interval value of fuzzy member of epistemic uncertainty.

1.9 Objectives and Statement of the Problem

Deriving fragility curves for a building requires the determination of a structure's response surface against strong ground motions due to earthquakes and also the probability of response surface exceeding in different limit states. For this purpose, employing appropriate models and methods in facing different sources of uncertainties and their combination for a final reliable result and a criterion for accurate decision-making seems critical. Different factors including human, construction, building maintenance and modeling errors produce uncertainties in the structure's seismic

response and as a result, uncertainties in estimating the probability of achieving a predefined limit state. In order to determine a more reliable response surface of the structure and prepare more accurate fragility curves, all the uncertainties in the existing data and used models should be appropriately studied.

In addition to epistemic and aleatory uncertainties sources described in the previous sections, consists of effective descriptive parameters in the structure's response and hence, its collapse fragility curve (e.g. changes occurring in the material stage compared to assumptions in the primary design, which are usually descriptively demonstrated with material quality parameter). Studies on the determination of structures' collapse fragility curve usually suggest separate vulnerability analyses for low-ductility and ductile buildings. For instance, in the study of Liel et al. [22] ductile concrete structures (designed and built according to new design guidelines) and low-ductility concrete structures (designed and built according to old guidelines and methods) are investigated. Unfortunately, the material quality parameter in the developing countries is very adversely effective in the behavior and ductility of structures that are even designed according to new guidelines. Reports on the damages and fatalities caused by buildings' collapse in recent earthquakes suggest that the material quality parameter has been considerably effective in the expected ductility of structures that were recently designed and built according to new guidelines. Therefore, it is assumed that elimination of this parameter in the structure's vulnerability analysis, where high quality is not assured, will cause a low estimation of earthquake consequences and its damages and fatalities. Beside introducing some approaches to promote the probability attitudes toward the involvement of epistemic uncertainties (like fuzzy-random and neural network methods), the present thesis has attempted to propose an approach in which related uncertainties of material quality are

focused on and the collapse fragility curve is obtained by the involvement and combination of that parameter with other effective uncertainties (aleatory and epistemic). Due to substantial economic losses after the structures' collapse in recent earthquakes and the fact that determining the structures' seismic hazard is directly related with their collapse, the collapse limit state is considered in the present thesis. On the other hand, selection of the ground motion is the main problem in time history analysis. In this thesis, clustering algorithm is proposed to select the ground motion for considering aleatory uncertainty in a better way.

Different mathematical methods have been proposed for material and synthesis of various factors which create uncertainty. Amongst these methods are the probability theory, algebra interval, convex modeling, fuzzy set theory, fuzzy-random theory and subjective probability[46].

Incorporating different sources of uncertainty in the structures' collapse fragility curve have been the subject of many recent studies [22, 24, 47]. Many of these studies have involved those uncertainties using probability theories like, FOSM [48], confidence interval [32], mean estimation [49], response surface estimation and the Monte Carlo simulation [22]. Probability methods assume that there are enough data to determine the probability distribution of variables with epistemic uncertainty. Thus, this perspective can only involve the part with aleatory uncertainty in the fragility curve [46]. However, uncertainties related to parameters that cannot be assigned to accurate probability distribution due to high dispersion and uncertainty sources which are expressed descriptively and non-numerically, cannot be involved in the structures' collapse fragility curve. There are a lot of researches involving the effects of these aleatory and cognitive uncertainties in the structures' reliability and dynamic response.

Determining a structure's response considering fuzzy parameters [50] and also determining that structure’s reliability using fuzzy variables[51] are examples of such studies conducted in this field. However, there have been few studies about the involvement of epistemic and cognitive uncertainties by using the probabilistic methods in the form of structures- collapse fragility curve and PEER equation (1-1). For this reason, an approach based on the fuzzy logic of the involvement of such uncertainties (especially that related to material quality parameter) in structures' collapse fragility curve is proposed in the present thesis. Thus, uncertainties of the modeling parameters and material quality are thereof respectively considered as epistemic and cognitive uncertainties. Moreover, a steel moment resistant structure, designed according to seismic standards, is considered to present the proposed methods. Uncertainties of other parameters like, the geometry of applied sections with live or dead loads applied to a structure's frame and irregularity effects such as weak and soft story and etc. is not examined in this study. By using proposed approaches for the involvement of different uncertainties and also classification of forenamed parameters as parts of aleatory, epistemic or cognitive uncertainties, they can examine the effects of such parameter in the collapse fragility curve.

1.10 Thesis Structure and Limitation

The collapse fragility curves and the concentrated plasticity model used in the steel moment resistant frame and the effect of ground motion are explained in the second chapter. In the third chapter, K-means algorithm is applied to properly select ground motion and the Fuzzy Inference System (FIS) and Cuckoo model is used to predict the performance of a structure by involving epistemic and cognitive uncertainties. The fourth chapter proposes the Fuzzy-PSO interval method for involving the uncertainties of parameters with no precise probability distribution being proposed. In addition, the

efficiency of the proposed method in involving the epistemic uncertainties related to modeling parameters of the sample steel frame is investigated. The results of calculating the collapse probability of a sample steel frame and also the mean annual frequency of collapse in the form of proposed methods are compared at the end of each chapter. In the last chapter, the conclusion of all chapters is put together. Finally a general description of the fuzzy inference system theory is considered in appendix A and the lists of records used in K-means method are represented in appendix B.

In all stages of the thesis, a steel moment resistant structure is used as a case study to illustrate the efficiency of the proposed methods.

There are some limitations in modeling and in the proposed methods of the study. The analytic model used for exhibiting a structure's dynamic behavior is a two-dimensional frame so that the effects of the influential parameters like the two-side loading (direction of the earthquake and the load applied on the structure), deflection of the structure's plan due to inappropriate distribution of the lateral load-bearing elements and ductility effects of diaphragms are not considered in a real three-dimensional building.

Moreover, since the sample building is a steel moment resistant building in this study, the effects of structural and non-structural components, are not included in the structure's lateral load-bearing system but effective in its stiffness and they are not investigated. The considered damage state for all the limit states is considered to be due to the formation of plastic hinges in beams and columns which cause the lateral instability. Although this damage mode is justified for those structures designed and built according to new guidelines with high quality, other modes should also be considered for the sample frames with low-index material quality. In addition, the

effects of soil-structure interaction are not examined in the thesis. In the moment-rotation model, considered for concentrated plasticity model, the effects of the axial force interaction on moment-rotation behavior of the target member is not considered (this is due to the lack of experimental data for the calibration of moment-rotation parameters). Finally, the modeling uncertainty parameters are not connected at the panel zone and therefore, are considered as deterministic parameters.

Chapter 2

FRAGILITY CURVES IN SIDESWAY COLLAPSE LIMIT STATE

2.1 Introduction

A structure's displacements due to strong ground motions from earthquakes thereof producing a force demand exceeding the final capacity of its components make the structure instable and weak. This limit state is called as the sideway collapse limit state. The generated forces in the structure’s components under the impact of cyclic loads by earthquake deteriorate the stiffness and strength of its components and as a result lead to a total or a partial collapse of the building. The structure’s collapse limit state can be divided into two sideway and vertical collapses. Reciprocal displacements of components and their resulting P-Δ effects activate the declining process of stiffness and strength which are considered as a part of the lateral loading system. It is continued to the point that the intensified demand (due to P-Δ effects), existing in the structure's components, exceeds the reduced strength (due to stiffness and strength deterioration) and the structure loses its ability to oppose the lateral load which leads to its lateral instability. On the other hand, if demand in the components of gravity load-bearing system exceeds their capacity, the structure is prone to a vertical collapse which is caused by its vertical instability.

Analytical models used by the scientists for predicting a structure’s collapse can be classified into a collection of system analyses with one degree of freedom [52] for real

structures or more complex models with several degrees of freedom [53, 54] based on the analysis of a structure's limited members. The main feature of analytical models for the prediction of its collapse capacity and its related uncertainties is the ability to determine and consider the parameters of stiffness and strength deterioration of the structural components under reciprocal loading. Reciprocal loadings, produced during strong ground motions in earthquakes, are applied to the structural components and the activation of different states of stiffness and strength deterioration causes more accurate prediction of a structure's collapse capacity. Therefore, creating an appropriate model for analyzing this collapse and developing the fragility curve of this limit state is critical [24]. In this section, the analytic moment-rotation models existing in steel moment resistant structures are studied and then, the modified Ibarra-Krawinkler moment-rotation model, capable of involving different modes of stiffness and strength deterioration, is introduced.

The aleatory state of the parameters of strong ground motions produced by earthquakes and also the inaccuracy of analytical models in determining a structure's seismic response complicate the determination of the collapse fragility curve. Different probability models [32, 47, 55] for different sources of uncertainty and their involvement in a structure's collapse capacity and also their combination for developing the collapse fragility curve are proposed. Various probability methods about the involvement of different uncertainties in the collapse fragility curve as well as their synthesis methods used in the next chapters are discussed in the second part of this chapter. At the end, modeling hypotheses of sample structures based on the laboratory data are discussed to determine modeling parameters and the modified Ibarra-Krawinkler moment-rotation model. Therefore, the presented values for these modeling parameters obtained using experimental studies on probability distributions,

from the basis of the further discussion on the effects of modeling and construction quality uncertainties which are expressed descriptively in the next chapters.

2.2 Appropriate Parameters of Seismic Demand and Intensity

As mentioned before, for a structure's incremental dynamic analysis and to determin its fragility curve, an appropriate intensity measure and engineering demand parameters are selected. Many studies used the first mode spectral acceleration (S_a (T_1)) as the intensity measure to examine the collapse limit state [24]. It shows that [28] prediction of a structure's response to the parameters of maximums of strong ground motion (e.g. maximum ground acceleration, velocity and displacement) and spectral parameters (e.g. spectral acceleration, velocity and displacement) include more changes. Therefore, selection of appropriate spectral values as IM is more efficient than selection of the record's maximums. Moreover, the hazard curves related to spectral acceleration parameter, which present mean annual frequency, can be obtained by using the probabilistic seismic hazard analysis. However, according to Baker et al., [16] using the vector intensity measure parameters instead of scalar parameters make the spectral acceleration more efficient. The proposed vector parameter is paired with the first mode spectral acceleration and is presented as the epsilon parameter (S_a (T_1), ε). The epsilon parameter indicates the changes present in the prediction model of the first mode spectral acceleration (reduction equation in seismic hazard analysis). Baker et al. suggested that ignoring the epsilon in a structure's incremental dynamic analysis leads to an overestimation of its seismic response and analytical collapse fragility curve. The first mode spectral acceleration parameter is used as the intensity measure in incremental dynamic analysis in this study.

Selecting an appropriate engineering demand parameter mostly depends on the understudy problem. A structure's engineering demand parameter should be then

measurable and have a logical relation with the objectives of that problem (determining the fragility curve for different limit states). Since a structure's lateral collapse, considered as the limit state of the present thesis, is caused by the structural lateral displacement under strong ground motions, intensified P-Δ effects and dynamic instability of structure, the Maximum Inter-story Drift Ratio (MIDR) is considered as the engineering demand parameter in this study [47, 56].

Former studies [47] illustrate that the stiffness and strength deterioration of those components under reciprocal loadings significantly affect the estimation of a structure's lateral collapse capacity. Thus, for an exact estimation, such analytical modeling approaches that are able to involve the effects of stiffness and strength deterioration should be used. The Hysteresis models capable of such actions are discussed here.

2.3 Hysteresis Models with Considering Strength and Stiffness Degradation

Considering an analytical model of structural component capable of involving the effects of stiffness and strength deterioration in reciprocal loadings due to strong ground motions is critical in estimating the structure's collapse capacity. Comparing the experimental results of two similar cases under static and cyclic incremental loadings it is evident that in monotonic loading after reaching the capping point, the strength will have a negative slope. It illustrates the necessity of involving the negative-slope branch in the hysteresis curve. In reciprocal loading, the maximum strength is also decreased with the number of loading cycles and cycle domains (it is true for both before and after the cap point) which have been shown by (1) and (2) in Figure 2.1.

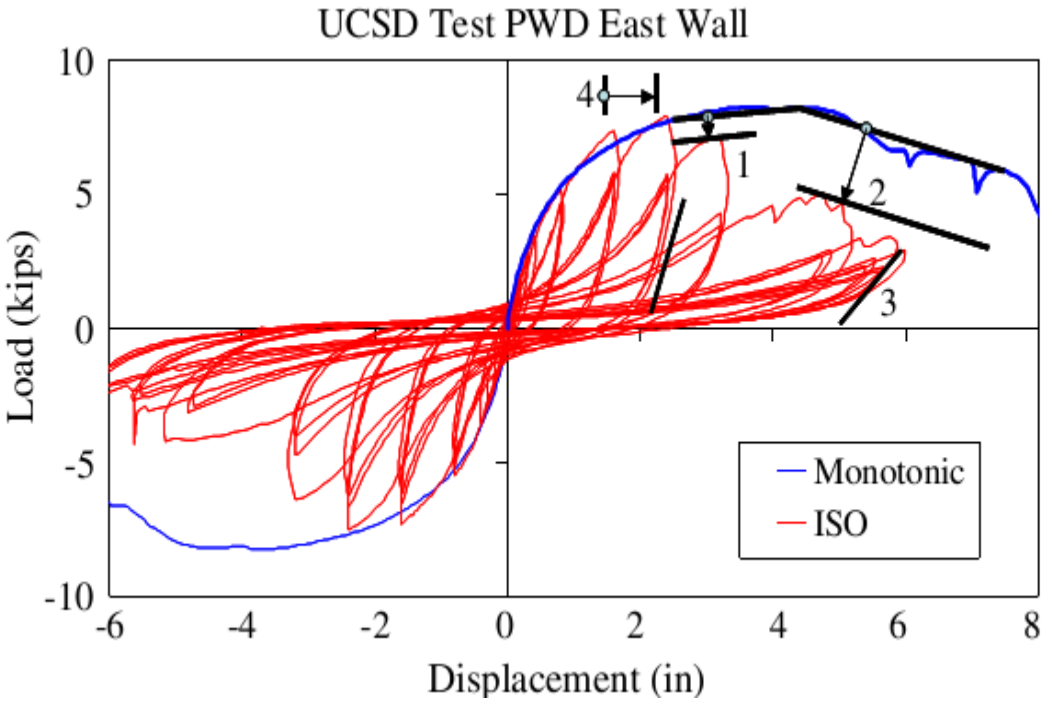

Figure 2.1: Various stiffness and strength degradation in ISO loading[57]

In addition, the unloading stiffness is reduced in reciprocal loading which is shown by (3) in Figure 2.1. Another mode of deterioration occurs in the stiffness of repetitive loading which is shown by (4) in Figure 2.1[57].

Various models have been developed for the determination of a structure's response under cyclic loading. Given the fact that a structure's lateral collapse is the limit state considered in the present study, the selected model for anticipating the structure's response in the form of engineering demand must involve the effects of stiffness and strength deterioration under the structure's dynamic loading. Many analytical models for estimating the structures' seismic response include the hysteresis models in which either the stiffness deterioration has been eliminated (e.g. bi-linear model) or has been taken into account by changing the direction in which the reloading occurs (e.g. peak-oriented and pinching models). Takeda et al.[58] proposed a model with tri-linear push curve the unloading stiffness of which reduced according to the maximum sample

displacement. This model is specifically employed for concrete samples. The developed model by Sivaselvan et al.[59], proposes some regulations regarding the involvement of stiffness and strength deterioration and pinching effects. However, no negative-slope branch in the hysteresis push curve has been considered in their proposed model.

Moreover, the proposed model by Song et al.[5] can involve the stiffness deterioration effects but given its limitations, it cannot involve the strength deterioration before the cap point (mode (1) in Figure 2.1) [57]. Various proposed hysteresis models and their abilities to involve different parameters are shown in Table 2.1.

Table 2.1: Applying various models to consider cyclic deterioration mode

Model	**Cyclic Deterioration Mode**			
	Basic Strength Deterioration	PostCap Strength Deterioration	Unloading Stiffness Deterioration	Accelerated Stiffness Deterioration
Takeda Model				
Bouce-Wen Model				
Ramberg-Osgood Model				
Kunath et. al Model				
FEMA-356 Model				
Song-Pinchiera Model				
Modified Ibarra-Krawinkler Model				

The Ibarra-Krawinkler model was firstly introduced by Rahnama et al. [60]and has been widely used ever since. The modified version of this moment-rotation model was provided by Ibarra et al.[57] Having a negative slope area and the ability to take into account different modes of stiffness and strength deterioration are among the characteristics of this model and it is defined based on the following:

- Push over curve which shows system's principal behavior regardless of its deterioration effects. The system's strength and deformation are defined in this curve.
- Some rules according to which the hysteresis behavior of target member, during the earthquake's reciprocal loading, are illustrated between the determined ranges in the push curve.
- Rules that define how to consider the deterioration modes rather than the base push over curve.

Using the hysteresis push curve determines its related strength and limitation of its deformation. The main parameters of the push curve in the Ibarra-Krawinkler model include the initial stiffness (K_e), yield strength (M_y), stiffness of hardening branch ($K_s = \alpha_s K_e$), maximum strength (M_c) and its corresponding displacement (θ_c), post-capping stiffness point ($K_c = \alpha_c K_e$), and residual strength (M_r) and its corresponding displacement (θ_r). The push-over curve and the above parameters are illustrated in Figure 2.2.

2.4 Ibarra-Krawinkler Backbone Model

A collection of rules that define the hysteresis model in the Ibarra-Krawinkler model are classified into bi-linear, peak-oriented and pinching models. The rules of each aforementioned model determine the repetitive loading and unloading behavior.

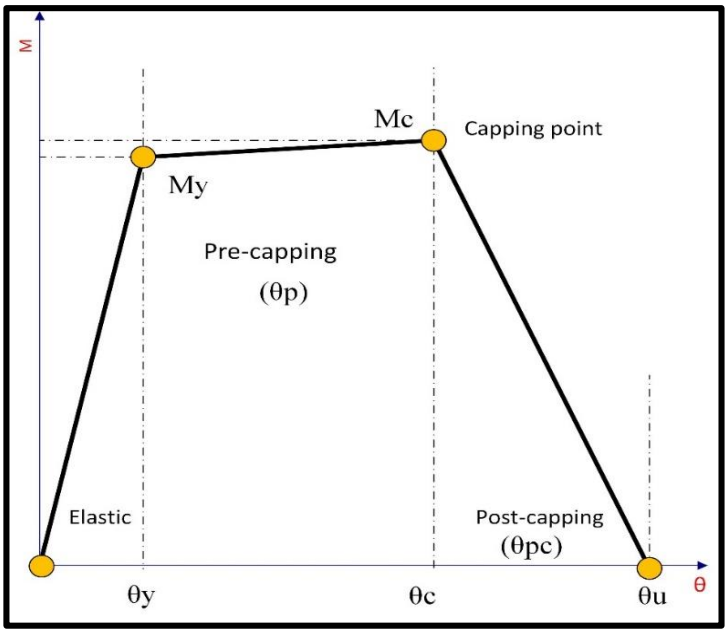

Figure 2.2: Moment-Rotation backbone curve of Ibarra-Krawinkler model

The reloading deterioration is not taken into account in the bi-linear model and occurs within the same slope of elastic curve. Figure 2.3 indicates the considered curve in this model. Experimental studies show that modeling the behavior of compact steel sections is made possible through this hysteresis model. Since the case studies of the present research are steel moment resistant structures, this approach is used to provide the modeling parameters of these structures' connections[47].

Bi-linear and peak-oriented modes are similar except that in the latter model, after unloading (parallel to the elastic area after reaching the reloading axis), the loading direction moves toward the target point located in a cycle before the one considered. The reloading process in the first cycle also occurs toward the yield point. The behavior of this model is shown in Figure 2.4.

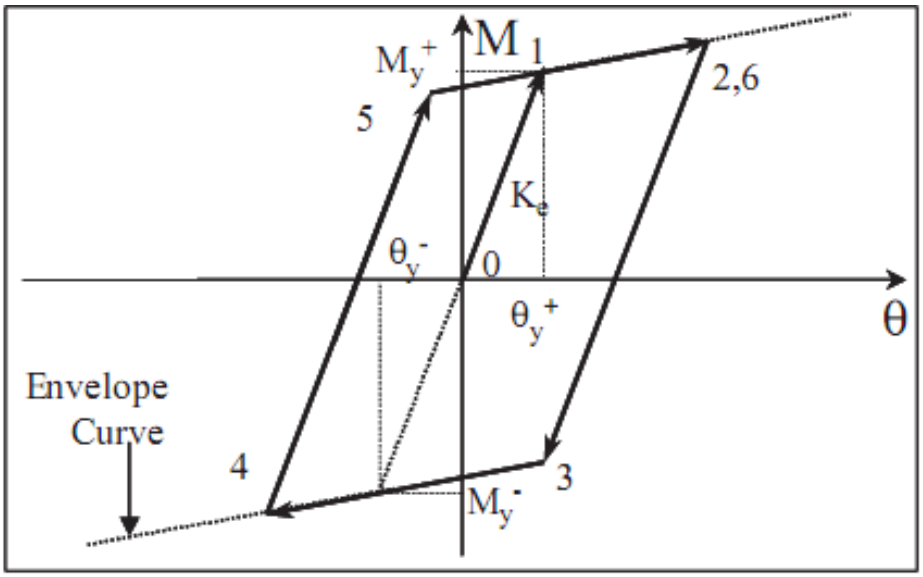

Figure 2.3: Bi-linear model [47]

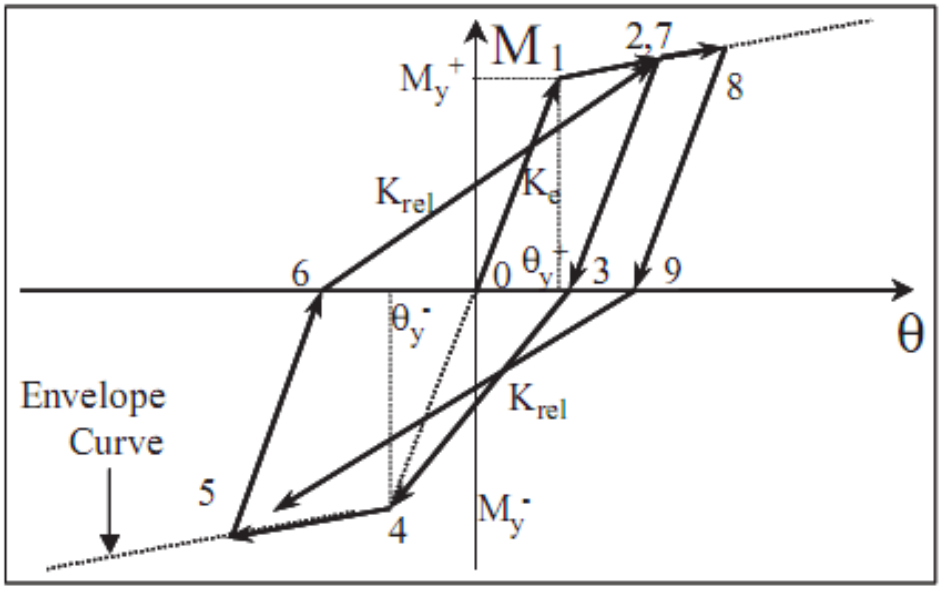

Figure 2.4: Peak-oriented model [47]

Finally, the pinching model is usually used for modeling the behavior of a crack's opening and closing and the adhesion effects of reinforcements in concrete sections. Movement of the reloading branch in the present model is firstly directed toward the

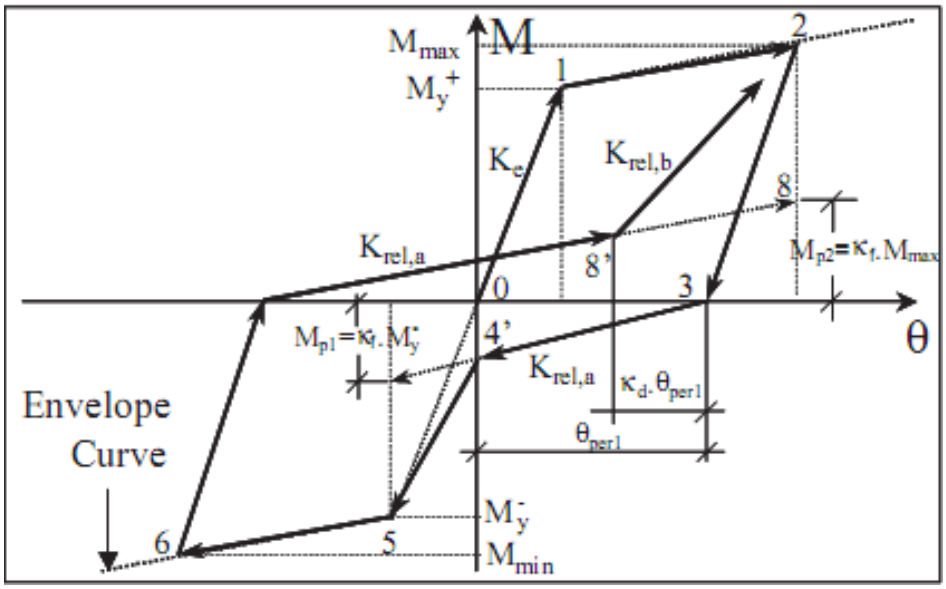

Figure 2.5: Pinching model [47]

breaking point and then is changed again toward the capping point, experienced in the former cycle. The behavior of this model is shown in Figure 2.5.

The third part of the hysteresis model deals with the involvement of stiffness and strength deterioration parameters. The four common modes of deterioration in reciprocal loading are: the basic strength, the post-capping strength, the unloading stiffness and the reloading stiffness deteriorations. Cyclic deterioration rules are the same for all hysteresis models except for the bi-linear model in which reloading deterioration is not taken into account. The cyclic deterioration ratio obeys the rule provided by Rahnama et al.,[60] which is formulated based on the dissipated energy in each cycle of the reciprocal loading. Each forming component of structure, regardless of the applied loading type, has a hysteresis capacity. Deterioration modes on the *ith* loading cycle are determined using κ_i (equation 2-1).

$$\kappa_i = \left[\frac{E_i}{E_t - \sum_{j=1}^{i} E_j}\right]^c \quad (2\text{-}1)$$

Where, E_i is the amount of dissipated energy on the *i th* cycle, ΣE_j is the dissipated energy in all previous cycles within the range of positive and negative loading and E_t is the base energy for the target component. The capacity of the base energy is determined by equation (2-2).

$$E_t = \gamma M_Y \theta_Y = \Lambda \theta_Y \quad (2\text{-}2)$$

According to equation (2-2), the capacity of hysteresis energy is defined as a coefficient to yield rotation. The capacity coefficient of dissipated hysteresis energy is determined by laboratory data and considered as an uncertainty modeling parameter. In equation (2-1), c is the deterioration velocity, the admissible value of which, according to Rahnama et al.[60] must be between 1 and 2.

The basic strength deterioration is determined by equation (2-3):

$$M_i^{\pm} = (1 - \kappa_{si}) M_{i-1}^{\pm} \quad (2\text{-}3)$$

Where in the equation (2-3), M_i is the basic deteriorated strength in the *i th* cycle and M_i is the basic strength before the *i th* cycle. Basic strengths can be observed both in positive and negative parts of the moment-rotation curve. κ_{si} parameter, in each cycle, is determined by using the equation (2-1). The basic strength deterioration also includes the deterioration of the slope of the strain's hardening branch which is similarly obtained by equation (2-4).

$$K_i^{\pm} = (1 - \kappa_{si}) K_{i-1}^{\pm} \tag{2-4}$$

The related mode of primary strength deterioration using the peak-oriented model is shown in Figure 2.6.

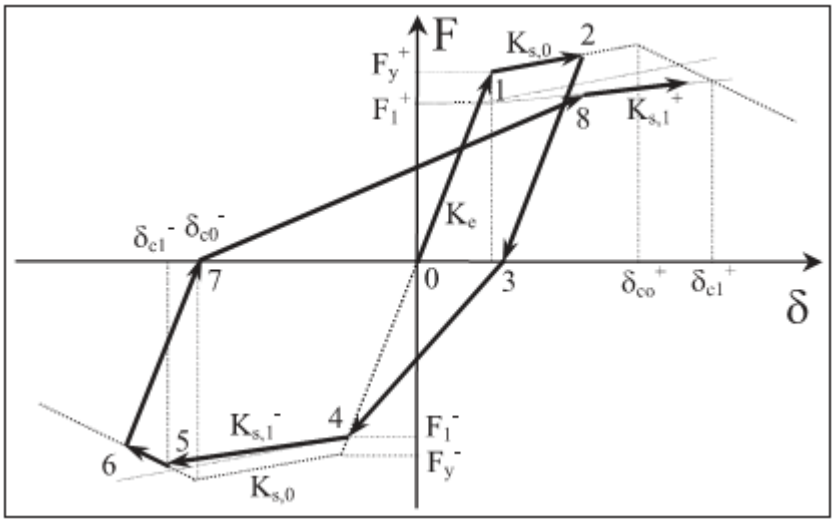

Figure 2.6: Primary strength deterioration model [47]

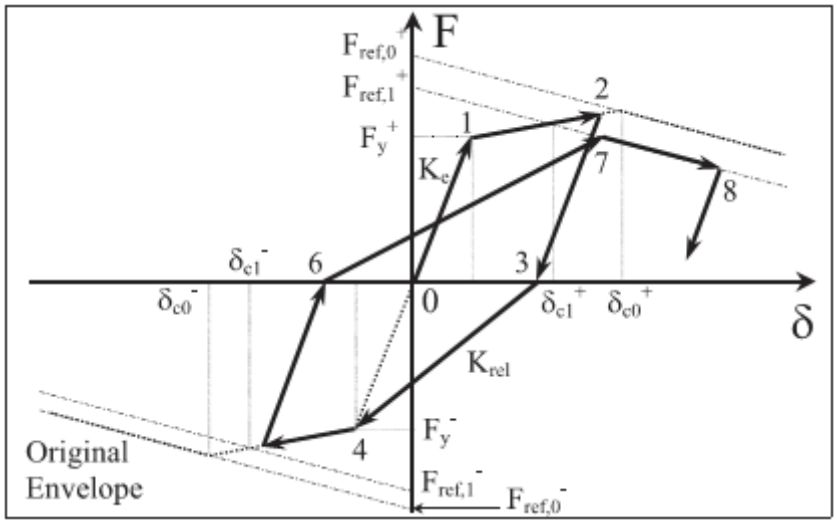

Figure 2.7: Post-capping strength deterioration model [47]

The related mode of post-capping strength deterioration, shown in Figure 2.7, is similarly obtained by equation (2-5).

$$M_{ref,i}^{\pm} = (1 - \kappa_{si}) M_{ref,i-1}^{\pm} \quad (2\text{-}5)$$

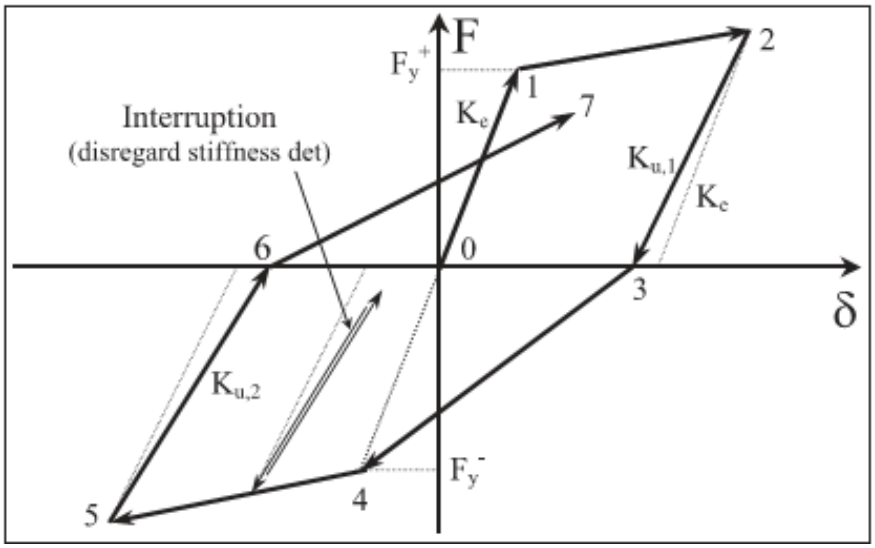

Figure 2.8: Unloading stiffness deterioration mode [47]

$M_{ref,i}$ is the cross-section of a vertical axis (moment axis) with the branch image after the maximum point. This deterioration mode occurs in positive or negative branches. The κ_{si} parameter is determined using equation (2-1).

The unloading stiffness deterioration mode is shown in Figure 2.8 and is similarly determined by the equation (2-6).

$$K_{u,i} = (1 - \kappa_{ui}) K_{u,i-1} \quad (2\text{-}6)$$

The reloading stiffness deterioration mode is shown in Figure 2.9 and is similarly determined by the equation (2-7). This deterioration mode increases the target rotation.

$$\theta_{t,i}^{\pm} = (1 + \kappa_{ai}) M_{t,i-1}^{\pm} \quad (2\text{-}7)$$

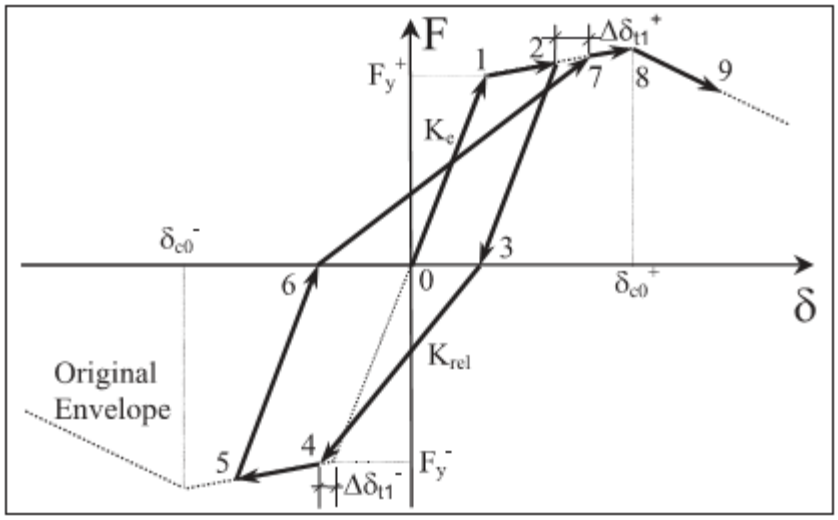

Figure 2.9: Reloading stiffness deterioration mode [47]

2.5 Physical Interpretation of Parameters in Ibarra-Krawinkler Model

By the implementation of such principles as increasing the connection capacity rather than the connected members (by 20%) and maintaining the relation between the weak beam-strong column, the current guidelines of the seismic design attempts to direct and concentrate the plastic deformations at the end of beams. But indeed, following the above regulations does not provide the required reliability for the maintenance of elastic deformations in connections. By observing the damages of welded beam-to-column connections in the Northridge earthquake indicates that even these regulations are not enough to prevent the plastic deformations of connections (Figure 2.10). Thus, the local ductility of node, including members and connections, should be defined and

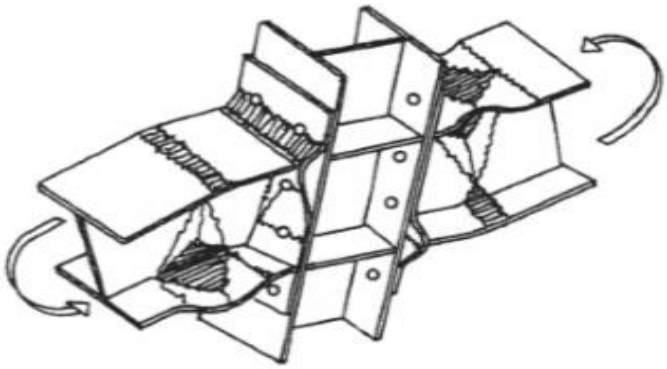

Figure 2.10: Plastic deformations of connections [24]

determined. It should be noted that there is a difference between the definitions of node, joint, connection and Panel zone areas which have been specified in Figure 2.11. For their inappropriate application, these areas are defined in technical literature as follows [24]: panel zone containing the column web within the height range of connection, joint containing the connection and panel zone, connection of structural parts in contact between the beam and column, node area containing the joint and a part of adjacent beam and column in which plastic deformations are likely to happen.

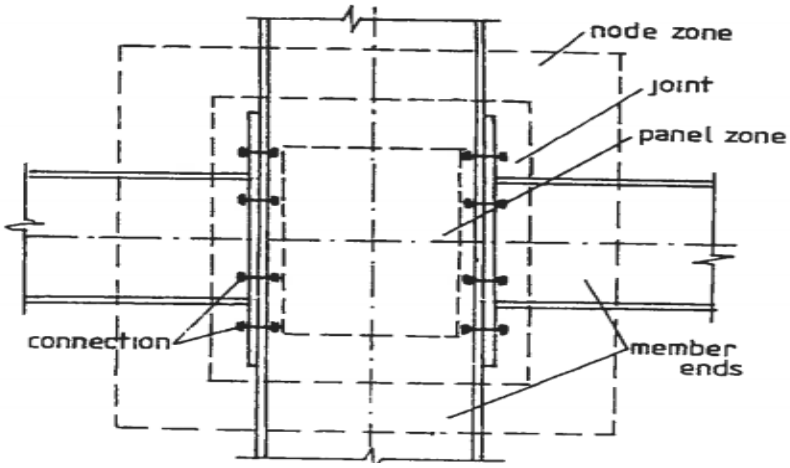

Figure 2.11: Panel, joint and node[24]

Different parts of the modified Ibarra-Krawinkler moment-rotation specify how plastic deformations extend through the beam and column members in the target connection.

Depending on the connection type and designed thickness of the target sections, extension of plastic deformations and plasticity of several connection parts (described above), differ. Assuming that plastic deformations firstly occur at beams, various parts of the moment-rotation curve can be described as follows [24].

The elastic part exists in the first step and to a larger extent, the beam section is located in this area ($\sigma_{max}<\sigma_y$). When the applied moment to the connection is increased, the upper and lower parts of the beam flange and gradually its web begin to yield. By increasing the applied moment in one section of the beam, the whole section reaches the yield state. The applied moment in this state equals to $M_y = Z.F_y$ (Z is the section's plastic moment). In this state, the rotation value equals to θ_y. The section's plastic rotation can be obtained by having the values of a section's elastic stiffness and yield moment.

Increasing the applied moment transmits the stress from its previous yield section to the strain's hardening area causing that section to tolerate a higher stress. This behavior is observed in the linear part of the yield and cap points. The ability of section rotation after the yield to the point where strength loss (due to web or flange buckling) is observed, the moment-rotation curve is then representative of θ_p. Therefore, the cap point moment value can be obtained by having the values of yield moment and the ratio of cap point moment to yield point moment (M_c/M_y).

The third branch of the moment-rotation curve indicates a drop in the section strength against the applied moment caused by the buckling of pressure flange or beam lateral buckling lying after the cap point. The rotation capacity of a section, reaching to a

point where its strength is completely lost, is represented as θ_{PC}. The final rotation of a member can be obtained by having θ_y, θ_p and θ_{PC} values.

Indeed, the final damage of a connection can be due to a combination of factors including the beam section yield, breakdown of bolted or welded connection, connection's panel zone yield and column section yield and buckling. Modeling of panel zone in the sample frames of the present thesis (to involve the yield effects of panel zone in the behavior of beam-to-column connection) is further explained in chapters three and four.

2.6 Calibration of Moment-Rotation Model by Experimental Results

The modified Ibarra-Krawinkler model, introduced in the previous part, is calibrated by the experimental results in a study by Lignos [23]. To calibrate the parameters of the moment-rotation model related to steel sections, he employed the experimental results of plastic deformations that occurred at the beam or column section and where the primary modes of deterioration contained local or torsional buckling. In some experimental results on steel section connections, the members have a brittle break (like break of weld) and are not considered in the calibration of the modeling parameters, nonetheless, the brittle break in rotation is remarkably greater than the plastic rotation. Various experimental results on connections of the steel structures have been used for parameter calibration. In general, experimental results in determining the modeling parameters related to sample beams are divided into two categories: reduced beam sections and other-than reduced beam section. However, experimental results of the box sections are used to calibrate the parameters of columns.

Some other-than reduced beam section experiments, used for the examination of beams' modeling parameters, are seen in Table 2.2.

The connection type of each experiment is provided in Table 2.3. In general, the results of 105 tests on the beams with different sections are provided. For box section columns, the results of 71 tests administered on the parameter calibration are used.

Therefore, to prove the validity of the results on structural dynamic analysis obtained by (OPENSEES, 2006) [61] are also used in determining the collapse fragility curve in the following chapters. A sample from Lignos [23] study is compared with the modeling results of a system with one degree of freedom in the same software. To determine the output of this software, this system is modeled as illustrated in Figure 2.12.

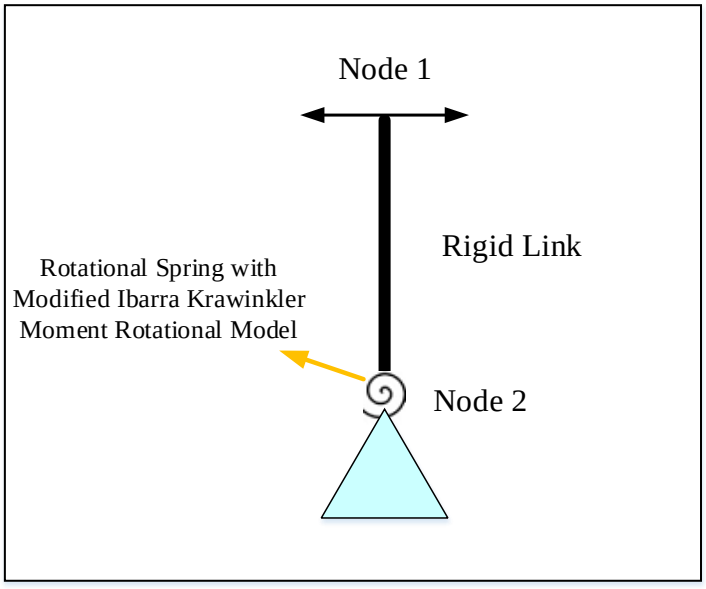

Figure 2.12: SDOF model for validating of the software result

Table 2.2: Some experimental results in beam calibration

Test ID	Reference	Con. Type	Test Conf.	Beam Size
1	Popov, E. P., Stephen, R. M., (1970)	WUF-B	N3SBNS	W24x76
2	Popov, E. P., Stephen, R. M., (1970)	WUF-B	N3SBNS	W18x50
3	Popov, E. P., Stephen, R. M., (1970)	WUF-B	N3SBNS	W24x76
4	Engelhardt, M. D., Sabol, T. A., (1994)	WFP	SSBNS	W36x150
5	Engelhardt, M. D., Sabol, T. A., (1994)	WFP	SSBNS	W36x150
6	Engelhardt, M. D., Sabol, T. A., (1994)	WSEP	SSBNS	W36x150
7	Engelhardt, M. D., Sabol, T. A., (1994)	WSEP	SSBNS	W36x150
8	Engelhardt, M. D., Sabol, T. A., (1994)	WFP	SSBNS	W36x150
9	Engelhardt, M. D., Sabol, T. A., (1994)	WFP	SSBNS	W36x150
10	Engelhardt, M. D., Sabol, T. A., (1994)	WFP	SSBNS	W36x150
11	Engelhardt, M. D., Sabol, T. A., (1994)	WFP	SSBNS	W36x150
12	Engelhardt, M. D., Sabol, T. A., (1994)	WSPFF	SSBNS	W36x150
13	Engelhardt, M. D., Sabol, T. A., (1994)	WSPFF	SSBNS	W36x150
14	Taejin, K., et al. (2000)	WFP	SSBNS	W30x99
15	Taejin, K., et al. (2000)	WFP	SSBNS	W30x99
16	Taejin, K., et al. (2000)	WFP	SSBNS	W30x99
17	Taejin, K., et al. (2000)	WFP	SSBNS	W30x99
18	Taejin, K., et al. (2000)	WFP	SSBNS	W30x99
19	Taejin, K., et al. (2000)	WFP	SSBNS	W30x99
20	Taejin, K., et al. (2000)	WFP	SSBNS	W30x99
21	Taejin, K., et al. (2000)	WFP	SSBNS	W30x99
22	Taejin, K., et al. (2000)	WFP	SSBNS	W30x99
23	Taejin, K., et al. (2000)	WFP	SSBNS	W30x99
24	Seismic Structural Design Associates -2000	SSDA	N3SBNS	W33x141
25	Seismic Structural Design Associates -2001	SSDA	N3SBNS	W27x94

Table 2.3: The various connection types in beam calibration[23]

Connection Type	Notation
Welded unreinforced flanges-Bolted Web	WUF-B
Welded unreinforced flanges-Welded Web	WUF-W
Free Flange	FF
Reduced Beam Section	RBS
Bolted Flange Plate	BFP
Bolted Unstiffened End Plate	BUEP
Bolted Stiffened End Plate	BSEP
Welded Flange Plate	WFP
Welded Flange Plate – Free Flange	WFPFF
Double Split Tee	DST
Slotted Web Connection	SSDA
Bolted Bracket connection	BB
Welded Stiffened End Plate	WSEP
Welded unreinforced flanges-Bolted Web, Welded Plate	WUF-BW
Ribs- Welded unreinforced flanges-Bolted Web	R-WUF-B
Bottom Haunch - Welded unreinforced flanges-Bolted Web	BH-WUF-B
Haunches - Welded unreinforced flanges-Bolted Web	H-WUF-B
Haunches – Bolted flanges-Bolted Web	H-BF-B
Haunches – Bolted flanges-Bolted Web, Bottom	BH-BF-B
Cover and Side Plate	MNH-SMTF
Japanese Welded unreinforced flanges-Welded Web	WUF-W-J
Japanese Welded – Bolted Web	WUF-B-J
Japanese Welded – Bolted Web – Tapered Flange	WUF – B – T - J
Korean – T – Stiffener – Welded	TS – W - K
Extended tee	T1
Extended tee with taper	MT1
Bolted split – tee with shear tab	MDST-ST
Bolted split – tee without shear tab	MDST
Tee-Bolted	TB

The model comprises two nodes (1and 2) connected to each other by a rigid element. Node number 1 is free and number 2 has an articulated support with a spiral spring. The behavior of the modified Ibarra-Krawinkler moment-rotation, discussed above, is applied to the spiral spring. According to this experiment, the history of displacement is applied to node 1. The value of the created moment against the created rotation of the spring illustrates the related moment-rotation behavior of loading. The software outputs are validated by comparing them with the experimental results.

2.6.1 Loading History and Comparison of Experimental and Analytical Results

To prove the validity of the software outputs, an experimental result from Lignos [23] study is studied. The experimental results obtained by Uang et al. [62], are related to experiments on the steel sections under cyclic loading. The obtained parameters in the modified Ibarra-Krawinkler model on the compatibility of the experimental results and the proposed model are shown in Figure 2.13.

The history of cyclic displacement applied to the target sample has been show in Figure 2.14. By applying the time history of cyclic displacement to a single-degree-of-freedom system (SDOF), the moment-rotation diagram is obtained (Figure 2.15).

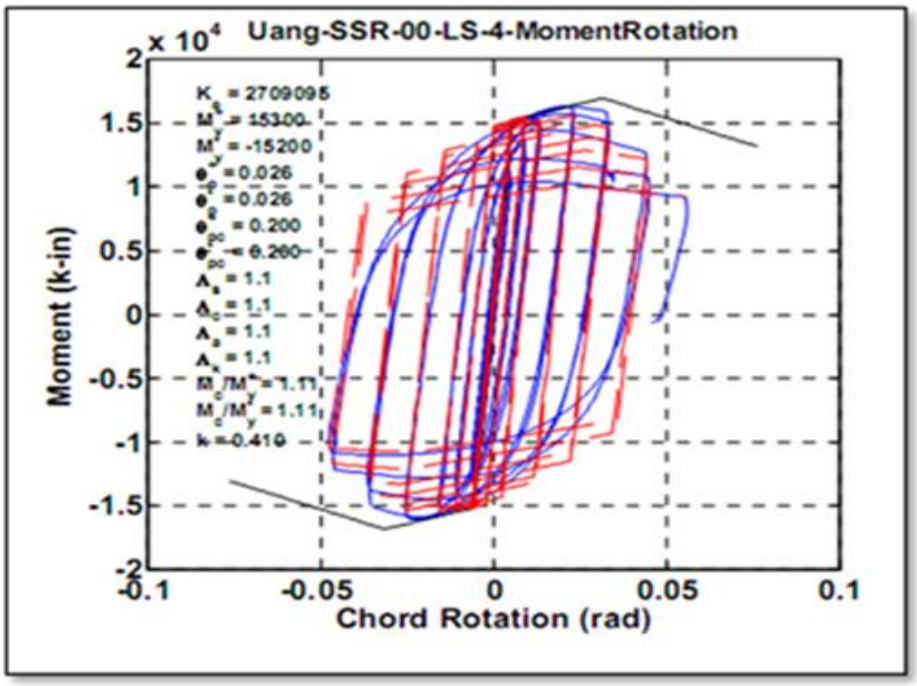

Figure 2.13: Modified Ibarra-Krawinkler model for compatibility of experimental results and the proposed model[23]

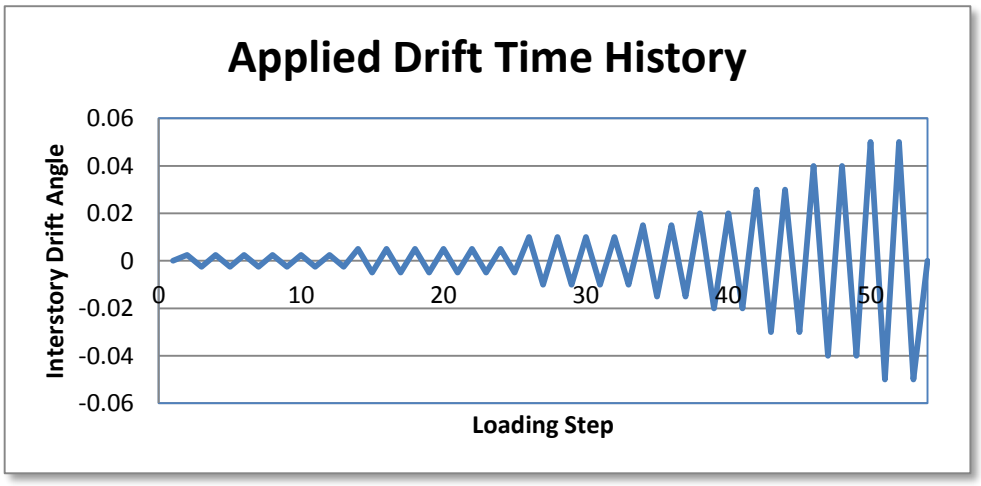

Figure 2.14: The history of cyclic displacement applied the sample structure

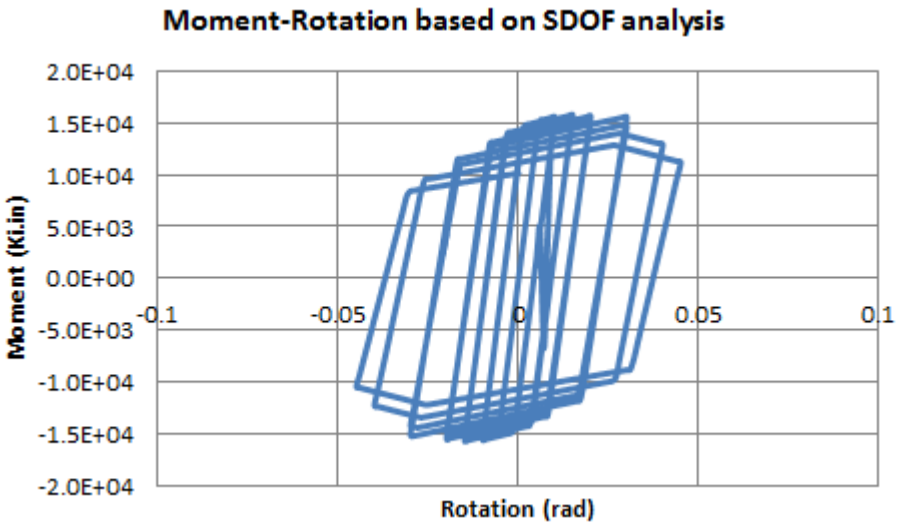

Figure 2.15: Moment-rotation diagram in the proposed method

2.7 Monte Carlo Method

To determine the collapse fragility curve, taking different sources of uncertainty into consideration, the Monte Carlo analysis, based on the response surface surfaces, a trained neural network and a fuzzy inference system is used in different parts of the study. This section describes how to employ the Monte Carlo simulation method according to a study by Liel et al.[22] In this approach, many simulations are generated for input parameters (including parameters of modeling, input layer of neural network and modeling variables and index of structural construction quality). The mean values and standard deviations of the fragility curve can be obtained using different approaches (response surface, neural or fuzzy inference network). According to the obtained mean and standard deviation values, the number of collapse fragility curves equal to the number of simulations. Each curve, then, indicates the collapse probability based on the applied intensity measure. The final fragility curve is gained using many collapse fragility curves. Nevertheless, the aleatory and epistemic uncertainties should

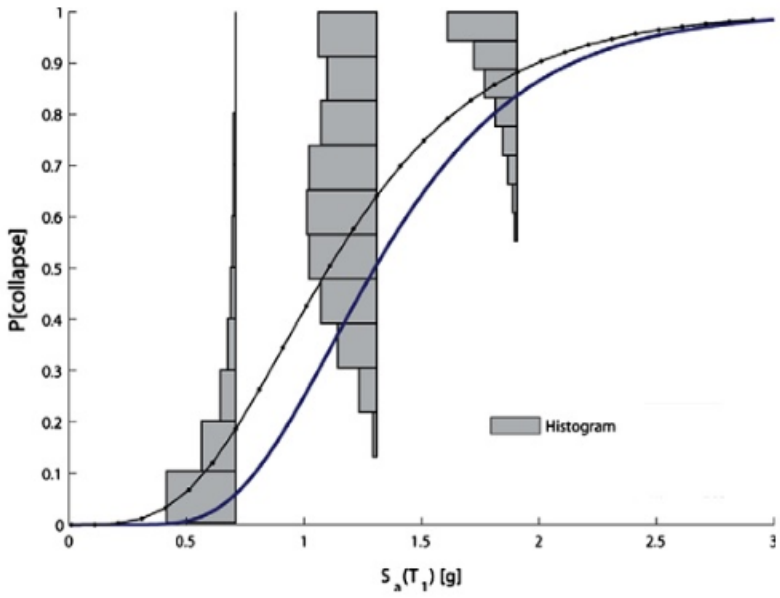

Figure 2.16: Collapse fragility curve obtained by the Monte Carlo simulation approach[22]

have been involved in the final probability distribution. For this reason, it is assumed that the final collapse probability in each interval equals to the expected value of the obtained probabilities form each collapse fragility curve. As an example, shown in Figure 2.16 are the results for the probability of collapse as S_a (T_1) = 1.91 g for all the 10,000 Monte Carlo realizations. The frequency of confidence intervals with different amplitudes is obtained and is shown in Figure 2.16.

The value of the expected probability for each amplitude indicates the probability of the final fragility curve. The values of the final probabilities for 1.91g are achieved 0.8, and are shown in Figure 2.16.

2.8 Appropriate Strong Ground Motions for Collapse Determination

Earthquake accelerographs are used for structural dynamic analysis against earthquakes in the IDA approach which leads to the intensity measure-engineering demand curves. Selected accelerographs should be then representative of the seismicity of that region in which the structure is located. Current studies on the

selection criteria of earthquake records are based on the earthquake magnitude (M) and distance of record place from the source of the earthquake (R). Other researchers have also introduced several approaches of the involvement of epsilon (ε) [16]. An important issue in the selection of strong ground motions is the involvement or elimination of particular effects like near-field effects, the soil type, etc. in the selected records. Due to the hammer effects present at their beginning, near-field records impose a huge input energy to the structure during their short time. Therefore, the first mode spectral acceleration (S_a (T_1)) is used as the measure for intensity for such records are not suitable (because they do not completely represent the record characteristics). Near-field records are defined with such parameters as pulse shape, period and amplitude. The findings of the study by Tothong [15] indicate that non-linear spectral displacement is a better parameter to be used as IM in near-field records.

2.9 Sensitivity of Collapse Fragility Curve to Modeling Parameters

Many studies have measured the sensitivity of collapse fragility curves for modeling parameters in steel moment resistant structures [22]. Considering the modeling parameters as the moment-rotation curves of the target springs in the Ibarra-Krawinkler model, θ_p, θ_{PC} and Λ are said to be the most important parameters related with the ductility capacity and stiffness and strength deterioration in the former studies [81]. In the following chapters (3 and 4), they are also considered as the modeling parameters with the uncertainty of which they should be involved in the collapse fragility curve. The considered parameters in chapter (3and 4) include the column ductility variables (θ_p, θ_{PC} and Λ for columns), beam ductility (θ_p, θ_{PC} and Λ for beams), column strength (M_c/M_y for columns) and beam strength (M_c/M_y for beams).

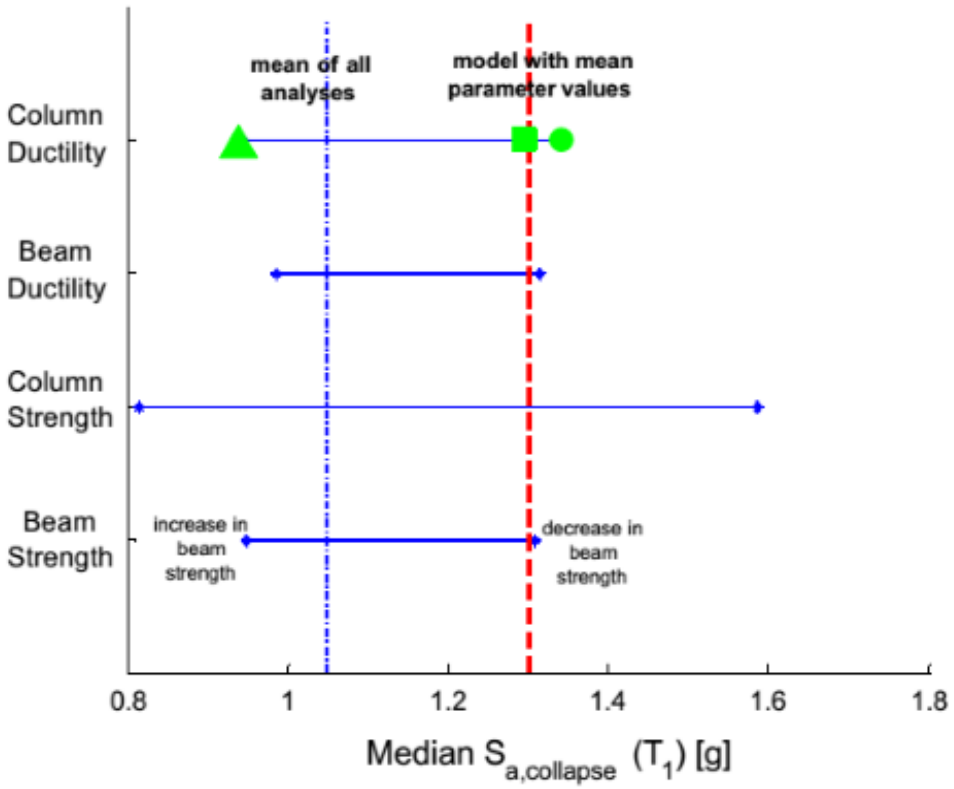

Figure 2.17: The result of sensitivity analysis for four meta variable [22]

Similar to the study of Liel et al.,[22] the construction quality parameter and its related uncertainty is used in chapter 5. For instance, the sensitivity of the collapse fragility curve parameters in the sample structure introduced to prove the efficiency of the proposed method is shown in this section. Figure 2.17 illustrates the median collapse capacity which is affected by changing the values of the modeling parameters (CD, BD, BS and CS). The effect of the epistemic uncertainty is considered as the mean of all analysis in this figure. The result of the sensitivity analysis for four meta variables are shown in Figure 2.17.[22]

2.10 Summary

This chapter seeks to define and further explain the analytical methods whilst determining the collapse fragility curve. Moreover, different uncertainty sources, their

determination and combination methods are described in this chapter. Statistical methods are used to show the effects of modeling uncertainties in a structure's collapse fragility curves and this requires access to the probability distributions of the modeling parameters. These probability distributions are determined by experimental results accompanied by an extended dispersion. The consecutive chapter investigates the application of the cuckoo, k-means algorithms and the fuzzy inference system approach to display the modeling and cognitive uncertainties in a structure's collapse fragility curve, fuzzy- PSO as a substitute for the response surface involving the epistemic uncertainties of the descriptive parameters. The efficiency of the proposed approaches in determining the collapse fragility curve of steel moment resistant structure is henceforth studied. Finally, the modified Ibarra-Krawinkler moment-rotation model is presented and the software outputs are validated by using the experimental models and results. The present chapter further quests to explain the Monte Carlo simulation approach used in all of the chapters for the determination of the collapse fragility curve.

Chapter 3

THE EFFECT OF COGNITIVE UNCERTAINTY

3.1 Introduction

Collapse is one of the main reasons for losses of life and property during earthquakes. Earthquake causes serious damages by both destroying buildings and rendering them unsafe and unusable [63]. Quantifying earthquake damage has become a major debate and a serious topic for research. Mainly structures may collapse in two ways. The first one is sideway collapse, which results in the loss of lateral stability of structures. Sideway collapse is itself the result of incremental and consecutive loss of the capacity of the elements which contribute to load-resisting system and used as a limit state to collapse in this paper. In contrast, vertical collapse is the result of direct loss of the components which constitute gravitational stability of the structure [64]. Structural uncertainties mainly include the uncertainties associated with the earthquake (record to record uncertainty), those associated with the model (modelling uncertainty) and those associated with the material quality (cognitive uncertainty). The first one stems from the random nature of seismic activity and lack of knowledge about deep geological causes. The second is part and parcel of modelling itself; and we can never deny the discrepancies which would exist between a model and the actual data collected on a phenomenon [22]. The third source of uncertainty is also of prime importance especially in countries where supervision is less rigorous. For the seismic assessment of structure, there are two relations: The first one is between intensity measure (IM) and collapse fragility probability and the second one is between hazard

curve and IM. Both performance criteria and methods for estimating them are discussed in this thesis. [64]. Effects of each of particular parameters e.g., material quality [65], irregular story [43], and building height [66] have been considered to achieve fragility curves by many researchers. Rajeev and Tesfamariam [45] have considered interactions among the parameters such as irregularities (weak story, irregular story, vertical discontinuities etc.,) and material quality to develop fragility curves. Liel *et al*. [64] has presented the effect of modelling uncertainty in collapse limit state in comparison with other limit state such as immediate occupancy and life safety in fragility curves. Zareian and Krawinkler [22] incorporated record to record (RTR) variability and modelling uncertainties through the IDA on deriving the fragility curves. Fuzzy logic is used for risk analysis, safety evaluation and structural analysis to consider the impact of modelling uncertainty [45, 46]. The study involves the effect of cognitive uncertainty in material quality compared to the modelling uncertainty in developing fragility curves for sideway collapse limit state of structures by using Cuckoo algorithm and Takagi-Sugeno-Kang (TSK) model. IDA is applied to consider RTR uncertainty while applied set of 40 strong ground motion that selected by k-means algorithm, which is expected to reduce the computation run time taken for proper selection of ground motion.

At the structural level, four meta variables namely Beam Strength (BS), Column Strength (CS), Beam Ductility (BD) and Column Ductility (CD) are considered for defining modelling uncertainty. Both RTR and modelling uncertainties are incorporated through Response Surface Method (RSM). Analytical equations of RSM

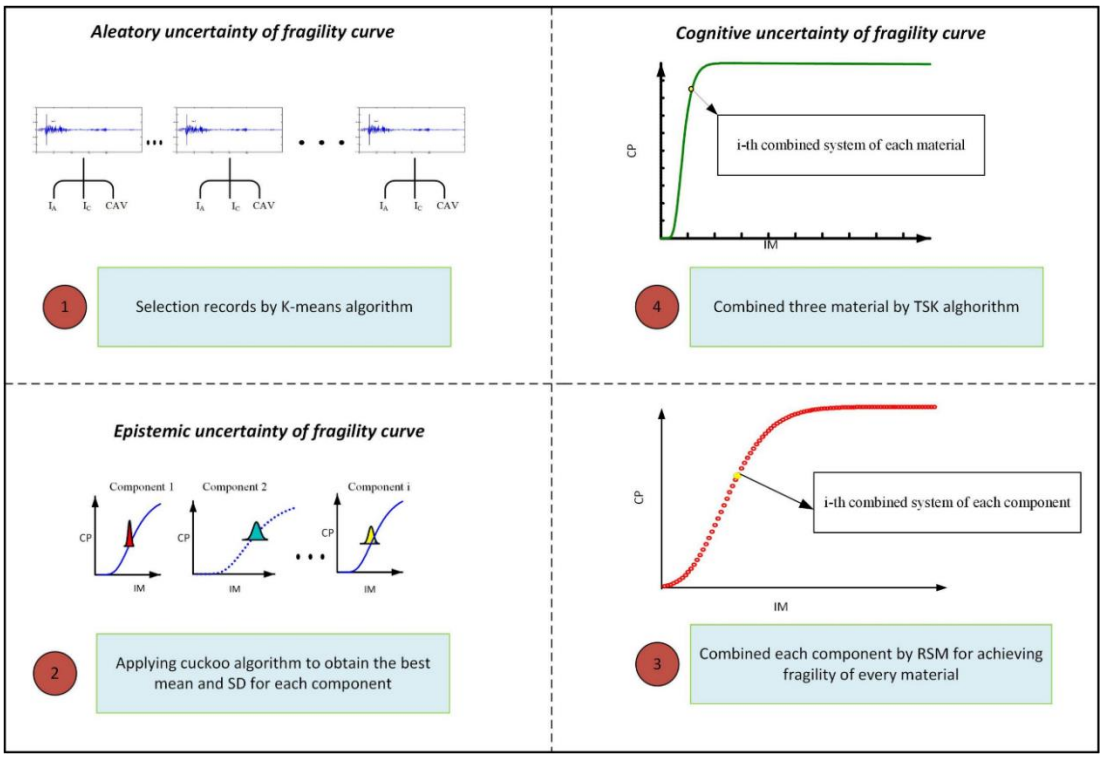

Figure 3.1: Uncertainty analysis of the system fragility curve by RSM and TSK method

are obtained through IDA results by Cuckoo algorithm, which predict mean and SD of collapse fragility curve. Three levels of Material Quality (MQ) are used to consider the effect of cognitive uncertainty. TSK model [67] is applied to predict the effect of material quality by response surface coefficient. Finally collapse fragility curve with various source of uncertainty are derived through large number of MQ values and meta variable inferred by TSK system based on RSM coefficients. To justify efficiency of the assumed method, the methodology is applied and demonstrated on five and ten story moment resistant frames as case study. Figure 3.1 demonstrates the uncertainties considered in this study. It is expected that the methodology adopted to consider the effect of different uncertainties, especially the cognitive uncertainty, will enhance the seismic performance assessment of large building stock in the regions with lack of quality control in materials.

3.2 Combination of Sources of Uncertainties

Main step in predicting the effect of modelling uncertainty is how to combine various uncertainty such as RTR with modelling uncertainties. In this target, RTR, modelling and cognitive are considered as various uncertainty [27]. Three common methods to incorporate effects of RTR and modelling uncertainties are confidence interval, mean estimate and Monte Carlo simulation approach [32, 33]. In mean estimate method, it is considered that mean value of fragility curves is remained and variance affecting modelling uncertainties is changed; on the other hand, confidence interval approach considers the variance of fragility curve unchanged.

Results obtained from this method are not sensitive to classes of uncertainties and in fact such classes are not evident from the results. Monte Carlo method implements thousands of simulations for modelling parameter values based on their probabilistic distributions and then sample is analyzed based on simulated values as modelling parameters of the structure. Thousands of the probability of collapse versus intensity measure values presented as collapse fragility curves including effects of modelling uncertainties resulted from this accurate analyses [22]. In recent studies [68], a new approach to consider modelling uncertainty achieved by combining the Monte Carlo method with the RSM, So Monte Carlo simulation approach requires a large number of simulations in order to incorporate various uncertainties, RSM in combination with Monte Carlo simulation is used for seismic vulnerability assessment in horizontally curved steel bridges [69], concrete building structures by Liel et al. [22] and Franchin et al. [70] and steel framed structure [71]. Also, RSM has been applied in previous relevant literature to derive the fragility curves [45, 72, 73]. At first, a sensitivity analysis is conducted to determine which modelling parameter contributes the most to

the mean and standard deviation (SD) of the fragility curve. Then, regression analysis is used to compile the fragility curve based on an analysis of sensitivity. To this end, the second order polynomial function given in equation (3-1) is used for the estimation of the mean and SD (using Monte Carlo method) for different scenarios of modelling uncertainty. Results obtained from employing the Monte Carlo method conform to estimations obtained from a variety of models [68].

$$y = \beta_0 + \sum_{i=1}^{k} \beta_i x_i + \sum_{i=1}^{k} \beta_i {x_i}^2 + \sum_{i=1}^{k-1} \sum_{j>i}^{k} \beta_{ij} x_i x_j \qquad (3\text{-}1)$$

3.3 Record to Record (Aleatory) Uncertainty

For the full definition of the strong ground motions, a lot of data are needed since the phenomena are relatively complicated. IM is the definition of a number of ground motion variables which simplifies the definition of an earthquake and at the same time connects the seismic hazard with the structural damage. The most important properties of a ground motion are the Arias Intensity (I_A) which reflects the amplitude, Characteristic Intensity (I_C) shows the frequency content and Cumulative Absolute Velocity (*CAV*) can represent the damage of building well by calculating duration of records. Arias Intensity (I_A) is described as given by equation (3-2):

$$I_A = \frac{\pi}{2g} \int_0^{\infty} [a(t)^2] dt \qquad (3\text{-}2)$$

Where *a(t)* is the acceleration intensity and the unit of (I_A) is meter per second. The infinity symbol in the equation of I_A is calculated based on whole duration not T_d (duration of the record).

Characteristic intensity (I_C) is described as:

$$I_C = \alpha_{rms}^{1.5} T_d^{0.5}, \qquad \propto_{rms} = \frac{1}{t_d}\int_0^{t_d}[a(t)^2]\,dt \tag{3-3}$$

Cumulative Absolute Velocity (*CAV*) is continuous accumulation of the acceleration during the earthquake and it is calculated by the following equation (3-4)

$$CAV = \int_0^{T_d} |a(t)|dt| \tag{3-4}$$

CAV is the best value to show structural damage for various earthquake disasters [74]. RTR uncertainty is considered through the IDA approach. Selecting the ground motion is the main step in applying IDA method for considering the effects of RTR uncertainty. In this paper, K-means algorithm is used to decrease the dispersion of uncertainty and proper selection of ground motion. At the beginning of the proposed method, 100 records (Appendix B) of natural earthquake are selected by site specification according to following properties:

- The ground motion records in an area with longitude 115° to 124° and latitude 32°–41°;
- Moment magnitude (M_w) is considered to be greater than 5;
- The minimum value for epicental distance (R) is set to150 km.

It has been introduced that Arias Intensity, Characteristic Intensity, and Cumulative Absolute are the main characteristics of each record such that effect of earthquakes are highly dependent on these characteristics. On the other hand, this first filtration for selecting ground motion data may not be convenient for analysis. In other words, it is not cost effective to use 100 data. However, random selection of data from the group

may cause dispersion of results. Therefore K-means approach is adapted for proper choice of earthquake records after the first elimination.

3.3.1 Lloyd's algorithm (K-means algorithm)

Proper selection of earthquake records may be performed through different steps such as classification and clustering. There are differences in classification and clustering. Classification is supervised learning algorithm, but clustering is unsupervised. Clustering doesn't need training data, however, the classification is created by training data. In general, the classification is applied to assign defined tag to sample on the basic features and clustering is used to categorize similar samples on the basic features and does not assign to every group. To solve clustering problem, Lloyd's algorithm [66] is one of the unsupervised algorithms. At the beginning of the analysis, the number of clusters k and the centroid of center (COC) of these clusters are determined. Any sample can be taken randomly or the first k samples in sequence as the initial centroids. The sequences of applying Lloyd's algorithm are below:

- Decide the centroid point
- Decide the distance of each sample to the centroid (see equation (3-5))
- Categorize the sample based on optimum distance

$$D = \sum_{j=1}^{k} \sum_{i=1}^{n} \left\| x_i^j - c_j \right\|^2 \qquad (3\text{-}5)$$

Where $\left\| x_i^j - c_j \right\|$ is a selected distance value between a data sample x_i^j and the cluster center c_j, is an index of the distance of n data samples from their relative cluster centers [66]. Finally, this algorithm aims at minimizing an objective function, in this case a squared error function. The objective function is shown in equation (3-5). Although it can be proved that the procedure will always terminate, the k-means algorithm does

not necessarily find the most optimal configuration, corresponding to the global objective function minimum.

3.4 Modelling Uncertainty (Epistemic Uncertainty)

In the IM-based (vertical statistics format) approach [38] the seismic fragility curves are shown as:

$$P(Collapse|IM = im_i) = P\left(im_i > IM_{collapse}\right) \quad (3\text{-}6)$$

According to [75], it is presumed that two-value (mean-η and log-SD-β) lognormal distribution functions could define the fragility curves F_R and the maximum likelihood approach estimates the two parameters. The likelihood function for the present goal is defined as follows:

$$L(\eta_1, \eta_2, \dots, \eta_n, \beta_1, \beta_2, \dots, \beta_n) = \prod_{i=1}^{N} F_R(S_{A,i}, y_k) \quad (3\text{-}7)$$

While F_R shows the seismic fragility curve for collapse limit state, $S_{A,i}$ is intensity measure value to which *i-th* scenario of the sample is considered, N is the number of sample scenario is subjected. Therefore, F_R gets the following form:

$$F_R = \Phi\left[\frac{Ln(im_i/\mu_{ln(im_c)})}{\beta_{ln(im_c)}}\right] \quad (3\text{-}8)$$

In equation (3-8), μ is the mean and β is SD of collapse probability function and Φ is the standardized normal distribution function. It is clear that both mean and SD values of collapse fragility curve are affected if modelling uncertainty is involved. The modelling uncertainty is considered ±1.7 β away from the mean and ±1 β with

correlation of each meta variables that BD, BS, CS and CD is defined as meta variables in this thesis. This meta variable and combination as modelling uncertainty is explained in application. The two parameters μ and β are evaluated by maximizing Ln (L) through performing an optimization algorithm. In this study, a Cuckoo optimization algorithm is used to predict the mean and standard deviation of fragility curve.

3.4.1 Cuckoo optimization algorithm

The optimization algorithm applied for solving 2n value (η, β) problem max Ln (L) is the Cuckoo Optimization (CO) algorithm because it is obvious that the number of variable of CO is less than GA (Genetic Algorithm), PSO (particle swarm optimization) and it is more common to adopt to a larger optimization problems. CO algorithm is supervised algorithm and used as unconstrained form in this thesis. The procedure of CO algorithm is a population-based method. Starting the optimization algorithm, the matrix of $N_p \times N_{var}$ as candidate habitat is created to show the maximum number of cuckoos. Laying eggs from their habitats in a maximum distance is another habitat of real cuckoo. Egg Laying Radius (ELR) is computed based on the following equation (3-9) which represents maximum limit [76].

$$ELR = \omega \times \frac{Number\ of\ current\ cuckoo's\ eggs}{Total\ number\ of\ egges} \times (par_h - par_l) \qquad (3\text{-}9)$$

Where ω is an integer parameter, defined to apply the maximum value egg laying radius, par_h and par_l are the maximum and the minimum range of parameters, respectively. Each cuckoo starts egg laying in the bird's nests randomly. After the procedure of egg laying, S% (usually 10-15%) of all eggs, with low benefit values, will be detected and destroyed. It is very amazing that only one egg can live in each

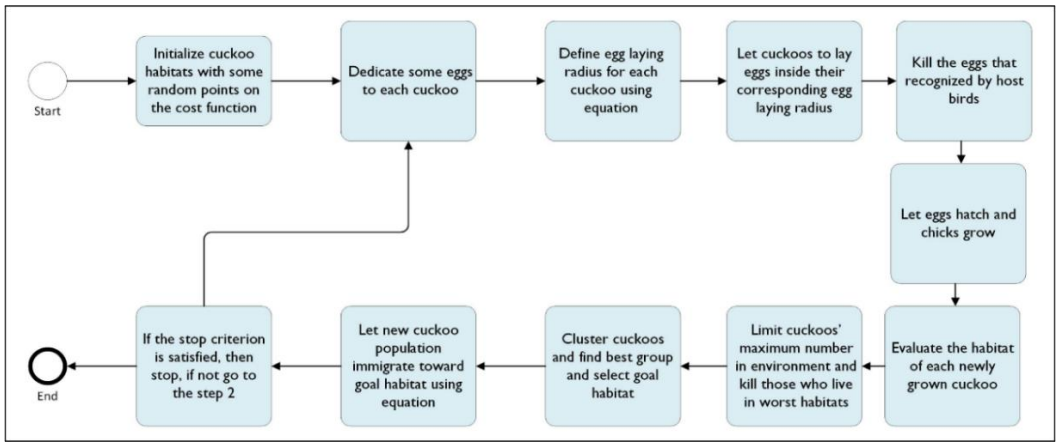

Figure 3.2: The pseudo code representation of Cuckoo algorithm

nest. When cuckoo grow, they begin living in their own community. In the period of egg laying, the young cuckoo immigrate to new area, while eggs are similar to host birds. The society with high benefit value is chosen as the target point for other cuckoo to immigrate after the cuckoo groups are formed in various environment. The procedure of new egg lying is defined by equation (3-10) [77].

$$X_{NextHabitat} = X_{currentHabitat} + F(X_{GoalPoint} - X_{currentHabitat}) \quad (3\text{-}10)$$

Here, *X* and *F* are the position and the motion coefficient, respectively. Figure 3.2 depicts the pseudo code of CO algorithm.

3.5 Theory of Inference in a Fuzzy Expert System (Cognitive Uncertainty)

Lotfi Zadeh [67] created fuzzy logic to present a way to map qualitative knowledge into exact reasoning. A fuzzy inference system is an expert knowledge-based (KB)

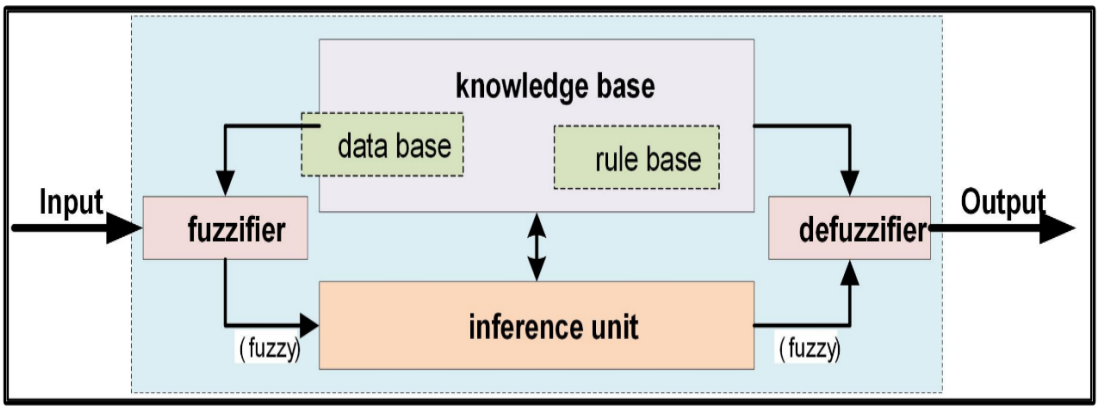

Figure 3.3: Fuzzy expert systems perform fuzzy reasoning

system which contains the fuzzy algorithm in a simple rule base. In this system, the knowledge which is encoded in the rule base, is emanated from human experience and intuition and the rules show the relationships between the inputs and outputs of a system. Numerical value of a linguistic variable (i.e. MQ in this study) could be presented by a fuzzy number. FIS (Fuzzy Inference System) consists of four parts: fuzzifier, inference engine, KB, and defuzzification of results (Figure 3.3) that means the conversion of real numbers of input into fuzzy sets. The knowledge base consists of a database and a rule base. Database includes membership functions of the fuzzy sets, while the rule base includes a set of linguistic statements in the form of IF-THEN rules that connected by AND operator (other operators such as OR, and NOT may be used). The inference engine which forms the core of a fuzzy inference system uses IF-THEN rules contained in the rule base to find out the output through fuzzy or approximate reasoning. The approximate reasoning process is to create conclusion from a set of IF-THEN rule in Sugeno type (also known as the TSK model) of FIS is written as follows:

$$Ri: \quad IF\ x\ is\ A \quad AND \quad y\ is\ B \ldots \quad THEN \quad z=ax+by+c \quad i=1, 2, \ldots, N$$

In which, rule number is shown by R_i, x and y is the parameter and A is the fuzzy set based on x,y. values a and b are constants and N is the number of rules [78]. The centre of area is the most popular defuzzification approach in Mamdani-type FIS. In Sugeno-type FIS, the final output is measured by the weighted average of all outputs (shown by equation (3-11)).

$$t = \frac{\sum_{i=1}^{N} w_i z_i}{\sum_{i=1}^{N} w_i} \tag{3-11}$$

$$w_i = \min(f_1(x_i), f_1(y_i), \dots) \qquad i = 1,2, \dots, N \tag{3-12}$$

In which, w_i is the firing strength of rule i and is described by equation (3-12) and $f_1(x)$ are $f_1(y)$ membership functions of variable x and y, respectively. Since the target of FIS in this work is to predict coefficients of response surfaces that are numerical variables, Sugeno inference system is used.

3.6 Consideration of Various Uncertainties on Sample Study Structures

3.6.1 Design of Structure

To assess the effect of cognitive uncertainty of intermediate moment steel buildings, one 5 story structure and a 10 story structure have been assumed situated in a very high seismic hazard environment.

It is further assumed that the soil on which these structures are situated is of type 2 soil (shear wave velocity between 360 to 750 m⁄s) [79]. The structures have regular plans (Figure 3.4) with three 5 meter bays on each side and 3.2 meter floor height (Figure 3.5). Floors are assumed to be rigid diaphragms with dead load distributions

similar to what we normally see in structures in Iran and in according to Iranian Seismic Code [79], the values of response modification factor (i.e. R) is considered 7 for the sample structures.

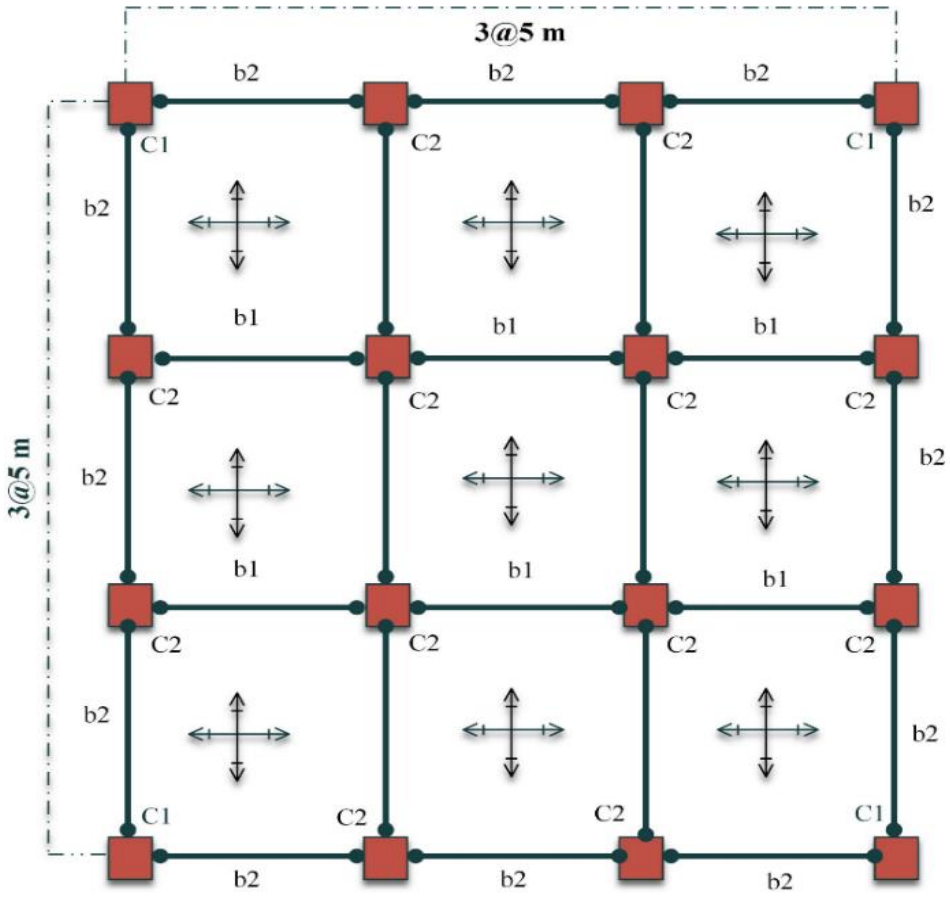

Figure 3.4: The Plan of sample structures

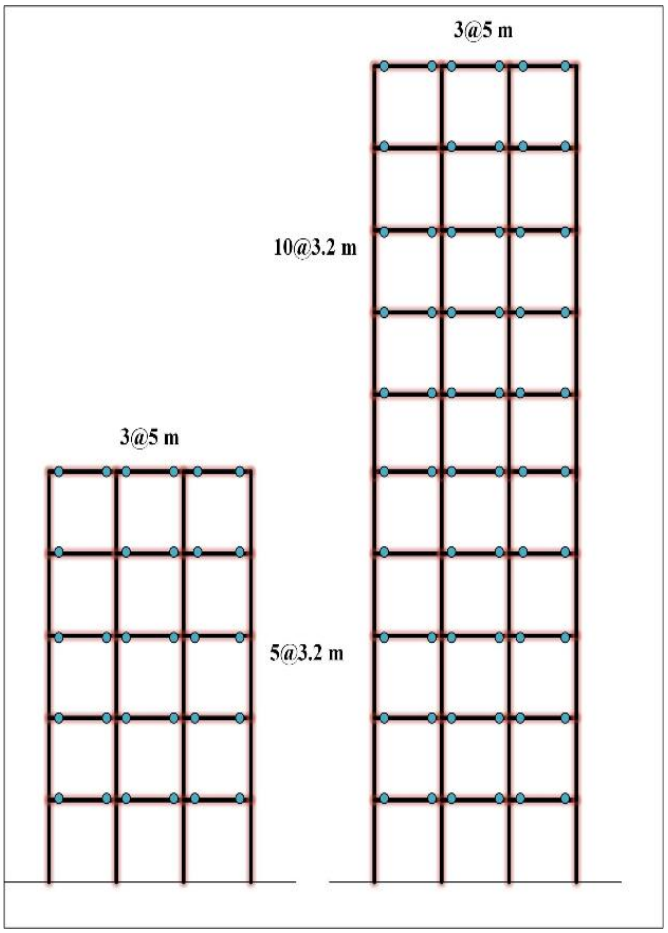

Figure 3.5: Elevations view of samples

Table 3.1: The design properties for 5 and 10 story buildings.

	Story	C_1	C_2	b_1	b_2
5-STORY	1,2	TUBO 180×180×20	TUBO 300×300×20	IPE 450	IPE 330
	3,4,5	TUBO 160×160×20	TUBO 200×200×20	IPE 400	IPE 300
10-STORY	1,2	TUBO 240×240×20	TUBO 400×400×20	IPE 500	IPE 400
	3,4,5,6	TUBO 220×220×20	TUBO 340×340×20	IPE 500	IPE 400
	7,8,9,10	TUBO 180×180×15	TUBO 280×280×20	IPE 400	IPE 360

The nominal yield strength of steel is 240 MPa. Table 3.1 shows cross sections for all members. Numerical modelling of the sample interior frame of a set of identical frames is implemented applying openSEES (2006) finite element program. To consider modelling uncertainty, nonlinear springs of Ibara-Krawinkler [22] model have been

assumed. Lumped plastic hinges of columns, beams and panel zones are incorporated in the model for the same purpose [22]. The backbone curve of considered moment-rotation model is represented in Figure 3.6. The backbone curve is defined by following variables: yield strength (M_y), the post yield strength (M_c), plastic rotation capacity (θ_p), post-capping plastic rotation (θ_{pc}), ultimate rotation capacity (θ_u) and cyclic deterioration (λ). (θ_p), (θ_{pc}) and (λ) are considered as the ductility variables.

The hysteretic behavior of the connection is described based on deterioration rules that are defined according to hysteretic energy dissipated in each hysteretic cycle. The deterioration of basic strength, post capping strength, unloading stiffness and reloading stiffness could be noticed in this model [22]. Capacity of energy dissipation of the component, by which deterioration rules are formulated, is described as equation (3-13).

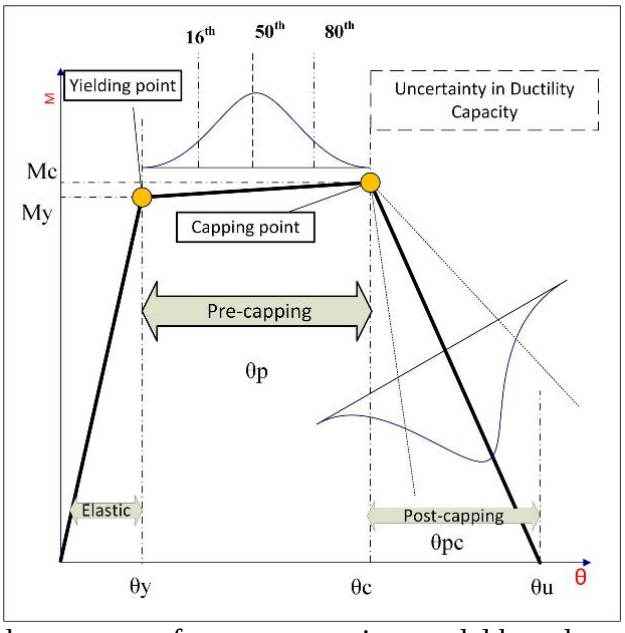

Figure 3.6: Backbone curve of moment rotation model based on modified Ibarra-Medina-Krawinkler

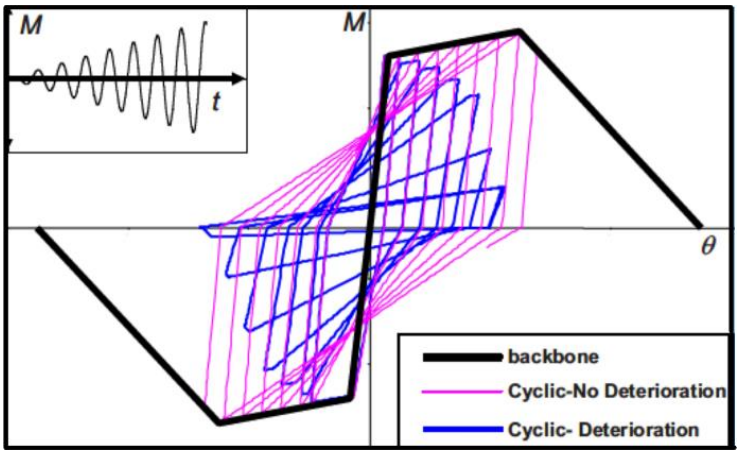

Figure 3.7: Effects of cyclic deterioration modelling on M-θ backbone curves[23]

$$E_t = \lambda \times M_y \tag{3-13}$$

λ is the rate of cyclic deterioration and is considered according to calibration of experimental outcomes. The deterioration of basic strength, post capping strength, unloading stiffness and reloading stiffness can be noticed in this model. Comparison of considering and neglecting cyclic deterioration of component behaviour is represented in Figure 3.7. The ratio of (M_c/M_y) is assumed as the strength variable.

Table 3.2: The modelling parameters for beam and column for uncertainty analysis

Component	Random variable	Mean	Standard deviation
Beam	θ_p	0.025	0.43
	θ_{pc}	0.16	0.41
	λ	1.00	0.43
	M_c/M_y	1.11	0.05
Column	θ_p	0.011	0.57
	θ_{pc}	0.07	0.92
	λ	0.4	0.96
	M_c/M_y	1.11	0.05

These variable distributions are lognormal (SD and means) which are summarized in Table 3.2[23]. No uncertainties are assumed for the panel zones because the structures are based on the new guidelines which assume that rupture first occurs in the beams and not in the joints. The suggested method is used to an interior frame. M2-WO panel zone model is noticed while yielding in the beams, columns and panel zones is shown well by this model that is presented in Figure 3.8[80].

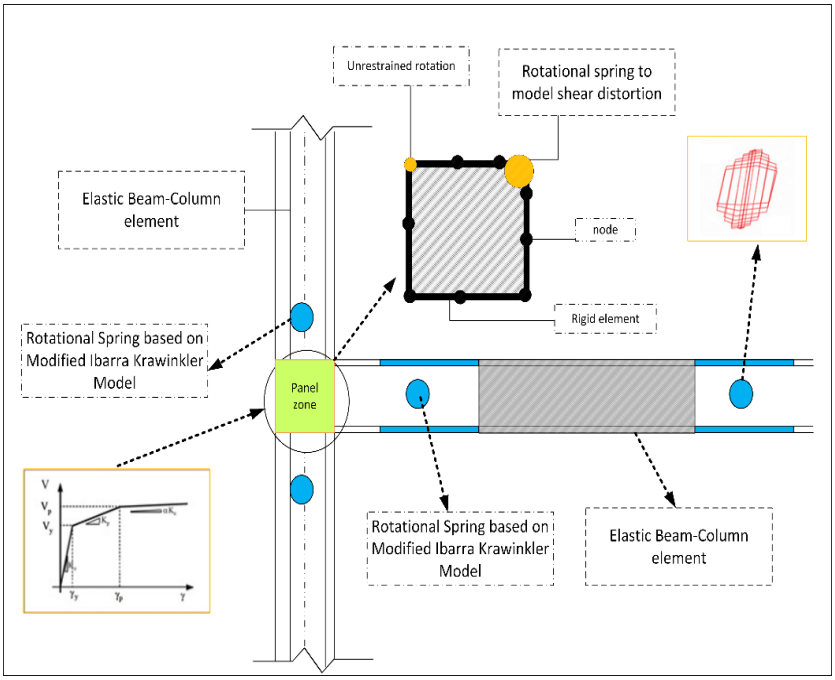

Figure 3.8: M2-WO panel zone

Four meta random variables are assumed on the beam strength (BS) (i.e. Mc/My for beams), column strength (CS) (i.e. Mc/My for columns), beam ductility (BD), (i.e. θ_p,θ_{pc} and λ for beams) and column ductility (CD) (i.e. θ_p,θ_{pc} and λ for columns) which represent strength and ductility for each element [22].

3.6.2 Numerical Tests

In the first mode, acceleration is assumed to be a measure of the intensity (S_a (T_1)). This IM is used in different research and is represented to accomplish sufficiency and efficiency criteria in the prediction of structural damage, which is the main target in this work. Intersory drift ratio is selected as engineering demand variable since it shows global behavior of the structure, which has a good correlation with global collapse. Mean and (SD) of modelling variables are affected by the quality of material. Low material quality leads to lower mean value and higher dispersion [81]. Three levels of material quality (good-average-low) are considered. Experimental values (Mean and SD) are unchanged for good MQ. The mean value is decreased 25% and 40% for average MQ and Low MQ, SD is increased 25% and 40% for average and low MQ with respect to their values for good MQ. This pattern was used in previous investigations [45]. Considering the above explanation, we have four main meta variables [82] and 33 combinations of these meta variables (hence 33 scenarios) are used for the sensitivity analysis and IDA. Eight of these scenarios correspond to only one variable and the other 25 scenarios correspond to interaction of variables taken two at a time. In the eight scenarios where one main meta variable is counted in the model, its value is set at ±1.7 times the SD from the mean. In the other scenarios, the value of each main meta variable is set at ±1 SD from the mean. In general, (33×3×2) IDA analyses have been conducted on the 40 selected records that selected by K-means approach. Hunt&fill tracing algorithm [83] is applied to scale records in IDA analysis to achieve good performance. In K-means approach, first the COC is calculated in four clusters and then each cluster is defined based on records occur near the COC based on the similarity of three parameters of earthquake records. Finally, 10 records are selected from each cluster randomly. This method decreases desperation of samples.

Figure 3.9 shows the position of each sample for every cluster in 3 dimension view which is represented in Table 3.3. Figure 3.10 (a) shows the validation of the proposed method. If we accept fragility curves based on 100 records as accurate one, it is clear that proposed method is very close to the accurate one rather than worst condition selection. In the worst condition case, all records are selected in the first cluster randomly. Moreover Figure 3.10 (b) shows reason of using 40 records to consider the aletaory uncertainty. It has been resulted that the fragility curve based on 40 records is suitable for both accuracy and computational run time compared with the others. Figure 3.11 shows IDA curves for different quality levels of building material for sample structure. The effect of the quality of building material on fragility is pretty obvious.

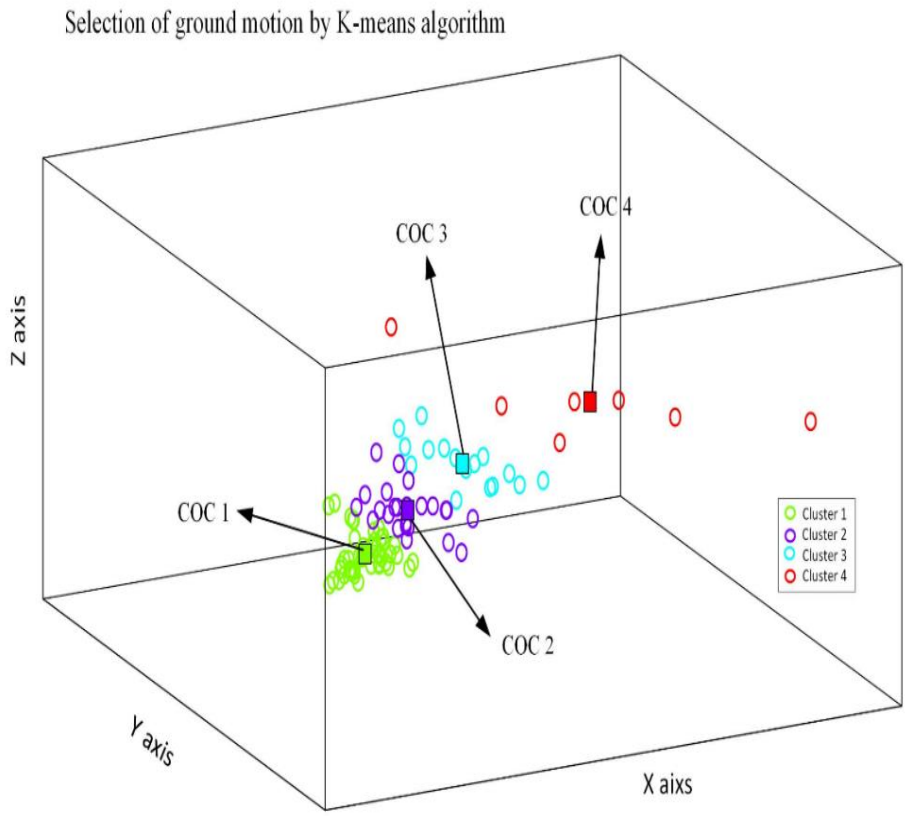

Figure 3.9: K-means sampling in the three-dimensional space

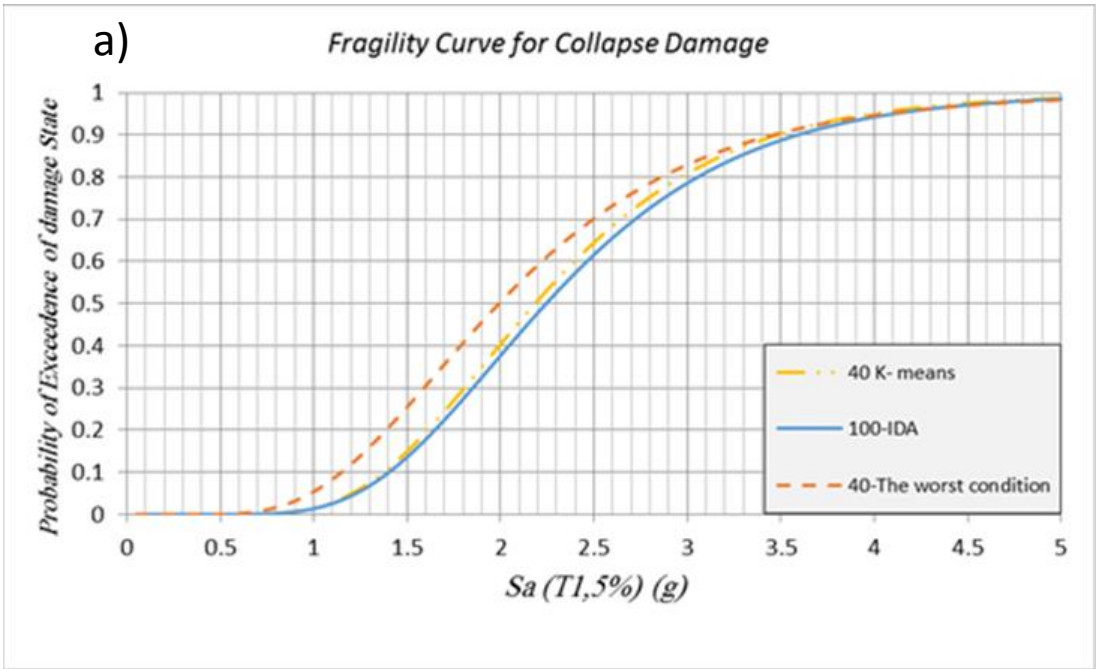

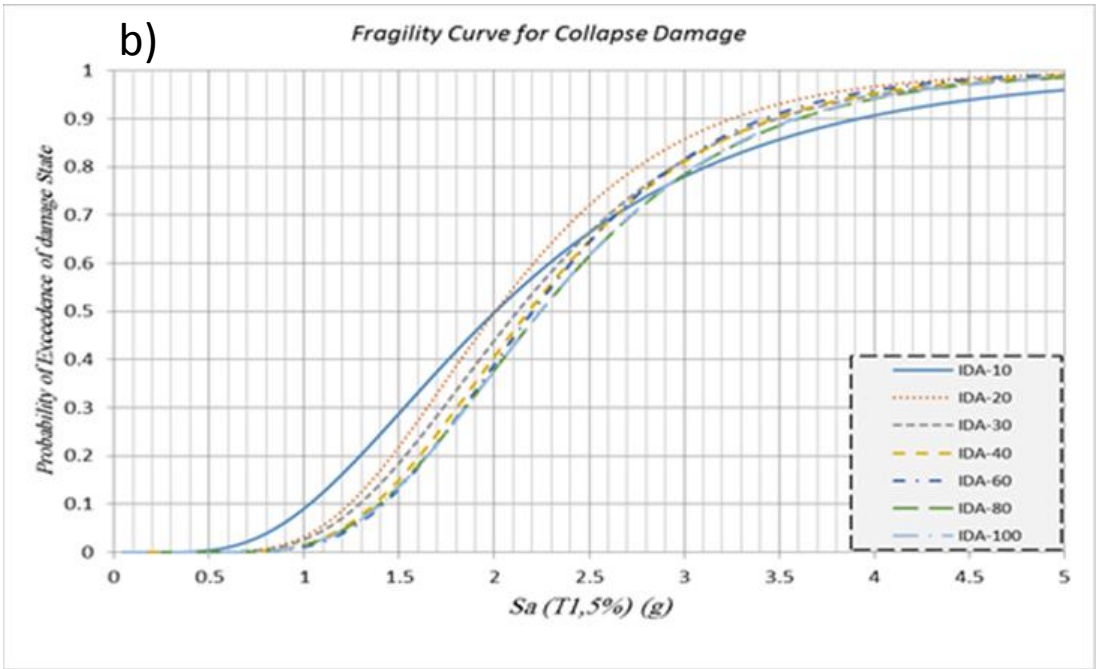

Figure 3.10: (a) The validation of selection of the ground motion based on the K-means, (b) fragility curve based on the various number of records

Table 3.3: The suit of 40 ground motion records

Record No	Year	Earthquake	M_W	Mech.[1]	Station	GM Characteristics	Dist.[2] (km)	PGA (g)	Arias Intensity (m/sec)	Characteristic Intensity (Ic)	Cumulative Absolute Velocity
1	1994	Northridge	6.7	RN	Leona Valley #2	Far-Fault	37.2	0.063	0.06252	0.00676	216.82
2	1994	Northridge	6.7	RN	Lake Hughes #1	Far-Fault	89.67	0.077	0.10962	0.0103	301.778
3	1994	Northridge	6.7	RN	LA, Hollywood Stor FF	Far-Fault	114.62	0.358	2.00474	0.08616	1185.35
4	1994	Northridge	6.7	RN	LA, Centinela St.	Far-Fault	31.53	0.322	0.99385	0.0547	799.35
5	1989	Loma Prieta	6.9	RO	WAHO	Far-Fault	17.50	0.672	6.27237	0.22791	2025.38
6	1989	Loma Prieta	6.9	RO	Halls Valley	Far-Fault	30.50	0.102	0.24847	0.018	467.845
7	1989	Loma Prieta	6.9	RO	Agnews State Hospital	Far-Fault	24.60	0.159	0.37439	0.02447	625.39
8	1989	Loma Prieta	6.9	RO	Anderson Dam (Downstream)	Far-Fault	4.40	0.24	0.80107	0.0434	721.197
9	1979	Imperial Valley	6.5	SS	Chihuahua	Far-Fault	8.4	0.254	1.18662	0.05813	1110.14
10	1979	Imperial Valley	6.5	SS	Bonds Corner	Far-Fault	4.01	0.588	3.90282	0.14418	1471.17
11	1987	Superstition Hills	6.7	SS	El Centro Imp. Co Cent	Far-Fault	18.5	0.258	0.67456	0.03806	814.968
12	1987	Superstition Hills	6.7	SS	Plaster City	Far-Fault	22.5	0.121	0.29862	0.02395	447.696
13	1987	Superstition Hills	6.7	SS	Brawley Airport	Far-Fault	29.91	0.116	0.24856	0.02091	427.309
14	1987	Superstition Hills	6.7	SS	Superstition Mtn Camera	Far-Fault	6.56	0.894	6.02742	0.22789	1908.88
15	1987	Superstition Hills	6.7	SS	Westmorland Fire Sta	Far-Fault	13.47	0.211	1.17613	0.05774	1073.18
16	1983	Coalinga	6.4	RN	Parkfield — Cholame 2WA	Far-Fault	44.72	0.114	0.19526	0.01502	422.411
17	1983	Coalinga	6.4	RN	Parkfield — Fault Zone 14	Far-Fault	29.48	0.274	0.88032	0.04647	844.768
18	1983	Coalinga	6.4	RN	Parkfield — Gold Hill 3W	Far-Fault	39.12	0.122	0.15312	0.01252	330.881
19	1983	Coalinga	6.4	RN	Parkfield — Stone Corral 3E	Far-Fault	34.00	0.106	0.12442	0.01217	270.909
20	1983	Coalinga	6.4	RN	Pleasant Valley P.P. — yard	Far-Fault	8.41	0.551	3.8457	0.14045	1506.25
21	1987	Whittier Narrows	6	RO	Alhambra—Fremont School	Far-Fault	14.66	0.413	0.87457	0.04624	593.004
22	1987	Whittier Narrows	6	RO	LA—Hollywood Stor FF	Far-Fault	24.08	0.124	0.15938	0.0129	351.832
23	1987	Whittier Narrows	6	RO	Altadena—Eaton Canyon	Far-Fault	19.52	0.151	0.18627	0.0145	309.673
24	1987	Whittier Narrows	6	RO	Brea Dam (Downstream)	Far-Fault	23.99	0.313	0.4169	0.02852	408.27
25	1979	Coyote Lake	5.7	SS	Gilroy Array #1	Far-Fault	10.67	0.132	0.07987	0.00849	170.129
26	1979	Coyote Lake	5.7	SS	Coyote Lake Dam (SW Abut)	Far-Fault	6.13	0.279	0.35919	0.02575	338.147
27	1979	Coyote Lake	5.7	SS	Gilroy Array #2	Far-Fault	9.02	0.339	0.5126	0.03422	399.466
28	1979	Coyote Lake	5.7	SS	Gilroy Array #6	Far-Fault	3.11	0.316	0.6798	0.0422	421.295
29	1992	Cape Mendocino	7.1	RN	Eureka—Myrtle & West	Far-Fault	41.97	0.178	0.33065	0.02177	579.139
30	1992	Cape Mendocino	7.1	RN	Fortuna—Fortuna Blvd	Far-Fault	19.95	0.114	0.23911	0.01707	491.474
31	1992	Cape Mendocino	7.1	RN	Petrolia	Far-Fault	8.18	0.662	3.82072	0.14349	1456.08
32	1981	Westmorland	5.8	SS	Brawley Airport	Far-Fault	15.57	0.171	0.18547	0.01574	303.306
33	1981	Westmorland	5.8	SS	Niland Fire Station	Far-Fault	15.5	0.176	0.17397	0.01377	339.247
34	1981	Westmorland	5.8	SS	Parachute Test Site	Far-Fault	16.81	0.155	0.49073	0.02998	670.89
35	1981	Westmorland	5.8	SS	Salton Sea Wildlife Ref	Far-Fault	8.15	0.176	0.51288	0.03366	542.232
36	1992	Landers	7.3	SS	Desert Hot Springs	Far-Fault	21.98	0.154	0.6776	0.03612	1050.99
37	1992	Landers	7.3	SS	Amboy	Far-Fault	69.17	0.146	0.75468	0.03916	1064.58
38	1992	Landers	7.3	SS	Lucerne	Far-Fault	3.71	0.789	6.58484	0.20068	2483.47
39	1992	Landers	7.3	SS	Joshua Tree	Far-Fault	11.34	0.284	2.34815	0.09472	1746.59
40	1992	Landers	7.3	SS	Morongo Valley	Far-Fault	17.58	0.188	0.95827	0.04305	1272.15

[1] *Faulting Mechanism = TH: Thrust; REV: Reverse; SS: Strike-slip; OB: Oblique ; RN (Reverse-Normal), RO (Reverse-Oblique), NO (Normal-Oblique).*

[2] *Closest distance to fault rupture (i.e., r_{jb})*

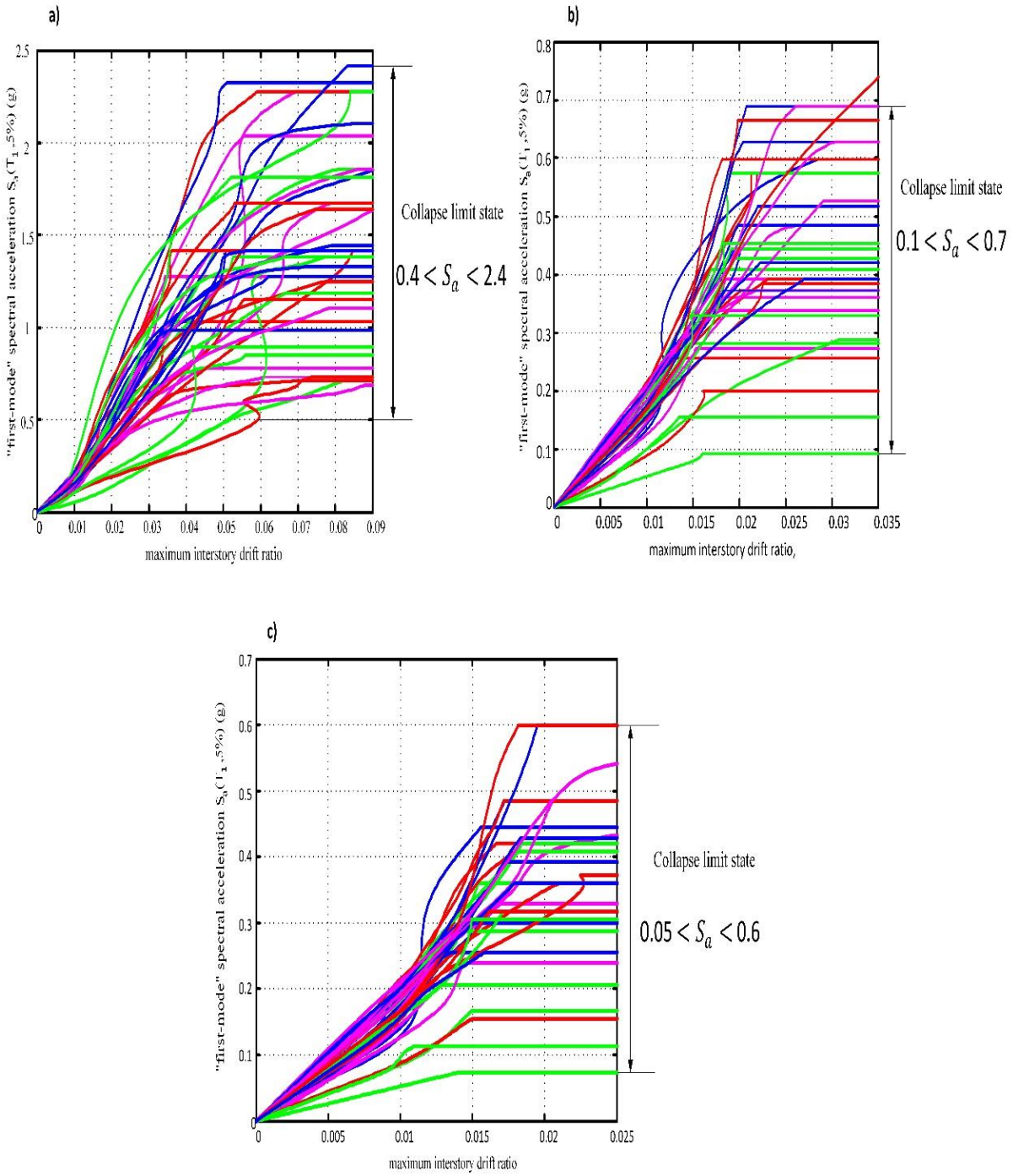

Figure 3.11: IDA curves for 5-story building, a) good quality b) average quality c) low quality

3.6.3 Sensitivity Analysis

According to the description of meta variables, sensitivity analyses are produced to determine the effects of each parameter of variable in various quality (MQ). The outcomes of sensitive analysis for sideways collapse of the sample 5-story structure are presented in Figure 3.12, where Figure 3.12 (a), (b) and (c) present created tornado diagrams of sensitivity outcomes and Figure 3.12 (d) and (e) show results of histogram of sensitivity analyses for each MQ.

As it is depicted in histogram dispersion of good material quality, structural response is large and it is reduced based on quality. In good quality as represented in Tornado Figure 3.12 of four random parameters, CS, BS and BD follow CD that has the largest effect on the mean collapse capacity and BS has an inverse effect on collapse. In average quality, CS has large effect while CD has no effect in mean collapse capacity. Finally in low quality, BD and CD have no effect in collapse. Monte Carlo simulation method has been used to incorporate the effects of modelling uncertainty in collapse fragility curve while thousands of sets for random variable and IDA analysis of structure for each realization are essential. Applying a predefined regressed function as response surface in Monte Carlo simulation, the nonlinearities and asymmetries in the relationship between the model random variables and the structural response have been represented.

In this method, the first step is to implement the IDA and vertical statistics for computing the two parameters μ and β of equation (3-7), which maximize Ln (L) by implementing the Cuckoo optimization algorithm. The parameters applied for the CO algorithm are based on proposed parameters as follows: Number of initial population (numCuckoos = 5), maximum number of eggs for each cuckoo (max Number of Eggs

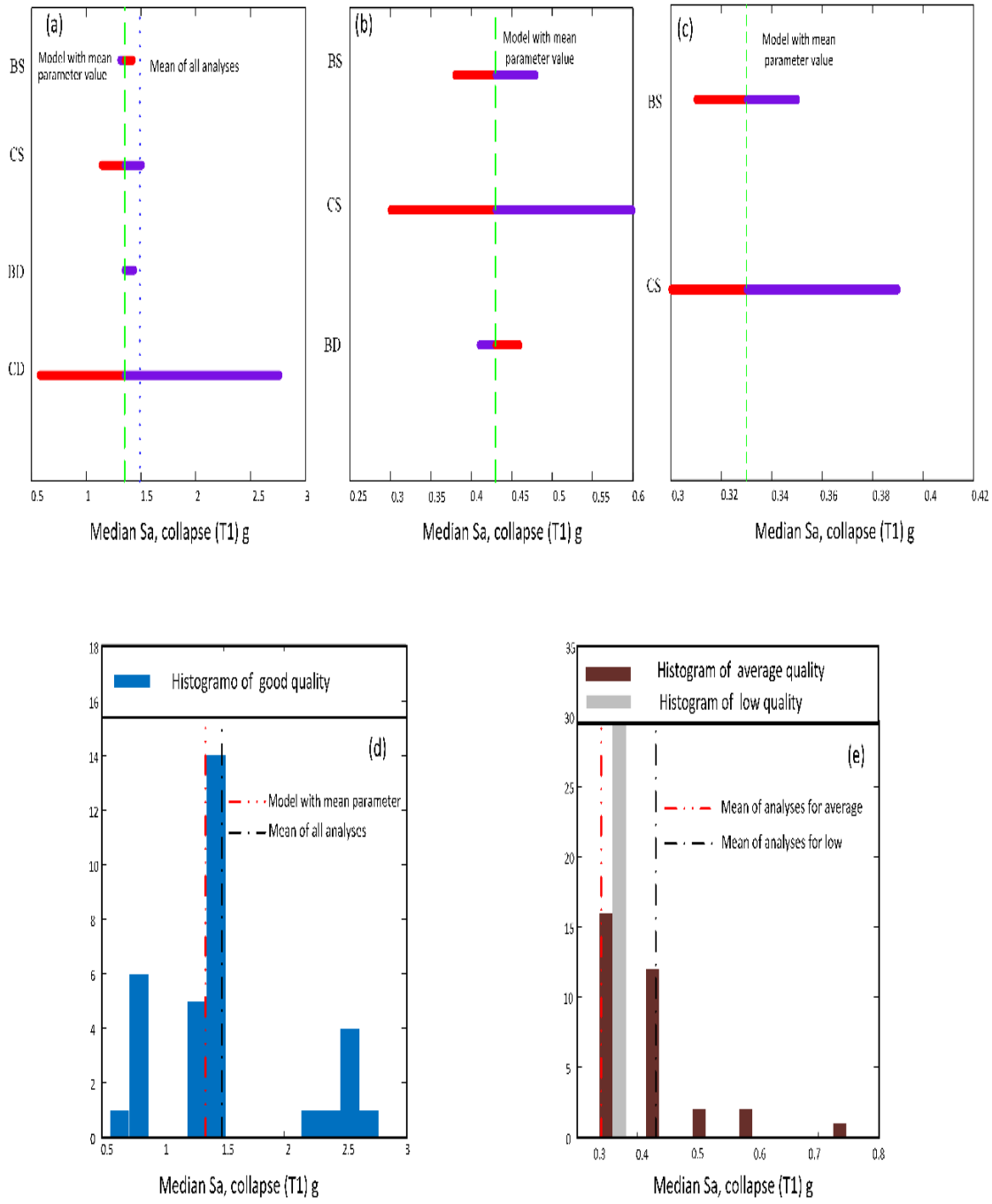

Figure 3.12: Tornado diagram from sensitivity analysis for 5-story building (a) good quality (b) average quality (c) Low quality, Histogram demonstrating the outcome of 33 sensitivity analysis for (d) good quality (e) average and low quality

= 4) and control parameter of egg laying is taken equal to 5. The optimization procedure is terminated when maximum iterations of the CO Algorithm reaches to 51. The sample of the best value of the objective function is shown in Figure 3.13.

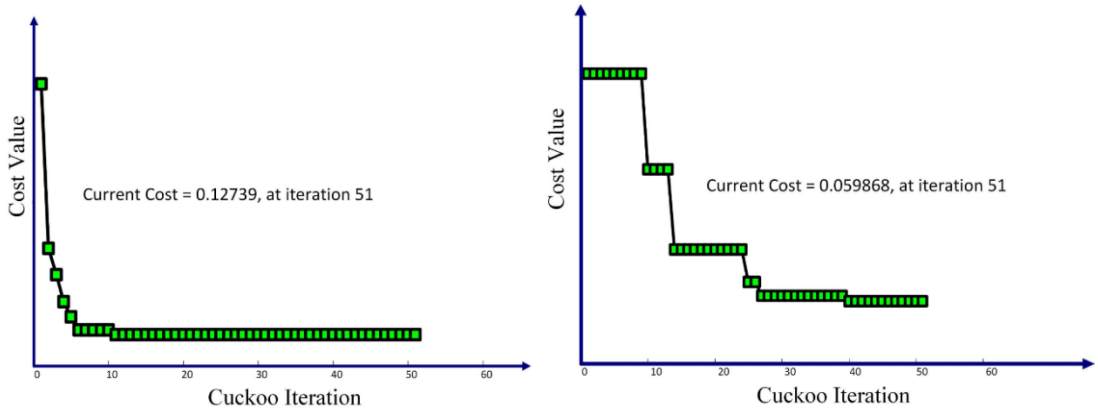

Figure 3.13: Best value of CO algorithm

Vertical statistics is performed for all quality of MQ. In the following step, the functions of response surface in equation (3-1) are used for prediction of means and SD of fragility curve for a limited number of realization for modelling parameter for each quality which is mentioned in numerical test section. The surface function is calculated by Pinv(x) function by using Matlab [84].

In the 5-story sample, the surface for collapse capacity limit state, mean of various material quality of collapse fragility curves are given by the following equations (3-14), (3-15) and (3-16):

$$\mu_{Good} = 0.389 + 0.0277(CD) + 0.004(BD) + .0047(CS) + 0.00043(BS) - 0.0086(CD)(BD) + 0.0172(CD)(CS) + 0.0021(CD)(BS) + 0.00195(BD)(CS) + 0.001425(BD)(BS) + 2.5 \times 10^{-5}(CD)(BS) + 0.00122(CD^2) - 0.0029(BD^2) - 0.00107(CS^{2)} - 0.000748(BS^2) \quad (3\text{-}14)$$

$$\mu_{Ave} = -0.833 - 0.00213(BD) + 0.129(CS) + 0.0141(BS) + 0.0065(BD)(CS) + 0.0057(BD)(BS) + 0.0129(BD^2) + 0.0286(CS^2) + 0.107(BS^2) \quad (3\text{-}15)$$

$$\mu_{Low} = 0.024(CS) - 0.0006(BS) + 0.015(CS^2) + 0.0068(BS^2) \quad (3\text{-}16)$$

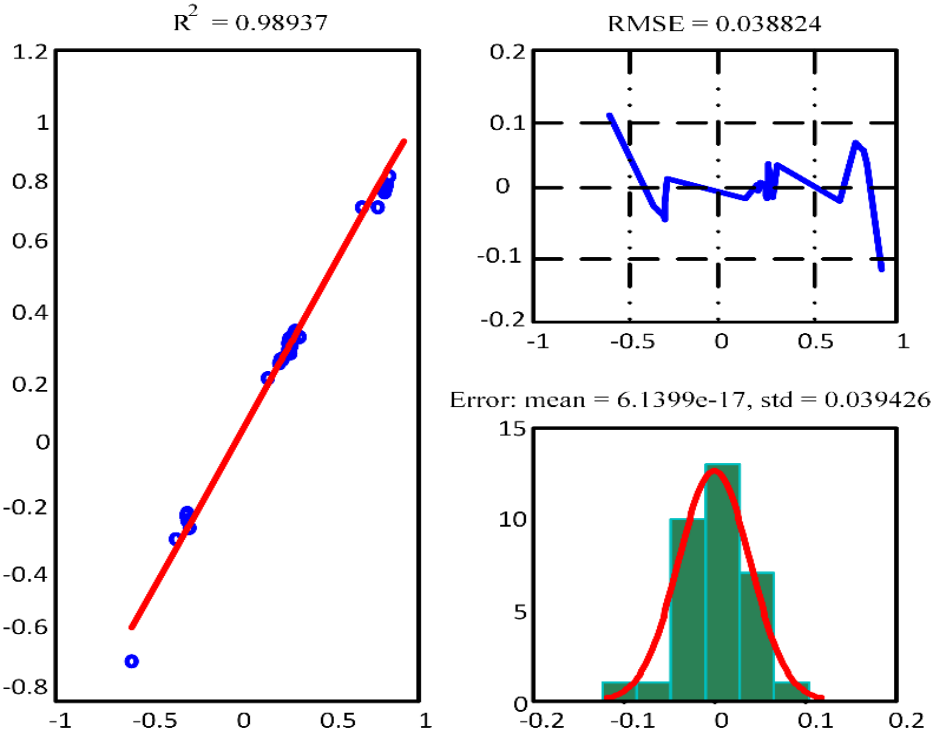

Figure 3.14: Statistical value for regression analysis of RSM

The best combination of values of the main variables for estimating the mean collapse capacity based on statistical data such as R^2, *RMSE* and *error* are given in Figure 3.14. Figure 3.15 shows the mean effect of collapse curve in RSM graphically.

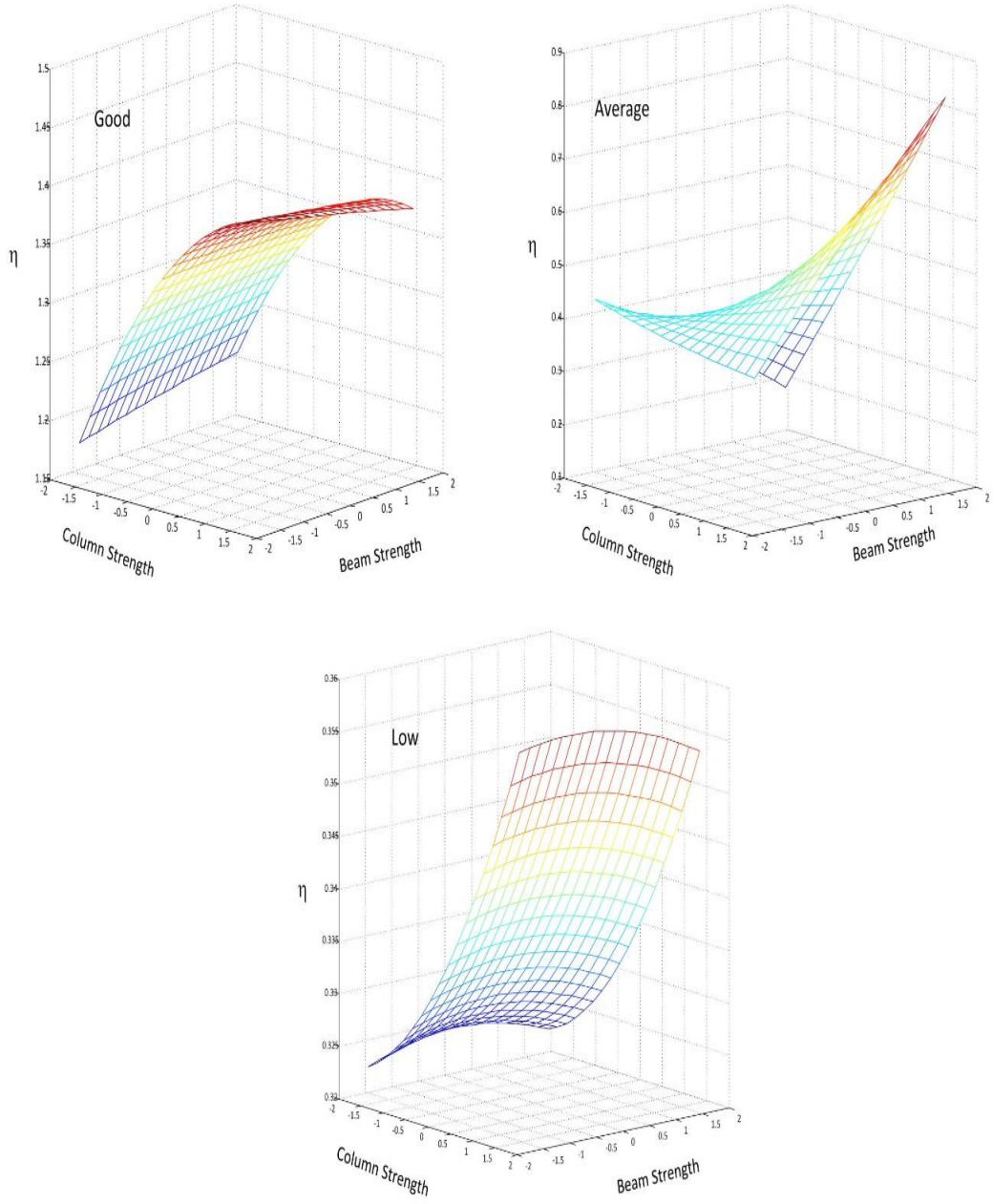

Figure 3.15: Response surface curves for collapse limit state for each quality level of 5-story sample structure

It can be seen that strength and ductility of columns as well as ductility of beams are desirable while strength of beams is not in good quality. Sugeno-type fuzzy expert has been used for considering quality uncertainty. Three rules are considered according to constant coefficient (one input, three rules, and 30 outputs) that are derived based on RSM coefficient which are summarized in Figure 3.16.

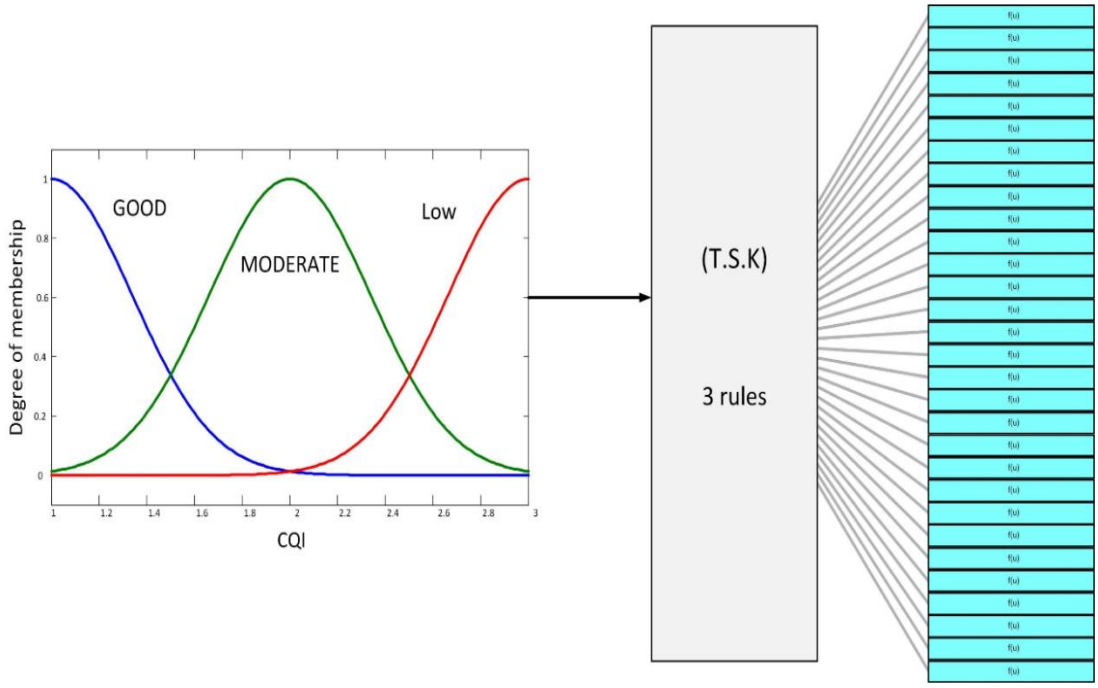

Figure 3.16: The structure of TSK system

Gaussian membership function for index of MQ as input and linear type as output is applied in Sugeno- type fuzzy expert system. Also weighted average, sum and prod method are used for defuzzification, aggregation and implication, respectively. Monte Carlo simulation is used for deriving fragility curve involving RTR, modelling and cognitive uncertainty effects. First of all, 10000 realizations of Monte Carlo are simulated by two parts.

The first one is 100 values of MQ based on uniformly-distributed in interval [1,3] and the second one is 100 values of modelling simulation of meta variable are obtained by

random number based on lognormal distribution. Finally mean and SD values are obtained by the expected value of collapse probabilities, which are calculated according to 10000 collapse fragility curves that is represented as the collapse final fragility probability.

Fragility capacity can be evaluated based on the following criteria: (a) the mean value of collapse capacity corresponding to the MCE (maximum considered earthquake acceleration) in the IDA curve, (b) probability of collapse at the MCE intensity,

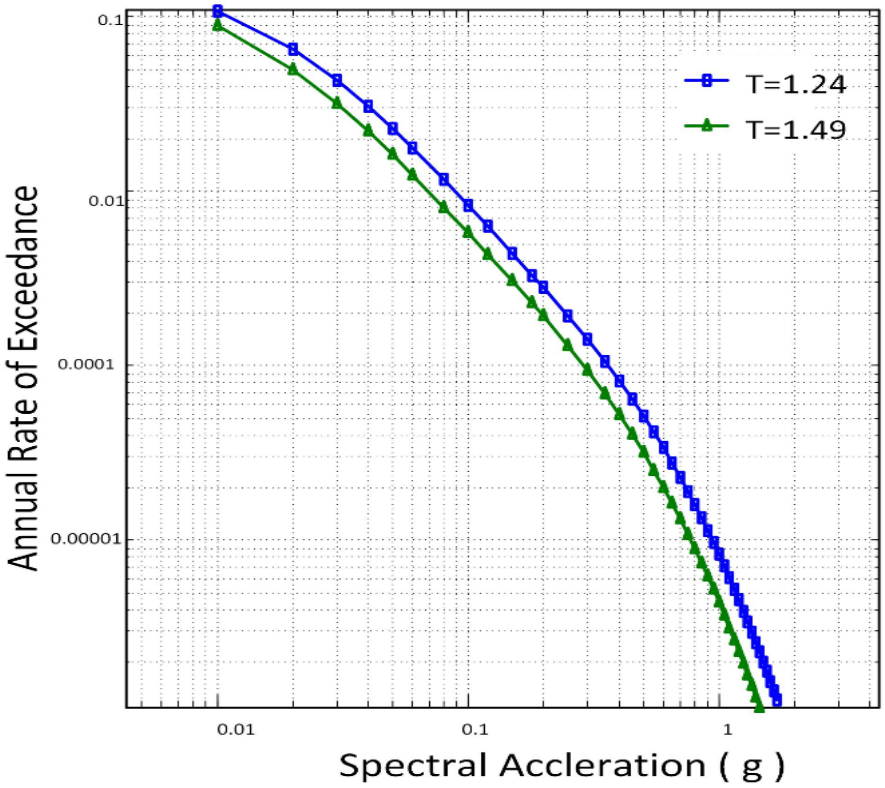

Figure 3.17: Seismic hazard curve

(c) Mean Annual Frequency Exceedance (MAFE) of the collapse which the value is estimated by integrating over the fragility curve over the hazard curve of a specific site (equation (3-17)). The Probabilistic hazard analysis have been done for Tehran region [85] and relevant hazard curve which was estimated (α) by fitting the functional

form $\beta_0(s_a)^{\alpha}$ in hazard curve (Figure 3.17). Based on the hazard curve, MPE (maximum probable earthquake spectral acceleration) and MCE are 0.477g, 0.716g for 5-story and 0.42g, 0.62g for 10-story frame.

$$MAFE = \int F_R \times d\lambda_{IM} \tag{3-17}$$

Incorporating modelling uncertainty and material quality for 5 and 10 story sample structures is shown in Figure 3.18. Combining the uncertainties into one entity causes the fragility curve to shift to the left and become more widely distributed. In other words, the curve depicts a critical state which becomes more pronounced when the material-related uncertainty comes into play.

Neglecting material quality causes underestimation of collapse fragility probabilities (Table 3.4), for example in 5-story structure, which is shown in Figure 3.18 (a) and (c), considering quality material uncertainty, mean is decreased to 63% while if it is only modelling uncertainty, mean is changed 3%, which there is no consideration of modelling uncertainty in the base case. In Figure 3.18 (d) and (e), fragility curves are obtained by using the RSM for each material quality level separately. It can be observed, MQ uncertainty is most important factor in deriving fragility curves.

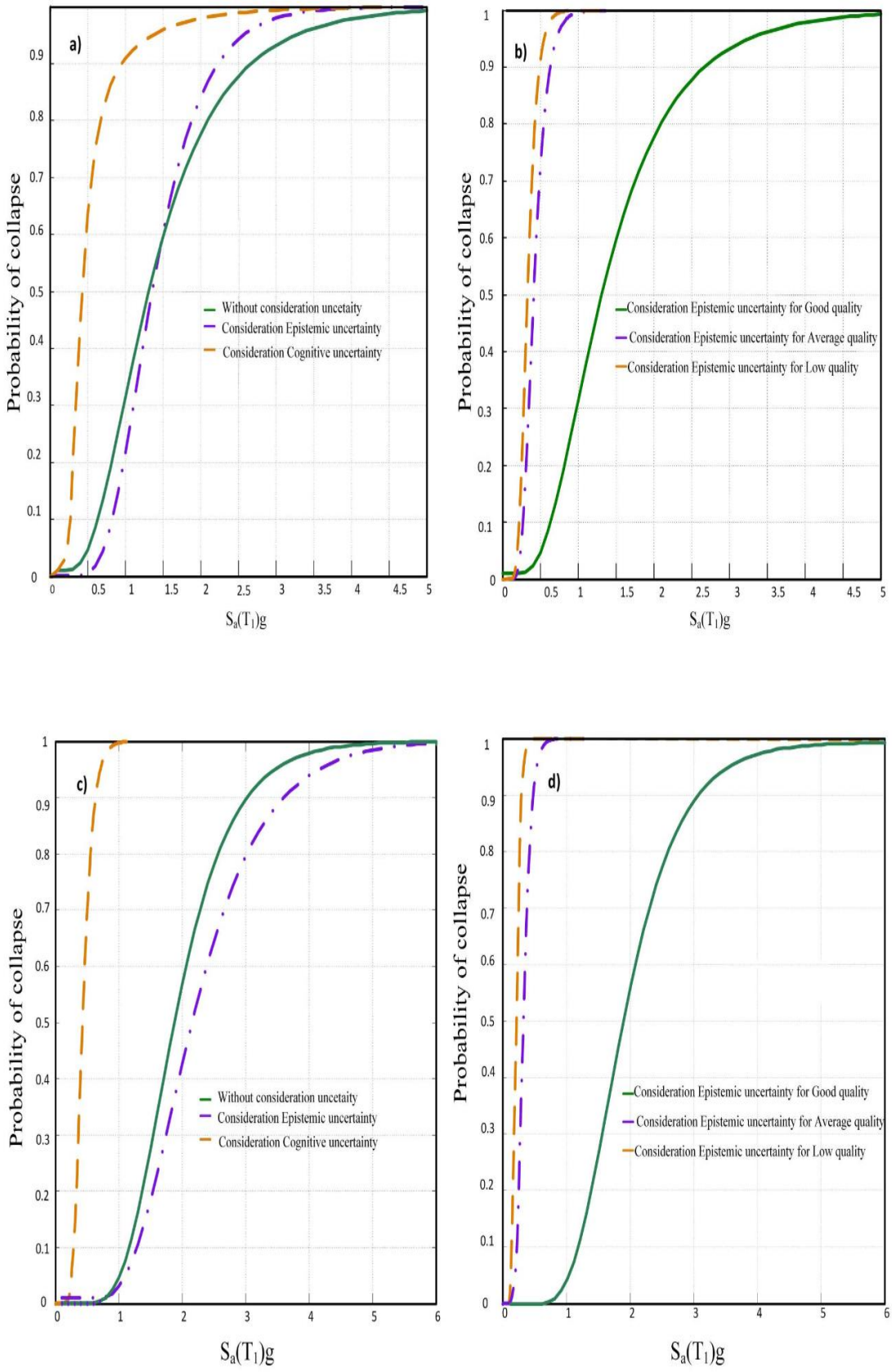

Figure 3.18: Collapse fragilities obtained for (a) 5-story building with modelling and MQ quality (b) 5-story with various quality (c) 10-story with modelling and MQ quality (d) 10-story with various quality

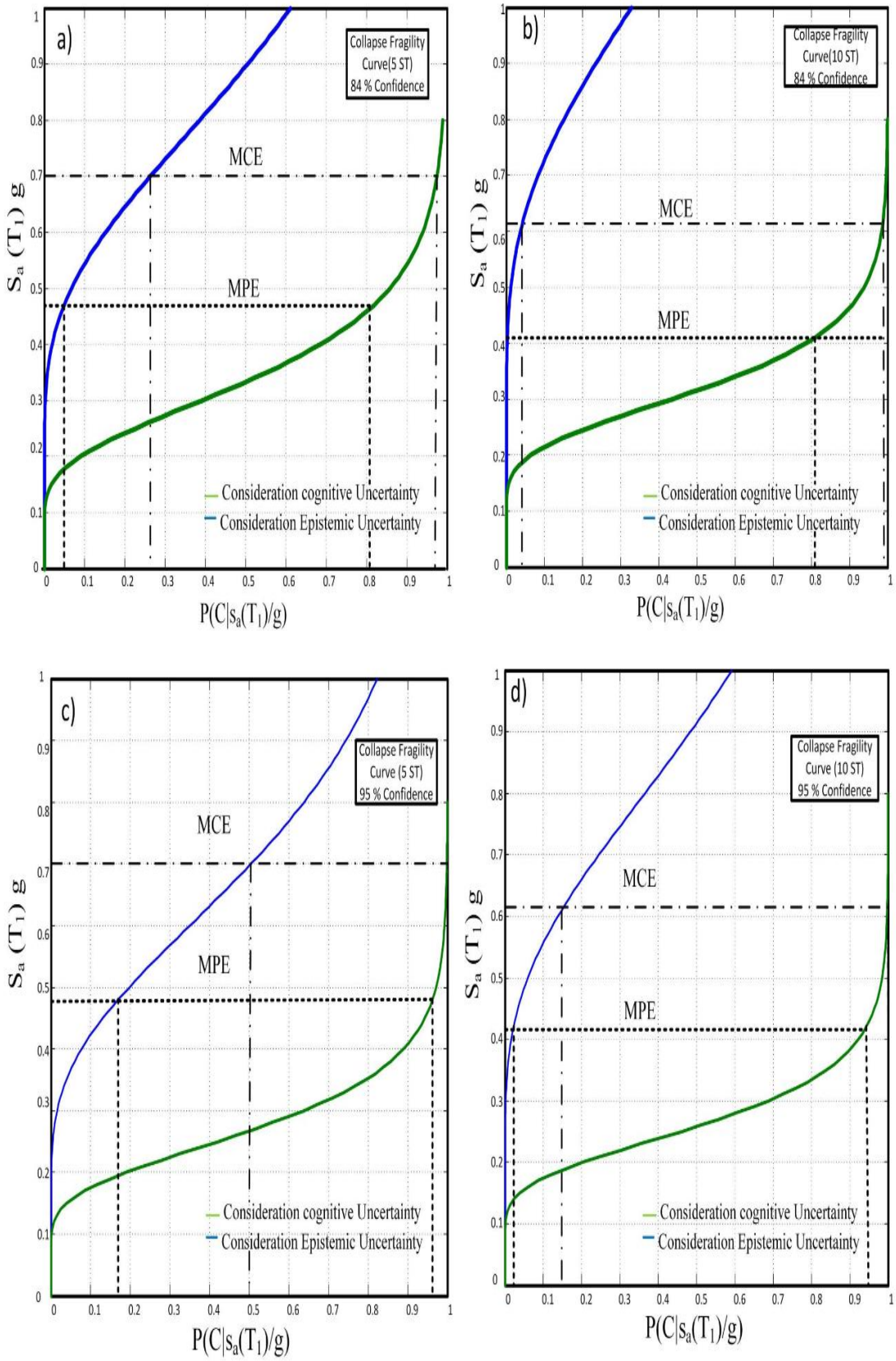

Figure 3.19: Fragility curve for collapse safety, considering modelling and material quality uncertainty for (a) 5-story building in 84% confidence (b)10-story in 84% (c) 5-story in 95% (d) 10-story in 95%

Table 3.4: The variation interval of collapse fragility curve by uncertainty analysis

	Method	MQ	Change in mean (%)	Change in dispersion (%)
5-ST	RSM	Good	-3	0.5
		Average	-69	13
		Low	-75	18
	TSK	MQ	-64	12
10-ST	RSM	Good	-8	1
		Average	82	19
		Low	89	31
	TSK	MQ	77	18

Table 3.5: Probability of collapse and mean annual frequency with considering various uncertainties

	Method	Uncertainty	P(Collapse|MCE)	P(Collapse|MPE)	MAFE $\times_{(10^{-5})}$
5-ST	RSM	No consideration	0.044	0.005	5.31
		Good	0.1334	0.0465	5.59
		Average	0.9381	0.72	54.6
		Low	0.9987	0.9154	82.9
	TSK	MQ	0.88	0.58	41.079
10-ST	RSM	No consideration	0.001	0.00016	2.80
		Good	0.02	0.01	3.38
		Average	0.87	0.72	89.6
		Low	100	0.99	195
	TSK	MQ	0.86	0.42	50.5

MQ: incorporation of quality and modelling uncertainty

According to the Table 3.4, the mean of the fragility curves in low quality for 10-story structure changes 89%, which it is much extended shift in fragility curves. Figure 3.19 illustrates probability of collapse in discreet hazard levels (MCE, MPE) and Mean annual frequency of exceedance (MAFE) in two sample structures. It can be observed that modelling and MQ uncertainty increase 75%-80% and 40%-50% approximately in MCE and MPE hazard levels respectively.

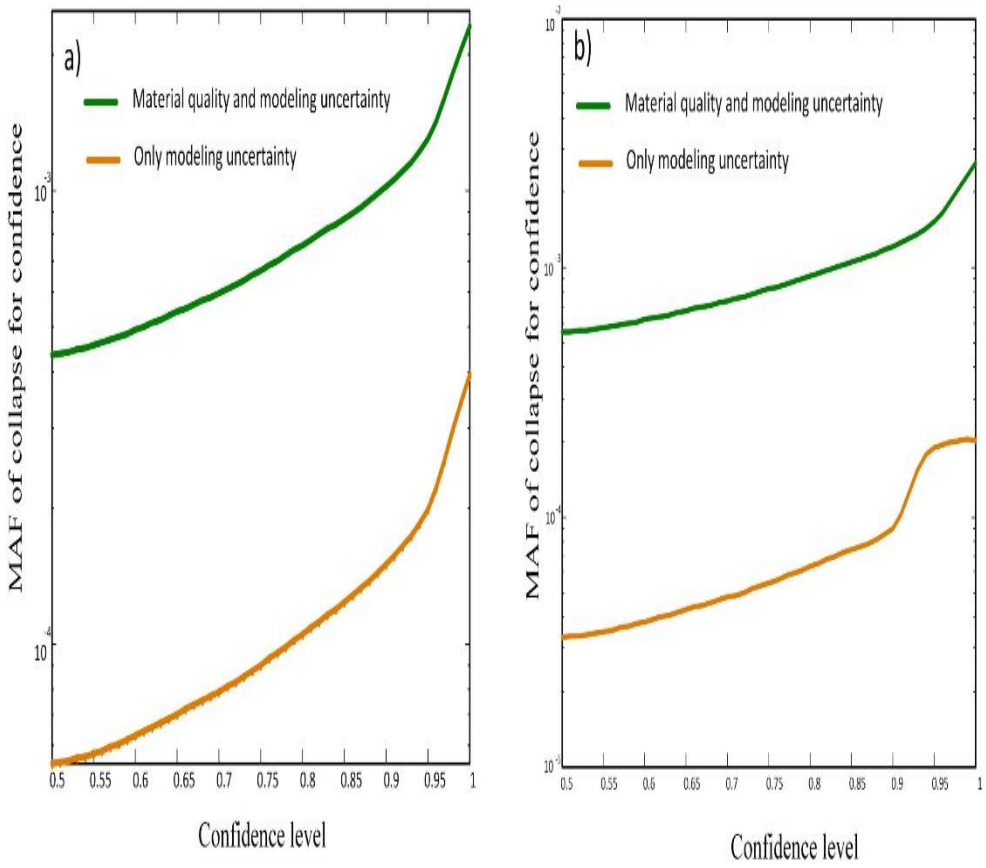

Figure 3.20: Effect of confidence level on of MAF with considering comprehensive sources of uncertainty (a) 5-story building (b) 10-story building

MAFE is an important factor in risk management and decision making that can be concluded material quality is dominant factor in mean annual frequency. Confidence approach has been applied for incorporating the effects of two uncertainties (modelling and material quality) in estimating of probability of collapse given in IM.

Then by using Figure 3.19, one can show the effect of MQ uncertainty for estimating of probability in certain Y confidence level of each sample structure. For example, according to Figure 3.19, it can be concluded that in the 5-story building, the collapse probability at MCE and MPE hazard level with 95 confidence level are 54% and 15% (95 confidence means 100-95=5% probability that the actual value of collapse is less than 15%) while considering only modelling uncertainty and probability of collapse are 94% and 99% when considering incorporating modelling and quality uncertainty. FEMA guideline requires the probability of collapse for a 50 year period to be smaller than 2% at a confidence level of 95%. Figure 3.20 shows MAF variation in the fragility of the 5 and 10 story structures at different confidence levels. It can be seen that the variation is too high and the criteria given for designing the sample structures become unacceptable when all the uncertainties come into play.

3.7 Summary

It is observed that almost in all cases disregarding the uncertainties effect is conservative. The dispersion increases in the response fragility when modelling and cognitive uncertainties is incorporated. The mean of curves may reduce approximately by 70% for cognitive uncertainty and 10% for modelling uncertainty. This reduction will be increased when the number of stories is added. Cognitive uncertainties have more impact than other uncertainties.

It can be considered that material quality is an important factor in the probability of collapse. Also, while MQ=low, the structure is more brittle. In studying nonlinear variable in sensitive analysis, it is observed that the effect of ductility in MQ=good is more than other variables while in MQ=low the strength is more effective. It is obvious that at different level of seismic design load, collapse probability will be different.

However, effect of uncertainties considered for the sample frames reveal that uncertainties may affect collapse probability significantly compared with the deterministic approach (not considering epistemic and cognitive uncertainties). Generally it can be concluded that in developing countries where problems of material quality might be observed, the cognitive uncertainty should be considered in fragility curves and mean annual frequency of collapse, which is a main point for decision making and risk management seriously. One of the possible solutions for this problem is applying advanced laboratory tests for diagnosing the quality of material.

Chapter 4

INTERVAL ANALYSIS BY FCM-PSO APPROACH

4.1 Introduction

Huge economic losses and collateral damages caused by seismic activities brought increased concern and focus in the seismic resistance evaluation of structures based on criteria, direct or indirect. The Seismologists, Civil Engineers and project engineers are all co-operating arrive at reliable evaluation methods which take into account the functionality of the buildings and bridges [1]. Determination of the seismic performance of buildings via probabilistic approach is developed at the Pacific Earthquake Engineering Research Center (PEER) [86]. This program focuses on determining the seismic performance of buildings taking into account the sources of uncertainty. In this program, the variables which determine the seismic performance of buildings are considered as the representing parameters including direct losses caused by the earthquakes, indirect losses caused by the building's loss of functionality, and loss of human lives. To determine the values of these parameters, the analysis is divided into:

- Analysis of earthquake risks
- Analysis of the response of the structure towards the earthquake
- Analysis of the damage caused by this response
- Analysis of the losses (direct or indirect) resulting from the damage [11].

The importance of identifying and determining the sources of uncertainty and using proper methods to combine them and to determine the probability distribution of the final decision making variable is obvious. Hence identifying the sources of uncertainty and incorporating them into fragility curves is similarly an important part of our recommended method in determining the seismic performance of buildings. Taking into consideration the number of possible uncertainties and the need for understanding their effects on the earthquake engineering concepts, we need to classify them properly. Generally speaking, there are two types of uncertainties. One, which emanated from the inherently random nature of the phenomena called the aleatory uncertainty. The other resulted from the inaccuracy of the model used when defining the phenomenon, called the epistemic uncertainty. The former is part of the phenomenon's nature and cannot be reduced while the latter can be reduced by choosing a more accurate model. Uncertainty itself can be modeled using either the classical method or the Bayesian method [87]. In the classical method, uncertainty can be handled via confidence of intervals. That is, the calculated mean of a random variable is itself taken as a random variable whose standard deviation is inversely proportional to the square root of the number of the sample points. The more the sample points are, the smaller the standard deviation is, and this is an indication of decreasing uncertainty. The Bayesian method is based on a radically different philosophical approach. In this method, new information collected from a sample is added to the already existing information, thus updating the existing information level. The new existing information level can then be updated again by adding newly acquired information from the sample. This can be repeated until the existing information level is deemed well enough. Here, the optimization algorithm, based on the statistical method, for deriving fragility is used. There are two important

parameters affecting fragility: engineering demand and the capacity of the system. The capacity of a structural system can be viewed as a normally distributed random variable X with mean μ and standard deviation β. Because of the high variability of data points, estimating the value of β wouldn't be easy and hence we indulge the smart optimization when estimating this value. Artificial neural networks and fuzzy systems are used in few studies for the compilation of the fragility curves of structures. Lagaros et al. [88] used the method of artificial neural networks to compile the fragility curve for different hazard levels. Papadrakakis [89] used artificial neural network based on the Monte Carlo method when analyzing concrete dams. The use of random-fuzzy method for incorporating epistemic uncertainties in a model is discussed by Moller and Beer [90]. In their method, parameters with aleatory uncertainty are considered as random variables with probability distributions while parameters with epistemic uncertainty are taken as fuzzy numbers. In this article, first functions of the mean and standard deviation of the fragility curve are determined, using the incremental dynamic analysis, as functions of parameters which possess an epistemic uncertainty; then the parameters of the model are determined as fuzzy variables; in the next stage, mean and standard deviation values of the fragility curve (themselves presented as fuzzy values) are calculated for certain combinations of the model parameter values. The calculation is performed using the advanced fuzzy method and the target parameters being optimized via particle swarm optimization. The reason for using this method is the result of the great variability of the mean and standard deviation values; however, we need accurate estimation tools. After the mean and standard deviation values of the probability distribution of fragility are calculated as fuzzy parameters, the probabilities of collapse are expressed as the probabilities of intervals. These probabilities reflect

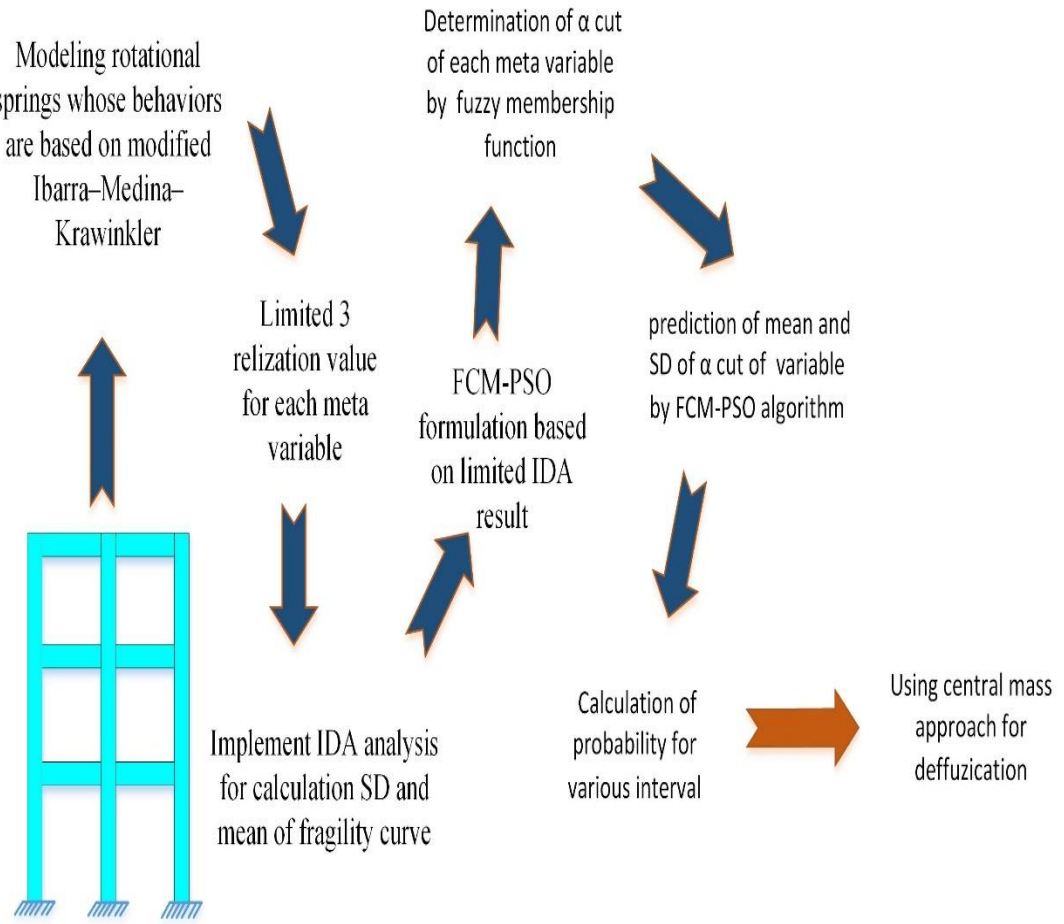

Figure 4.1: Proposed approach flowchart for incorporating epistemic uncertainty associated with fuzzy randomness

uncertainties inherent in the Incremental Dynamic Analysis (IDA) and the fuzzy nature of the parameters that reflect an epistemic uncertainty. Finally, the fuzzy values are turned into regular numbers using a defuzzifying algorithm. Figure 4.1 depicts the stages explained above. The emphasis here is on the use of a general variable which can account for the epistemic uncertainty on both beams and columns and the use of an optimized smart algorithm for the accurate estimation of means and standard deviations. Results are compared with those obtained using the Monte Carlo method which is currently considered as the most accurate way of accounting for uncertainties. It can be seen that the fuzzy method with optimized algorithm yields a comparable accuracy while it greatly improves the time taken for the estimation.

4.2 Basic Concepts of Hyperspectral Clustering

Clustering is a kind of learning algorithm in which similar objects are gathered in the same cluster. The first stage of this algorithm assumes objects that accomplish information of classes. Clustering can be applied in two different methods: crisp and fuzzy clustering. In the first method, the clusters are distinct and without coinciding in collection. Any sample could relate to just one class in this situation. In the second approach, a sample may relate to all the classes by a fuzzy membership function [91]. Each case in the pattern set is then nominated to the closest Cluster Centert (CC) which is updated by using the median of the associated cases. The procedure is repeated until some criterion is attained. The FCM [92] is the most important algorithm in the field of fuzzy clustering. In the FCM algorithm, a within cluster sum function Jm is optimized to create the proper CC as follows:

$$J_m(U,E) = \sum_{k=1}^{n}\sum_{i=1}^{c}(\mu_{ik})^m||x_k - e_i||^2 \qquad (4\text{-}1)$$

m is constant, and $m > 1$. Cluster i is displayed as e_i (i = 1, 2… c). The membership between case k and cluster i is displayed as μ_{ik} (i = 1, 2 … c, k = 1, 2… n) given c clusters, we can decide their CC, e_j for i = 1 to c through following expression:

$$e_i = \frac{\sum_{k=1}^{n}(\mu_{ik})^m X_k}{\sum_{k=1}^{n}(\mu_{ik})^m}, 1 \le i \le c \qquad (4\text{-}2)$$

4.2.1 Particle Swarm Optimization (PSO)

The PSO optimization algorithm logic is introduced by Kennedy and Eberhart [93]. In PSO algorithm, there are sets of particles called swarm defined as individuals. Search

space is used for solving the problem in PSO. Each candidate solution is selected in search space from various positions to find the best solution. The velocity equation which moves based on each particle of swarm is calculated as [93]:

$$v_{id}(t+1) = wv_{id}(t) + c_1 r_1\big(p_{id}(t) - x_{id}(t)\big) + c_2 r_2\left(p_{gd}(t) - x_{id}(t)\right) \quad (4\text{-}3)$$

$$x_{id}(t+1) = x_{id}(t) + v_{id}(t+1) \quad (4\text{-}4)$$

In equations (4-3) and (4-4), $x_{id}(t)$ is the position of particle i at time t, $v_{id}(t)$ is the velocity of particle i at time t, $p_{id}(t)$ is the best position found by particle i itself so far, $p_{gd}(t)$ is the best position found by the whole swarm so far, w is an inertia weight scaling the previous time step velocity, $c_1$and $c_2$are two acceleration coefficients that scale the influence of the best personal position of the particle $p_{id}(t)$ and the best global position $p_{gd}(t)$, $r_1$and r_2 are random variables between 0 and 1.

4.2.2 Fuzzy C-means Algorithm Based on PSO

The FCM algorithm requires less function assessment than the PSO algorithm because of the fast converging in FCM, although it often gets stuck in local optima. FCM-PSO is a hybrid clustering algorithm which has the advantage over the both two mentioned algorithms in one place. This algorithm implements the FCM in a way that swarms of particles from each eight generations pass through four repetitions, with each repetition the conformity increases as it should [94]. Each particle is a real k ×S vector, with k being the number of clusters and S being the dimension of the data on which the cluster executes. The target function of this algorithm is explained by equation (4-1), which is a function conforming to the hybrid clustering algorithms. The hybrid FCM-PSO algorithm can be defined as given in Figure 4.2.

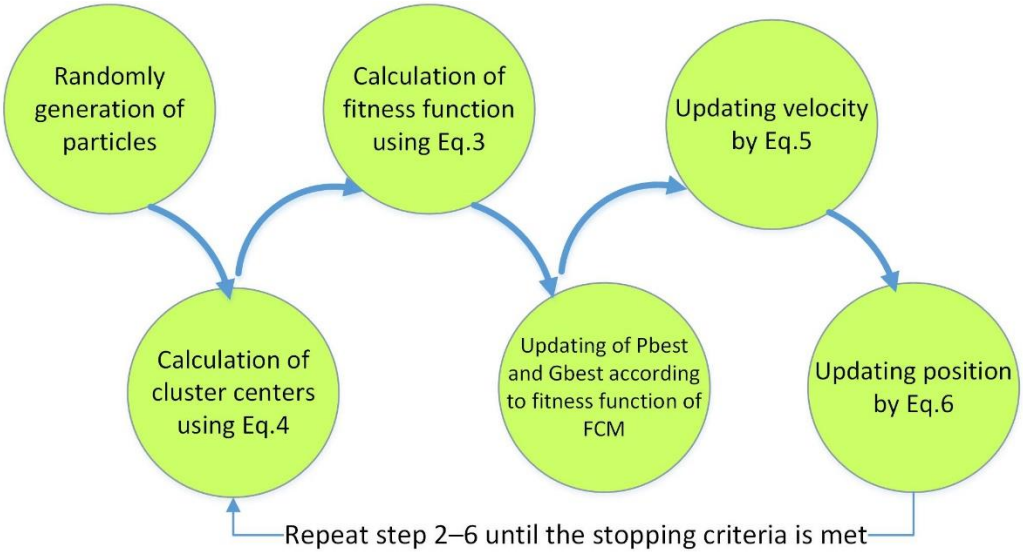

Figure 4.2: Flowchart of the optimization of fragility curve by FCM-PSO method[94]

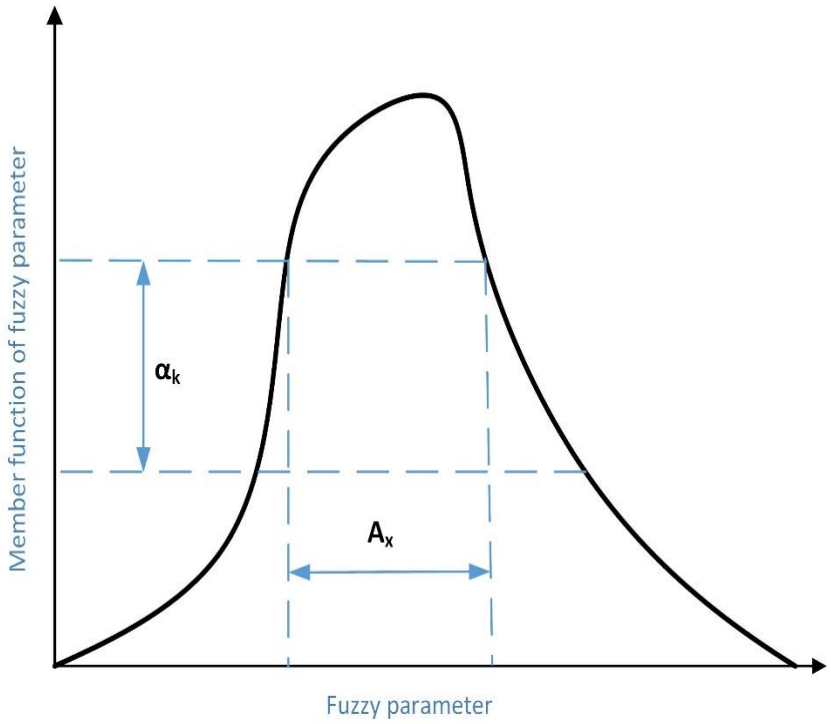

Figure 4.3: α-section definition of fuzzy parameter of X

4.3 Research Methodology

In this study the fuzzy random variables are suggested for the propagation of modeling uncertainties. Application of the fuzzy random approach, in modeling the behavior of uncertainty, is presented. In this approach the parameters of the epistemic uncertainties are presented by fuzzy values as defined by Zadeh [95]. A powerful numerical algorithm is developed by applying α-section to the fuzzy random variables which establishes the prerequisites for the application of α-level optimization expressed by the equation (4-5) and α crisp set A, is obtained as shown in Figure 4.3.

$$A_\alpha = \{X | MF(X) \geq \alpha\} \tag{4-5}$$

MF(X) is membership function value for parameter *X*. A range of values for the implementation of interval analysis methods has been developed by Rao and Berke [96]. The flowchart of the proposed method is shown in Figure 4.1. In this thesis, the effects of informal or epistemic uncertainty on beam strength (BS), column strength (CS), beam ductility (BD) and column ductility (CD), are considered by the lognormal distribution for each meta-variable by mapping the distribution function into their components [22]. Aleatory uncertainty from random nature of strong ground motion of earthquakes is considered to achieve the collapse fragility curve of a typical steel moment resisting frame as the case study. Effect of the aleatory uncertainty in this study is considered by selecting the appropriate 40 records given in Table 3.3. The selection strategy is based on K-means algorithm when considering the seismic hazard properties of the region interest. Modeling uncertainty effect is incorporated with the response surface method, which is used in the previous relevant literature [68]. The first step in the proposed method is to prepare mean functions and standard deviation

of collapse fragility curve as the function of values for the 20 modeling parameters. To achieve this, the mean values and the standard deviation of the collapse fragility curve is determined for some of the modeling parameter values by the use of IDA method. Each random parameter is perturbed in confident intervals individually, and in combination with other random parameters. Totally 81 perturbations of the incremental dynamic analysis is run with a subset of 40 earthquake records. FCM-PSO is applied to derive an analytical relationship between the predictor variables (BD, CD, BS, and CS) and response parameters (collapse fragility curve mean and standard deviation). The applied FCM-PSO functions are formulated as predictors. In the second stage of the proposed method, modeling variables are taken as fuzzy parameters by using triangular membership functions. The most likely point (peak in the membership function) equals to the modeling variable mean value and mean values minus standard deviation and mean plus one standard deviation are considered as low and high membership functions. By looking at various values of α and determining sections for membership functions of the modeling variables, different intervals of modeling variables are obtained. With the use of FCM-PSO obtained in the previous section, minimum and maximum mean value and collapse fragility standard deviation are determined by solving the optimization problem in various ranges. The obtained minimum and maximum values as mean value and standard deviation based on the low and high ranges of the membership functions are related to α-section mean and standard deviation values. Changes in values obtained for mean and collapse fragility distribution standard deviation indicate the validity of values for fragility function. In other words, the effects of modeling uncertainties are presented by the fuzzy-probability method with the help of optimization algorithm. After obtaining mean values and fragility distribution standard deviation as fuzzy parameters, values for

collapse probability are presented as intervals. Collapse probability is an indication of random uncertainties (due to intense land movements in IDA analysis) and changes provided as probability correctness interval (based on fuzzy-probability method) are indication of the effects of modeling uncertainties (due to changes in modeling parameters). If $Z_1 = \frac{IM_1 - \tilde{\eta}}{\beta}$ and $Z_2 = \frac{IM_2 - \tilde{\eta}}{\beta}$, collapse probability in the interval, [IM_1, IM_2] is calculated based on the fuzzy probability theory[97], and is written as:

$$\tilde{P}[IM_1, IM_2][\alpha] = \left\{ \int_{Z_1}^{Z_2} f_{IM_C}(IM) d(im) \middle| \eta \in \tilde{\eta},\ \beta \in \tilde{\beta} \right\} = [p_1(\alpha), p_2(\alpha)] \qquad (4\text{-}6)$$

In which probability density function f_{im_c} is follows as:

$$f_{IM_C}(im) = \frac{1}{(im)\,\tilde{\beta}\,\sqrt{2\pi}}\, exp\left(\frac{-(Ln(im) - \tilde{\eta})^2}{2\tilde{\beta}^2}\right) \qquad (4\text{-}7)$$

Where $\tilde{\eta}\ and\ \tilde{\beta}$ are the fuzzy mean and standard deviation of collapse probability distribution. It is proved that the probability, which is presented by BD, CD, BS, CS is a fuzzy number itself. The α-section number of this fuzzy value is represented by max and min of $p_1(\alpha)$, $p_2(\alpha)$. The defuzzier algorithm can be applied to show the result as a number after the result is achieved as fuzzy parameter. The center of gravity method would perform defuzzyfying to achieve collapse probability.

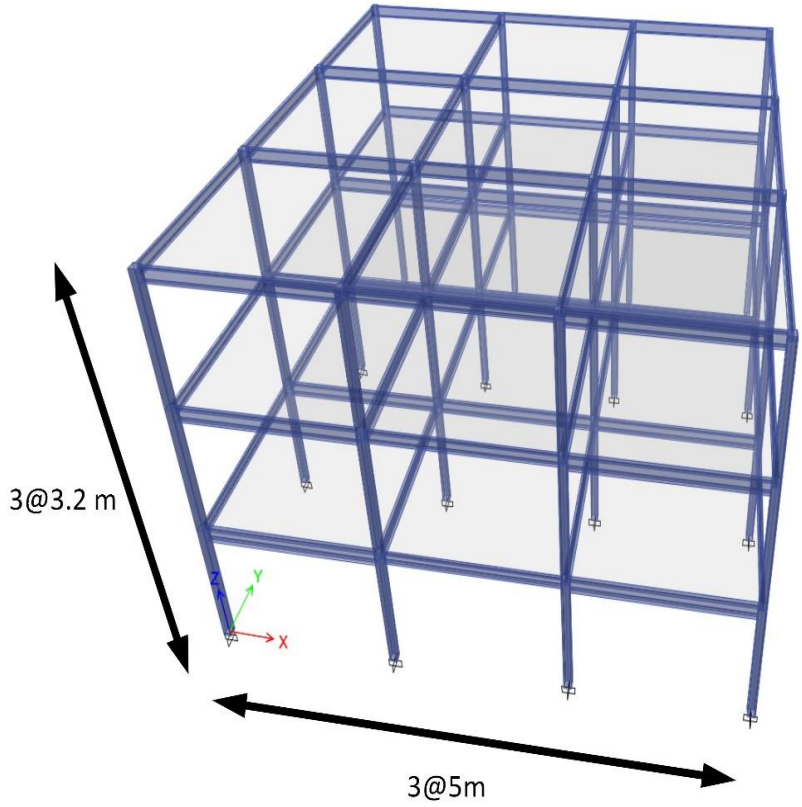

Figure 4.4: 3D view of sample structure.

4.4 Sample Study

4.4.1 Structural Model

Incorporating modeling uncertainty in a three storey ductile steel moment-resisting frame structure designed in accordance with the UBC-97 code [26] and the Iranian Seismic Code standard specifically for the relatively high risk region of Tehran where each storey has three bays and is 3.2 meters high (as seen in the Figure 4.4) is considered.

To better focus on the modeling parameters, we used the sample structure of the moment-resisting system. Sections of columns and beams are used for the analysis which is shown in Figure 4.5. The period of the building is calculated (using Open Sees [61]Software) as 0.98 second in the first vibration mode. The nominal yield

strength of the steel and the elasticity module are assumed as 240 MPa and 200 GPa, respectively. Beam to column connections are assumed to follow the Ibarra-Krawinkler moment-rotation behavior [98], with the elastic and rotational spring model. More specifically, the structure is assumed to have contain three elements, two beam elements with rotational springs situated on both sides of a column element with elastic behavior [57].

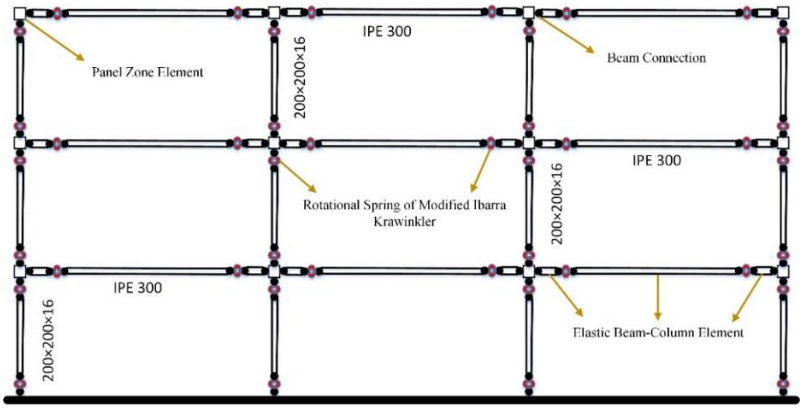

Figure 4.5: The analytical model of three-story, three-bay moment resisting frame

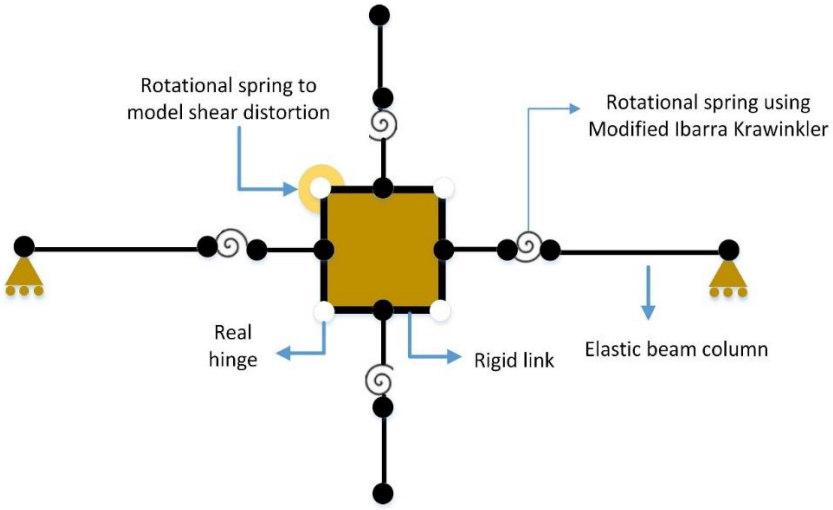

Figure 4.6: Subassembly model in OpenSees software

To adhere to such assumptions in our modeling, the related hardness coefficients of the elastic beams and the coefficient of contribution of mass matrix on the damping force should be modified accordingly. The latter should be modified in such a way that the work done by the damping force on the main element (lumped plasticity) becomes equal to the work done by this force on the beam's elastic element. To model the panel zone behavior, we have used the M2-WO model as explained by Foutch and Yun [99], generated by Open Sees Software.

As shown in Figure 4.6, dimensions of the panel zone are set in a way to be in accordance with the rigid elements assumption. The displacement of the panel zone can be expressed as the bilinear response of two elastic elements, creating a trilinear response.

With this model, the strength difference between the real behavior and the model of the panel zones (especially in large displacements) can be drastically mitigated. After yielding, the model shows an extremely rigid behavior, an indication that yielding has started but the whole section has not gone into yielding yet. After the whole section is affected by the yielding, behavior of the panel zone changes into one characterized by a very small gradient (typically 2%, sometimes even zero).

As seen in Figure 3.6, the four parameters are taken into account in the Krawinkler's model for the determination of the nonlinear behavior of elements [23] (pre-capping plastic deformation (θ_p), post-capping deformation capacity (θ_{pc}) and cyclic deterioration (λ) and ratio of capping strength to yield strength (Mc/My)).

Based on the laboratory experiments [23], values of these parameters are assumed to follow log-normal distributions with means and standard deviations that describe uncertainties as to $\theta_p,\ \theta_{pc}\ and\ \lambda$. To reduce the time taken by the analysis, simplifying assumptions are adopted. For instance, it is assumed that the ductility variables of beams are so interrelated that one single variable can account for the beam ductility (BD). The same is assumed for beam strength (BS), column ductility (CD), and column strength (CS), leaving us with four Meta variable in total. The meta variable BS includes the ratio *(M_c/M_y)* for beams, meta variable CS includes the ratio (M_c/M_y) for columns, meta variable BD includes the variables (θ_p),(θ_{pc}) and (λ) for beams, meta variable CD includes the variables (θ_p),(θ_{pc}) and (λ) for columns. The statistical parameters of these modeling variables are given in Table 3.2.

Meta-variables of strength and ductility defined are fully correlated with similar component. Defining lognormal distribution for each meta variable, and the probability of each meta-variable can be mapped into probability of its components.

4.4.2 Interval Based on FCM-PSO

To obtain the input data in evaluating FCM-PSO, each meta variable is perturbed 1β away from mean individually and in the combination of the other variables. Totally $3^4 = 81$ realizations are considered. The tree diagram of the realizations for input variables is shown in Figure 4.7. For each realization of input variables, IDA is implemented and S_a associated with two distinct limit states are derived for each record. The 3-storey ductile moment frame building is considered as a sample frame and two distinct limit states are defined as: (a) exceedance of 2% interstory drift and (b) sidesway collapse. Then the mean and standard deviation of the fragility curve is

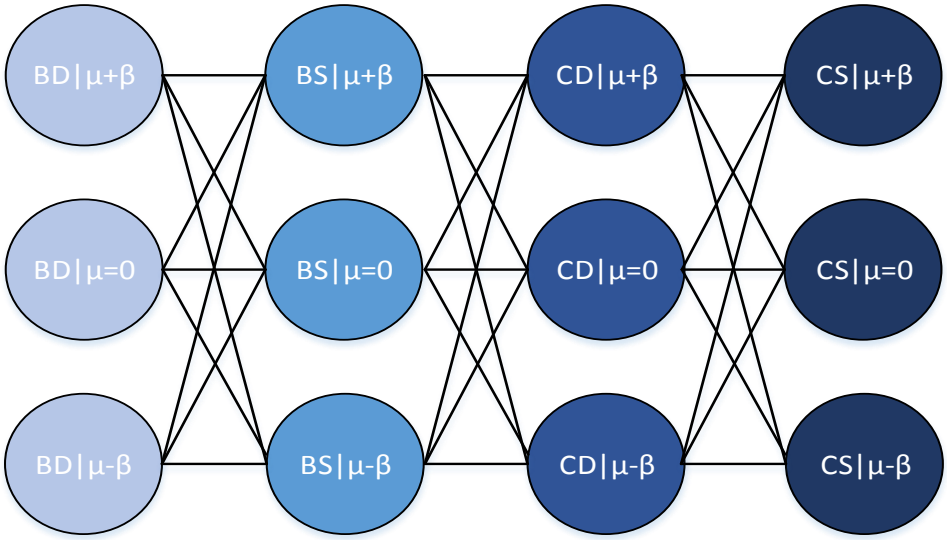

Figure 4.7: Tree diagram for pre-assumed values of epistemic uncertainty

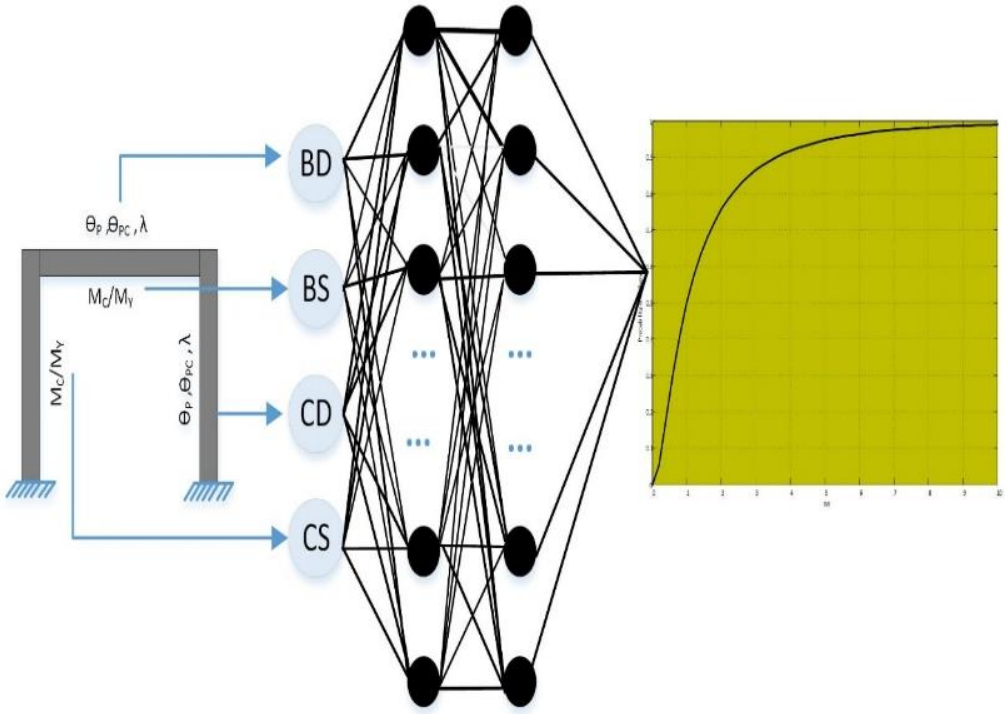

.

Figure 4.8: Proposed FCM-PSO approach to predict mean and standard deviation

achieved based on the 40 records by fitting a log-normal probability distribution. The architecture of proposed FCM-PSO is presented in Figure 4.8. The fragility curves and samples of IDA curves associated with the sides way collapse limit state are shown in Figures 4.9 and 4.10, respectively.

These means and standard deviations are considered as target data in proposed FCM-PSO model. Therefore, 64 realizations (65% of total realization) are utilized to train and test the proposed algorithm.

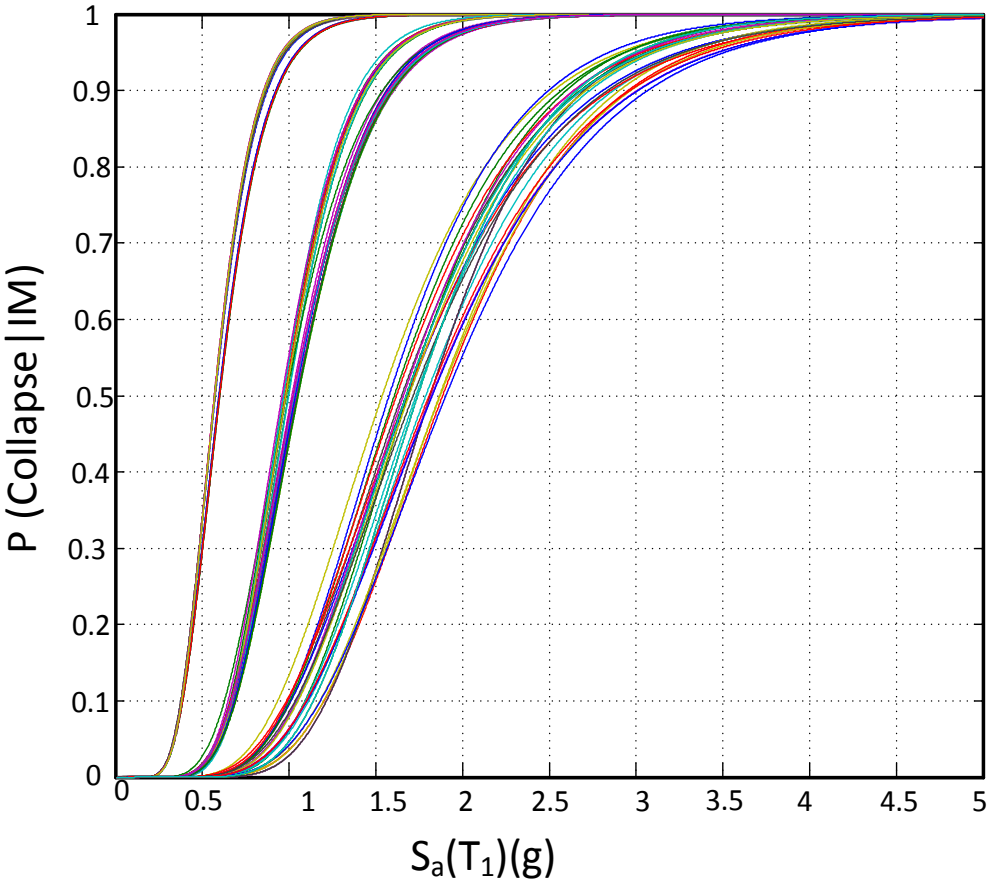

Figure 4.9: Sample collapse fragility curves for 81 cases

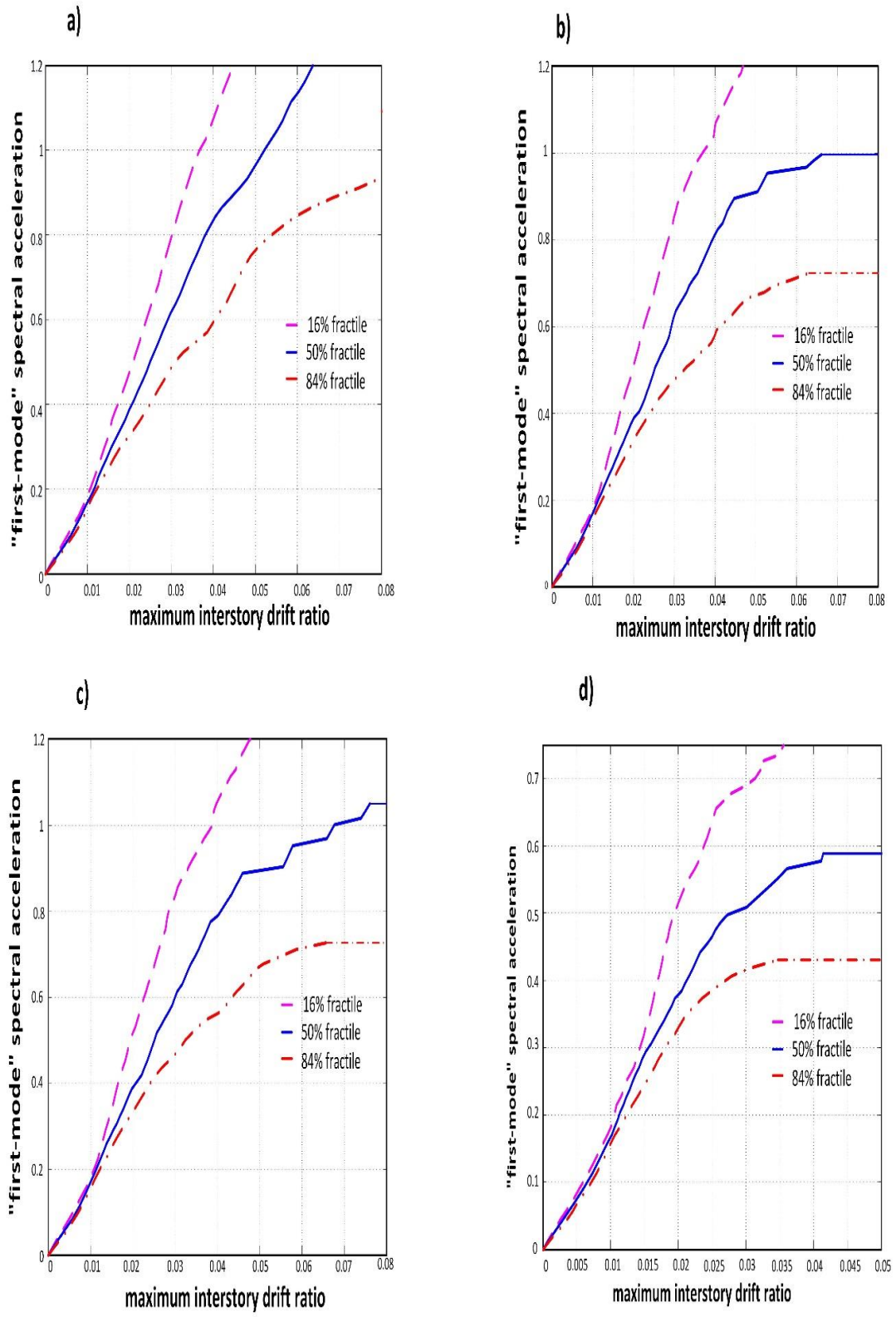

Figure 4.10: Median of sample IDA curves (β) a) BD=1,CD=1,BS=0,CS=0 b) BD=0,CD=0,BS=1,CS=1 c) BD=0,CD=0,BS=0,BS=0 d) BD=-1,CD=-1,BS=-1,CS=-1

The mean and standard deviation values evaluated by direct analysis considering three realizations of modeling parameters and values calculated based on IDA of sample structure, are compared in Figures 4.11 and 4.12. These figures show a good fit between estimated mean and standard deviation and the accurate ones.

In these figures, horizontal axis shows values that are evaluated by direct IDA and vertical axis as those which are estimated by FCM-PSO method. The solid black line shows the position where approximate values are equal to IDA-based values. In order to evaluate the accuracy of mean and SD predicted by FCM-PSO, the Mean Square

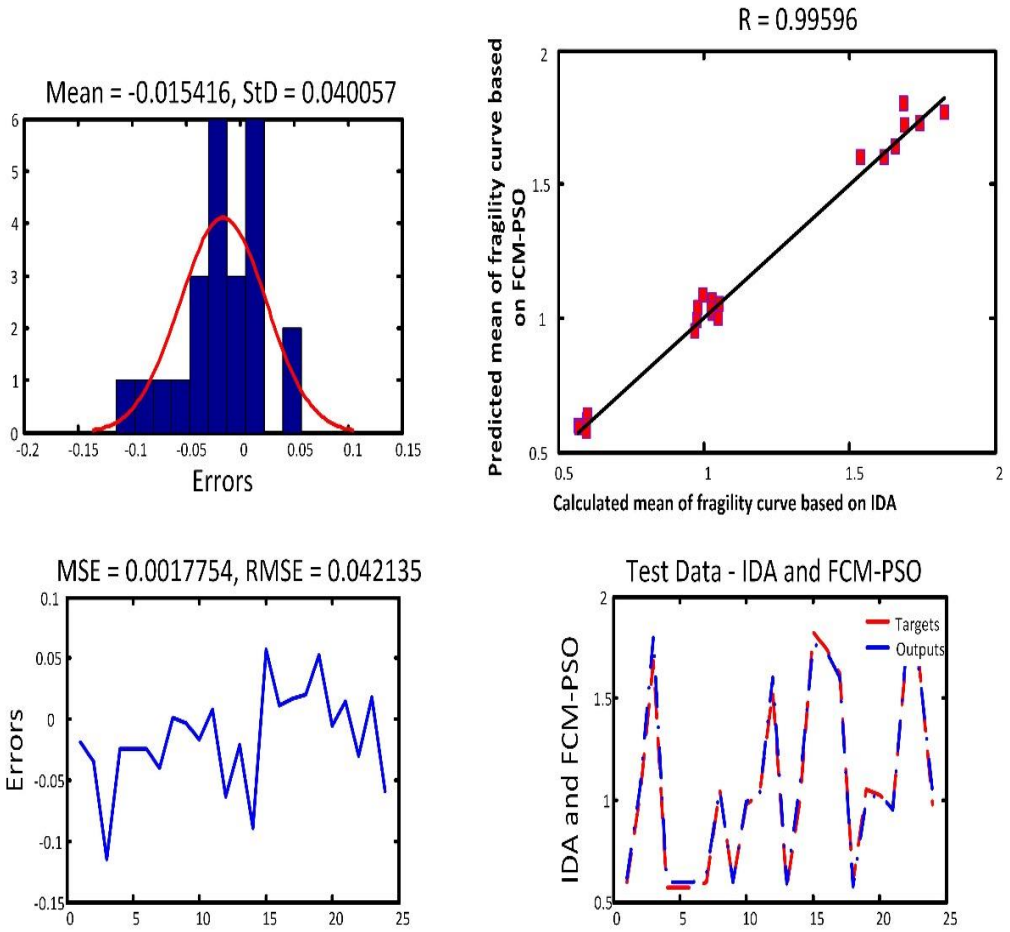

Figure 4.11: Comparison of mean values based on IDA versus estimated mean of fragility curve

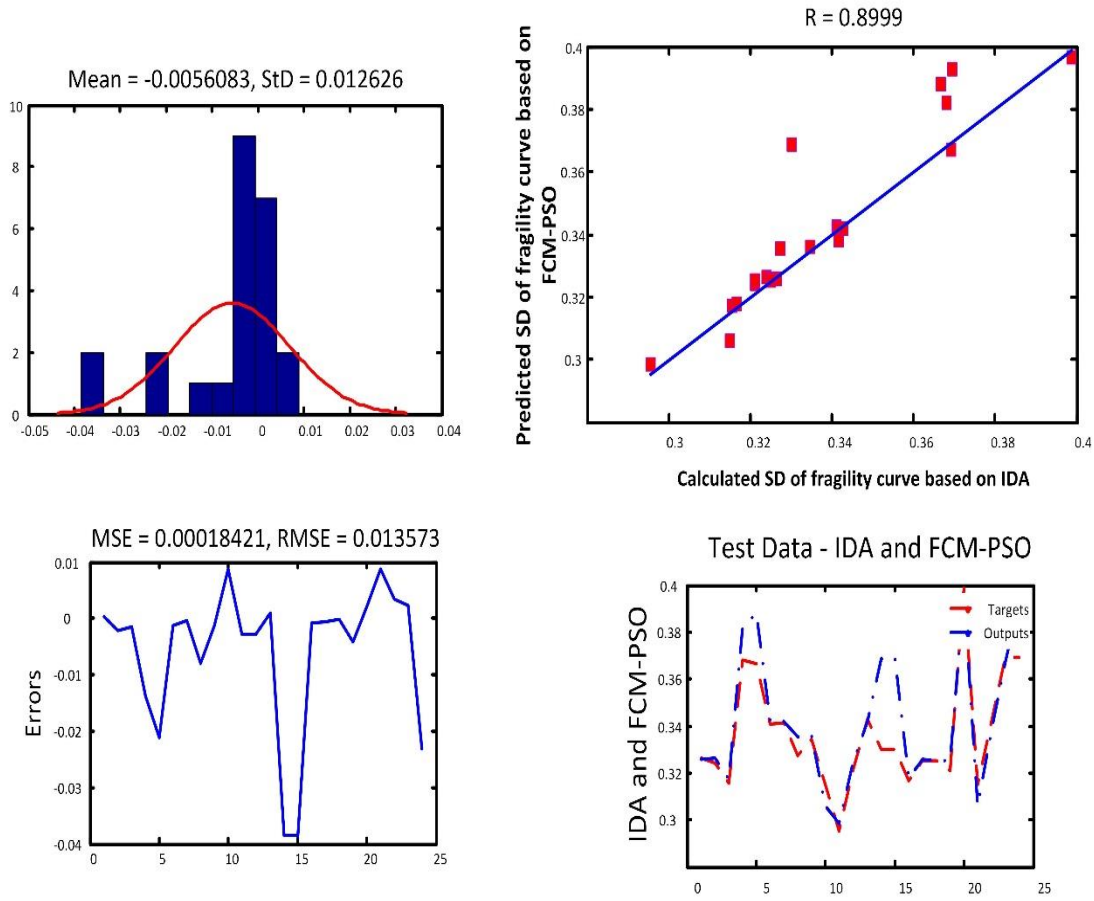

Figure 4.12: Comparison of SD values based on IDA versus estimated SD of fragility curve

Error (*MSE*), the Root Mean Square Error (*RMSE*) and R-square (R^2) statistic measurements are determined as the accuracy criterion through the test data. The *MSE*, *RMSE* and R^2 between the exact and predicted responses are as:

$$MSE = \frac{1}{n}\sum_{i=1}^{n} |y - \hat{y}_i|^2 \tag{4-8}$$

$$RMSE = \frac{n_i \sum_{i=1}^{n_i} (y_i - \hat{y}_i)^2}{(n_i - 1)\sum_{i=1}^{n_i} (y_i)^2} \tag{4-9}$$

$$R^2 = 1 - \left[\frac{\sum_{i=1}^{n_i} (y_i - \hat{y}_i)^2}{\sum_{i=1}^{n_i} (\hat{y}_i)^2}\right] \tag{4-10}$$

Where y and $\hat{y}$ are actual and predicted values, respectively; and n_i is the number of testing samples. The smaller *MSE* and *RMSE* and the larger R^2 are indicative of better performance in general. In order to achieve the best performances, different FCM configurations with variable number of clusters and the exponent of weights are considered.

The PSO algorithm is used to achieve the best configurations of FCM that are trained based on the performance error which is evaluated by equations (4-8) and (4-10). Using such a trial-and-error approach, the best FCM-PSO model corresponding to the least error measure is determined. The following parameters archived from trial-and-error approach used in the FCM-PSO to predict mean and SD of fragility curves:

- Population Size (Swarm Size): 300
- Number of Iterations: 420
- Inertia Weight: 1
- Observant acceleration constant: 2.05
- Social acceleration constant: 2.05

The mean square error applying trained FCM-PSO in prediction of the mean and standard deviation values are 0.177% and 0.018% respectively, which are considerably less than those of full Monte Carlo methods shown in the next section.

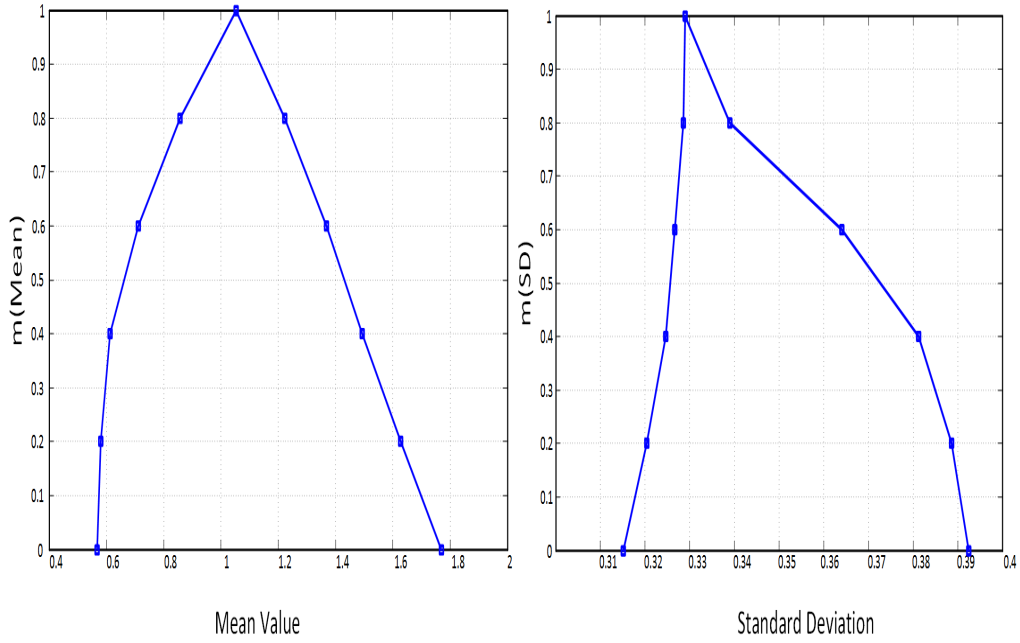

Figure 4.13: The membership function of mean and SD of fragility curve in interval analysis

After the prediction of the maximum and minimum values by the proposed algorithm, a triangular membership function is formed as a fuzzy function. Such membership functions are indicative of modeling uncertainty and their values are in fact the mentioned intersections for different intervals. These values are shown in Figure 4.13 and the membership value of mean and standard deviation of the fragility curve derived from the eight intersections expressive of the epistemic uncertainty is given in the Table 4.1. The obtained required fuzzy membership functions for mean and SD uses equation (4-6) that determines the probability of the collapse for different intervals and is shown in Figure 4.14. To determine the final probability of collapse by using the center of mass calculation method meanwhile taking into account the modeling uncertainty. The final fragility curves are given in Figure 4.15.

Table 4.1: Variation of epistemic uncertainty with different level of membership function

α-section		0.2	0.4	0.6	0.8
Mean of fragility curve	min	0.5796	0.6132	0.7122	0.8567
	max	1.6264	1.4927	1.3684	1.222
SD of fragility curve	min	0.3151	0.3246	0.3266	0.3286
	max	0.3925	0.3812	0.3641	0.329

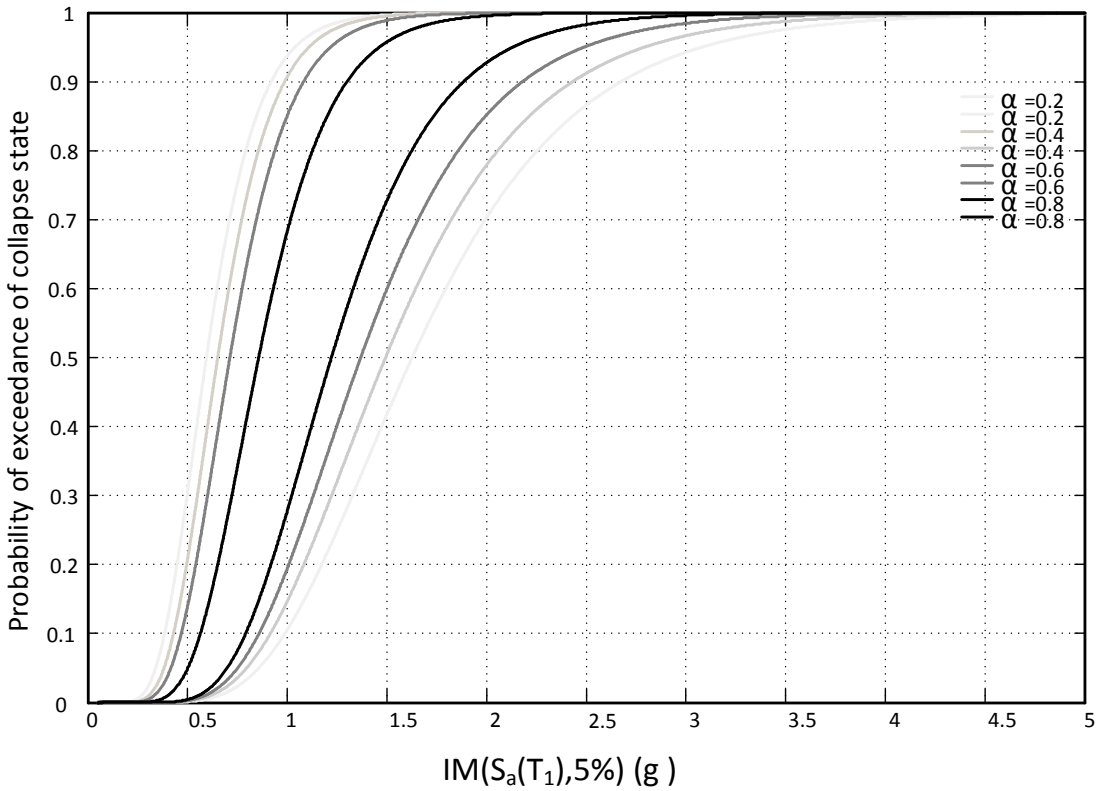

Figure 4.14: Collapse fragility curve for different interval of meta variable

4.4.3 Full Monte Carlo Method

Full Monte Carlo method is used for the comparison and validation of the proposed method. Monte Carlo method involves thousands of sets of random variable. In order to have a solid validation, more simulations are used for the proposed method.

The values for 5 different model parameters (mean, mean ±0.5× standard deviation, mean ±1.0× standard deviation) are simulated. Totally 125 combinations of the Meta variable are taken and then the IDA analyses are done for each combination in the sample structure. Mean and standard deviation values are then calculated for each of the predefined scenarios. These values are indications of the probability of collapse at different intensity measures. A surface formed by the intersection of a second order polynomial function at these values was then generated using Mathlab's pinv(x) function [84], the aim being the prediction of many simulated values for the input parameters. The second order equations used for the prediction of mean and standard deviation values for collapse conditions are shown in equations (4-11) and (4-12)). In all, 10000 Monte Carlo simulated realizations which are randomly taken as values of input parameters then the mean and standard deviations are calculated using the polynomial function. These 10000 simulations are sources of the aleatory and modeling uncertainties.

To account for this fact, it is assumed that for each interval the probability of the final collapse is the same as that obtained from the corresponding fragility curve. The collapse fragility curve of the frame according to the proposed method is compared with the full Monte Carlo methods and also with the collapse fragility curve neglecting effects of the modeling uncertainties (while modeling parameters are set to their mean

values in Figure 4.15. The fragility curve obtained by using the full Monte Carlo method has a mean square error of 0.28% for the mean and 0.05% for the standard deviation.

$$\begin{aligned}\mu = {} & 0.043406 + 0.5494(CD) - 0.00391(BD) + .025787(CS) \\ & + 0.013145(BS) - .00385(CD)(BD) \\ & + 0.028567(CD)(CS) + 0.018134(CD)(BS) \\ & - 0.00364(BD)(CS) - 0.00061(BD)(BS) \\ & - 0.00016(BS)(CS) - 0.01255(CD^2) \\ & + 0.003803\, BD^2 - 0.03846(CS^2) \\ & - 0.00471(BS^2)\end{aligned} \tag{4-11}$$

$$\begin{aligned}\beta = {} & 0.333207 + 0.020035(CD) - 0.00179(BD) \\ & + .00291(CS) + 0.005209(BS) \\ & - .003374(CD)(BD) - 0.00444(CD)(CS) \\ & + 0.004715(CD)(BS) + .003436(BD)(CS) \\ & - 0.000326(BD)(BS)0.003262(BS)(CS) \\ & - 0.02582(CD^2) - .00447BD^2 - 0.00966(CS^2) \\ & - 0.00201(BS^2)\end{aligned} \tag{4-12}$$

Table 4.2 shows the estimated values of mean and standard deviation of the fragility distribution curve, with different methods used for incorporating the epistemic uncertainty into the estimation model. It is observed, in both methods, that the effect of the incorporation of the epistemic uncertainty shows a decrease in the mean value and an increase in the standard deviation; and this falls into a total contrast with the standard guideline methods whose implementation would only result in changes in the standard deviation. Mean and standard deviation values are found to be 0.9977 and 0.4575, in the full Monte Carlo approach, respectively. In the FCM-PSO approach, mean and standard deviation values are 0.9665 and 0.48 respectively.

Table 4.2: The effect of epistemic uncertainty on mean and SD according the different approaches

Collapse damage	Mean	SD	Change in mean (%)	Change in SD (%)
Without consideration of epistemic uncertainty	1.07	0.3	-	-
FCM-PSO method	0.9977	0.4575	6.75	34.42
Full Monte Carlo Method	0.9665	0.48	9.67	37.5

Full Monte Carlo method, which is usually considered as the most accurate method for estimating uncertainties, is used for comparison purposes. From Figure 4.15, it can be seen that the new approach may yield more accurate results as compared to the full Monte Carlo method. Furthermore, for the 2% interstory drift ratio damage level; there is a little change in the parameters when we incorporate epistemic uncertainty into the model. That is because under such conditions the variation range of IM is too small. On the other hand, epistemic uncertainty considerable affects the model parameters when there is lateral damage. One should bear in mind that the main limitation of the probabilistic methods called the distribution of model parameters predefined, are of no point of consideration here. Furthermore, the fuzzy approach makes it possible to consider the variables which affect the seismic performance of structures, none the less can only be descriptively defined and evaluated (such variables as the material quality).

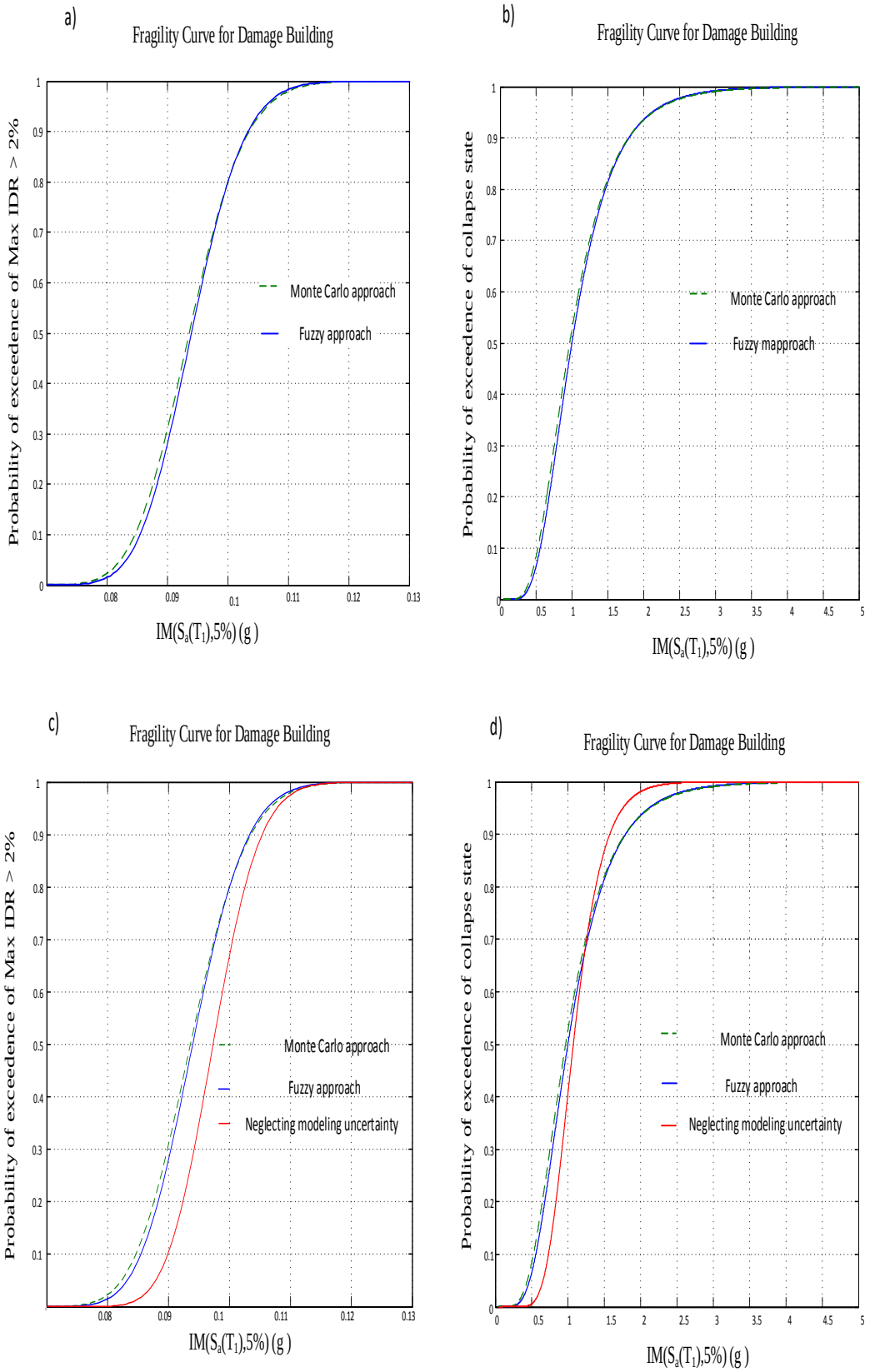

Figure 4.15: Structural response fragilities representing the collapse limit state and the 2% interstory drift (IDR) limit state

4.5 Summary

The Fuzzy algorithm, optimized and based on the particular swarm optimization algorithm, is used in determining the lower bounds of the mean and standard deviation values. This method is used based on the fact that the assessment of the mean and standard deviation is the most important part of the fuzzy method, and its usage is not limited to the structure under consideration. It can be seen that while the results perfectly conform with those obtained from the full Monte Carlo method (which was used as the base of comparison and validation of the proposed method), here there is a significant advantage with respect to time required to execute the algorithm. The presented method anticipates accurate results based on the 81 realizations while the full Monte Carlo method is used on the 125 realizations for the same performance.

In general, the Monte Carlo method needs a far greater number of simulations as compared to the method presented here. Nevertheless, the method presented here demonstrates a small prediction error and the results are in line with those obtained using the Monte Carlo method.

Chapter 5

CONCLUSIONS AND RECOMMENDATIONS

5.1 Summary

The first chapter elucidates probabilistic methods while deriving the fragility curve in order to incorporate the various sources of uncertainties. Second chapter focuses on the components and Meta variables described as epistemic uncertainty. In the third chapter, the earthquake-related risks of the structural collapse is accounted for using aleatory and epistemic (modelling) uncertainties as well as uncertainties related with the quality of the building materials used; i.e, a five-storey and ten-storey moment-resisting steel frame which is designed in accordance with the earthquake level of 10% probability exceedance with 50 years of seismic load design is considered. The structures designed according to the seismic code do not go beyond the "life safety" performance level during or after earthquakes. In order to ponder about modeling and cognitive uncertainties, the modeling parameters are applied based on the modified Ibarra–Medina–Krawinkler moment rotation model. A set of 40 records suggested by K-means clustering algorithm are considered for implementing the incremental dynamic analysis of the effect of RTR uncertainty. Hereafter, the mean and SD of the collapse fragility curve which are obtained by the IDA and Cuckoo optimization algorithm are predicted via the analytical response function. The interaction between the model variables and structural parameters is presented as response surface. The response surface qualitatively presents the uncertainty in three different levels (good, average, and low). The TSK system is given for combining these levels into one

qualitative uncertainty. Since the sensitivity method is used for predicting the response surface, the time taken for the prediction is considerably reduced. Otherwise, the IDA method is used to consider the aleatory uncertainty for each realization.

In the fourth chapter, the optimized fuzzy method is used in incorporating the epistemic uncertainties when deriving the fragility curve in the sample structure. As an example, a sample model of a three storey ductile frame structure is presented, with the joints modeled as part of the uncertainty and based on Krawinkler's model.

To demonstrate the optimized fuzzy C-means method, different realizations of combinations regarding epistemic and aleatory uncertainties are compiled. It is evident that uncertainties are generally created in the lower means and higher standard deviations in the fragility curves. In contrast with the probabilistic methods, the ranges of variations concerning the model parameters are wide enough resulting in fuzzy model parameters. Taking into account the different levels of Meta variables expressed based on the fuzzy value, the mean and standard deviation of the fragility curve can be obtained as fuzzy parameters. The effect of the epistemic uncertainty with a fragility curve based on the fuzzy parameter can thus be stated obviously.

The collapse probability values presented in Table 3.4 and Table 4.2 are indicative of the significance of modeling uncertainties on the collapse fragility curve. By involving modeling uncertainties, it is observed that the collapse probability of a hazard level with 2% exceedance probability over 50 years undergoes more changes than the hazard level with 10% exceedance probability over 50 years. Because the formers spectral acceleration is higher and the effects of modeling uncertainties contribute more to the final collapse fragility curve at this hazard level.

5.2 Conclusions

K-means algorithm enhanced earthquake selection by decreasing the dispersion. It is most suitable for considering the aleatory uncertainty rather than the random selection.

Cuckoo algorithm is more accurate than lognormal probability distribution when applying the Response Surface Method.

As expected, the considerable changes of the sample structure's collapse probability happen in two understudy hazard levels: considering the material quality parameter and the affectability of the mean annual frequency. All show that not combining the modeling and construction quality uncertainties has remarkable effects on the parameters indicative of the structure's collapse performance.

The FCM-PSO method is an appropriate approximator which is able to accurately predict the mean and SD values provided by the fuzzy membership function. This work demonstrates the efficiency of the FCM-PSO method against the full response surface method through a specific example.

5.3 Recommendations

Base on the study conducted in this thesis, the following future research topics can be suggested:

- Using the proposed approach to compute the desiccation variable based on the Pacific Earthquake Engineering research approach.
- Investigation of the higher mode effects in deriving fragility curve with consideration the epistemic and alateory uncertainties.

- The effect of the soil structure interaction in deriving the fragility curve based on the ANN method.
- Using the proposed method for various structural system.
- Introduce and investigate the new IM for deriving the fragility curve for decreasing the dispersion of uncertainty.
- Experimental analysis to achieve the back-bone curve of meta variable in different quality of material.
- Considering nonstructural components to predict damage of structure by proposed method.

REFERENCES

[1] Ghobarah, A.(2001). Performance-based design in earthquake engineering: state of development. *Engineering structures.* 23, 878-884.

[2] Jalayer, F., & Cornell, C. A. (2003). A technical framework for probability-based demand and capacity factor (DCFD) seismic formats.

[3] ASCE. (2006). Minimum design loads for buildings and other structures, ed: American Society of Civil Engineers, Reston, Virginia.

[4] IBC. (2000). International building code. International Code Council, Washington, DC.

[5] Song, J.K., & Pincheira, J.(2000). Spectral displacement demands of stiffness-and strength-degrading systems. *Earthquake Spectra.* 16, 817-851.

[6] SEAOC. (2000). A Framework for Performance Based Earthquake Engineering.

[7] ATC-40.(1996). Seismic evaluation and retrofit of concrete buildings. Applied Technology Council, Redwood City.

[8] FEMA 273.(1997). Second ballot version NEHRP guidelines for seismic rehabilitation of buildings. Seismic Safety Council, Washington DC, USA, ATC.

[9] FEMA 274. NEHRP Commentary on the Guidelines for the Rehabilitation of Building. Washington DC : Federal Emergancy Management Agancy.

[10] FEMA 356. Prestandard and Commentary for the Seismic Rehabilitation of Buildings: Rehabilitation Requirement.

[11] Whittaker, A., Hamburger, R., & Mahoney, M. (2003). Performance-based engineering of buildings and infrastructure for extreme loadings, in *Proceedings, AISC-SINY Symposium on Resisting Blast and Progressive Collapse. American Institute of Steel Construction.* New York.

[12] Cordova, P., Deierlein, G., Mehanny, S., & Cornell, C. A. (2000). Development of a two-parameter seismic intensity measure and probabilistic assessment procedure, in *The Second US-Japan Workshop on Performance-Based Earthquake Engineering Methodology for Reinforced Concrete Building Structures*.187-206.

[13] Hutchinson, T. C., Chai, Y., Boulanger, R., & Idriss, I.(2004). Inelastic seismic response of extended pile-shaft-supported bridge structures. *Earthquake Spectra.* 20, 1057-1080.

[14] Luco, N., & Cornell, C. A.(1998). Seismic drift demands for two SMRF structures with brittle connections. *Structural Engineering World Wide.*

[15] Tothong, P. (2007). Probabilistic seismic demand analysis using advanced ground motion intensity measures, attenuation relationships, and near-fault effects, Stanford University.

[16] Baker, J. W., & Allin Cornell, C.(2005). A vector-valued ground motion intensity measure consisting of spectral acceleration and epsilon. *Earthquake Engineering & Structural Dynamics.* 34, 1193-1217.

[17] Bazzurro, P., & Cornell, C.(2002). Vector-valued probabilistic seismic hazard analysis (VPSHA), in *Proceedings of the 7th US national conference on earthquake engineering*. 21-25.

[18] Shome, N.(1999). Probabilistic seismic demand analysis of nonlinear structures.

[19] Calvi, G., Pinho, R., Magenes, G., Bommer, J., Restrepo-Vélez, L., &Crowley, H.(2006). Development of seismic vulnerability assessment methodologies over the past 30 years. *ISET journal of Earthquake Technology*. 43, 75-104.

[20] Khurana, A.(2005). Report on earthquake of 8th October in some parts of northern India.

[21] Wyllie, L. A., Filson, J. R., Agbabian, M., &Der Kiureghian, A.(1989). Armenia earthquake reconnaissance report: Earthquake Engineering Research Institute.

[22] Liel, A. B., Haselton, C. B., Deierlein, G. G., &Baker, J. W.(2009). Incorporating modeling uncertainties in the assessment of seismic collapse risk of buildings. *Structural Safety.* 31, 197-211.

[23] Lignos, D.(2008). Sidesway collapse of deteriorating structural systems under seismic excitations: ProQuest.

[24] Zareian, F., Krawinkler, H., Ibarra, L., & Lignos, D.(2010). Basic concepts and performance measures in prediction of collapse of buildings under earthquake ground motions. *The Structural Design of Tall and Special Buildings.* 19, 167-181.

[25] Hamburger, R., Rojahn, C., Heintz, J., &Mahoney, M.(2012). FEMA P58: Next-Generation Building Seismic Performance Assessment Methodology, in Proceedings.

[26] UBC.(1997). 'Uniform building code, in Int. Conf. Building Officials.

[27] Der Kiureghian, A., & Ditlevsen, O.(2009). Aleatory or epistemic? Does it matter? *Structural Safety.* 31, 105-112.

[28] Vamvatsikos, D., & Cornell, C. A.(2002). Incremental dynamic analysis. *Earthquake Engineering & Structural Dynamics.* 31, 491-514.

[29] Foutch, D. (2000). State of the Art Report on Performance Prediction and Evaluation of Steel Moment-Frame Buildings, prepared for the SAC Joint

Venture, published by the Federal Emergency Management Agency, FEMA-355 F, Washington, DC.

[30] Jalayer, F.(2003). Direct probabilistic seismic anaysis: implementing non-linear dynamic assessments, Stanford University.

[31] Baker, J. W., & Cornell, C. A.(2008). Uncertainty propagation in probabilistic seismic loss estimation. *Structural Safety.* 30, 236-252.

[32] Cornell, C. A., Jalayer, F., Hamburger, R. O., &Foutch, D. A.(2002). Probabilistic basis for 2000 SAC federal emergency management agency steel moment frame guidelines. *Journal of Structural Engineering.* 128, 526-533.

[33] Ellingwood, B. R., &Kinali, K.(2009). Quantifying and communicating uncertainty in seismic risk assessment. *Structural Safety.* 31, 179-187.

[34] Rubinstein, R. Y., &Kroese, D. P.(2011). Simulation and the Monte Carlo method *John Wiley & Sons.*707.

[35] Pinto, P. E., Giannini, R., & Franchin, P.(2004). Seismic reliability analysis of structures.

[36] Helton, J. C., & Davis, F. J.(2003). Latin hypercube sampling and the propagation of uncertainty in analyses of complex systems. *Reliability Engineering & System Safety.* 81, 23-69.

[37] Lagaros, N., &Papadrakakis, M.(2004). Improving the condition of the Jacobian in neural network training. *Adv Eng Softw.* 35, 9-25.

[38] Mitropoulou, C. C., & Papadrakakis, M.(2011). Developing fragility curves based on neural network IDA predictions. *Engineering Structures.* 33, 3409-3421.

[39] Cardaliaguet, P., & Euvrard, G.(1992). Approximation of a function and its derivative with a neural network. *Neural Networks.* 5, 207-220.

[40] Li, X.(1996). Simultaneous approximations of multivariate functions and their derivatives by neural networks with one hidden layer. *Neurocomputing.* 12, 327-343.

[41] Chapman, O., & Crossland, A.(1995). Neural networks in probabilistic structural mechanics, in *Probabilistic Structural Mechanics Handbook*, ed: Springer, 317-330.

[42] Dimova, S. L., &Negro, P.(2006). Assessment of seismic fragility of structures with consideration of the quality of construction. *Earthquake Spectra.* 22, 909-936.

[43] Kappos, A. J., &Panagopoulos, G.(2010). Fragility curves for reinforced concrete buildings in Greece. *Structure and Infrastructure Engineering.* 6, 39-53.

[44] Erberik, M. A.(2008). Generation of fragility curves for Turkish masonry buildings considering in-plane failure modes. *Earthquake Engineering & Structural Dynamics.* 37, 387-405.

[45] Rajeev, P., &Tesfamariam, S.(2012). Seismic fragilities for reinforced concrete buildings with consideration of irregularities. *Structural Safety.* 39, 1-13.

[46] Möller, B., Graf, W., &Beer, M.(2003). Safety assessment of structures in view of fuzzy randomness. *Computers & Structures.* 81, 1567-1582.

[47] Ibarra, L. F., &Krawinkler, H.(2005). Global collapse of frame structures under seismic excitations: Pacific Earthquake Engineering Research Center.

[48] Haselton, C. B.(2006). Assessing seismic collapse safety of modern reinforced concrete moment frame buildings, Stanford University.

[49] Benjamin, J. R., & Cornell, C. A.(2014). Probability, statistics, and decision for civil engineers: Courier Corporation.

[50] Möller, B., Graf, W., &Beer, M.(2000). Fuzzy structural analysis using α-level optimization. *Computational Mechanics.* 26, 547-565.

[51] Adduri, P. R., &Penmetsa, R. C.(2009). System reliability analysis for mixed uncertain variables. *Structural Safety.* 31, 375-382.

[52] Adam, C., Ibarra, L. F., &Krawinkler, H.(2004). *Evaluation of P-delta effects in non-deteriorating MDOF structures from equivalent SDOF systems*.

[53] Sasani, M., & Kropelnicki, J.(2008). Progressive collapse analysis of an RC structure. *The Structural Design of Tall and Special Buildings.* 17, 757-771.

[54] Talaat, M., &Mosalam, K. M.(2009). Modeling progressive collapse in reinforced concrete buildings using direct element removal. *Earthquake Engineering & Structural Dynamics.* 38, 609-634.

[55] Haselton, C. B., Liel, A. B., Dean, B. S., Chou, J. H., &Deierlein, G.(2007). Seismic Collapse safety and behavior of modern reinforced concrete moment frame buildings, in *Proceedings of ASCE 2007 Structures Congress: New Horizons Better Practices*.16-19.

[56] Zareian, F., & Krawinkler, H.(2006). Simplified performance-based earthquake engineering, Stanford University.

[57] Ibarra, L. F., Medina, R. A., & Krawinkler, H.(2005). Hysteretic models that incorporate strength and stiffness deterioration. *Earthquake engineering and structural dynamics.* 34, 1489-1512.

[58] Takeda, T., Sozen, M. A., & Nielsen, N. N.(1970). Reinforced concrete response to simulated earthquakes. *Journal of the Structural Division.* 96, 2557-2573.

[59] Sivaselvan, M. V., &Reinhorn, A. M.(2000). Hysteretic models for deteriorating inelastic structures. *Journal of Engineering Mechanics.* 126, 633-640.

[60] Rahnama, M., &Krawinkler, H.(1993). Effect of soft soils and hysteresis models on seismic design spectra. *John A. Blume Earthquake Engineering Center Report.*

[61] OpenSEES.(2006). Open System for Earthquake Engineering Simulation, Pacific Earthquake Engineering Research Centre, University of California, Berkeley.

[62] Yu, Q. S., Gilton, C., &Uang, C.M.(2000). *Cyclic response of RBS moment connections: Loading sequence and lateral bracing effects*: Department of Structural Engineering, University of California, San Diego.

[63] Kircher, C. A., Reitherman, R. K., Whitman, R. V., &Arnold, C.(1997). Estimation of earthquake losses to buildings. *Earthquake spectra.* 13, 703-720.

[64] Zareian, F., Krawinkler, H., Ibarra, L., &Lignos, D.(2009). Basic concepts and performance measures in prediction of collapse of buildings under earthquake ground motions. *The Structural Design of Tall and Special Buildings.* 19, 167-181.

[65] Dimova, S. L., & Negro, P.(2006). Assessment of Seismic Fragility of Structures with Consideration of the Quality of Construction. *Earthquake Spectra.* 22, 909-936.

[66] Erberik, M. A.(2008). Generation of fragility curves for Turkish masonry buildings considering in-plane failure modes. *Earthquake Engineering & Structural Dynamics.* 37, 387-405.

[67] Sugeno, M.(Jul-Aug 1985). An introduction survey of fuzzy control. *Information Sciences.* 36, 59-83.

[68] Seo, J., &Linzell, D. G.(2013). Use of response surface metamodels to generate system level fragilities for existing curved steel bridges. *Engineering Structures.* 52, 642-653.

[69] Seo, J., &Linzell, D. G.(2012). Horizontally curved steel bridge seismic vulnerability assessment. *Engineering Structures.* 34, 21-32.

[70] Franchin, P., Lupoi, A., Pinto, P., &Schotanus, M. I.(2003). Seismic fragility of reinforced concrete structures using a response surface approach. *Journal of Earthquake Engineering.* 7, 45-77.

[71] He, J. N., &Wang, Z., Analysis on System Reliability of Steel Framework Structure and Optimal Design, in *Applied Mechanics and Materials*, 2012. 902-906.

[72] Rossetto, T., &Elnashai, A.(2005). A new analytical procedure for the derivation of displacement-based vulnerability curves for populations of RC structures. *Engineering structures.* 27, 397-409.

[73] Schotanus, M., Franchin, P., Lupoi, A., & Pinto, P.(2004). Seismic fragility analysis of 3D structures. *Structural Safety.* 26, 421-441.

[74] Kramer, S. L., *Geotechnical Earthquake Engineering*, 1 ed., 1996.

[75] Shinozuka, M., Feng, M. Q., Lee, J., &Naganuma, T. (Dec 2000). Statistical analysis of fragility curves. *Journal of Engineering Mechanics-Asce.* 126, 1224-1231.

[76] Rajabioun, R.(2011). Cuckoo optimization algorithm. *Applied soft computing.* 11, 5508-5518.

[77] Shokri-Ghaleh, H., &Alfi, A.(2014). Optimal synchronization of teleoperation systems via cuckoo optimization algorithm. *Nonlinear Dynamics.* 78, 2359-2376.

[78] Siler, W., &Buckley, J. J.(2005). Fuzzy expert systems and fuzzy reasoning: *John Wiley & Sons.*

[79] 2800, Standard. N.(2007). Iranian Code of Practice for Seismic Resistant Design of Buildings, vol. 3rd Edition, ed. Iran: Building and Housing Research Center.

[80] Foutch, D. A., & Yun, S. Y.(May-Aug 2002). Modeling of steel moment frames for seismic loads. *Journal of Constructional Steel Research.* 58, 529-564.

[81] Li, Q., &Ellingwood, B. R.(2008). Damage inspection and vulnerability analysis of existing buildings with steel moment-resisting frames. *Engineering Structures.* 30, 338-351.

[82] Pinto, P., Giannini, R., &Franchin, P.(2007). Seismic Reliability Analysis of Structures. *Earthquake Engineering & Structural Dynamics.* 36, 2081-2081.

[83] Vamvatsikos, D.(2007). Performing incremental dynamic analysis in parallel using computer clusters, in *Proceedings of COMPDYN2007 Conference on Computational Methods in Structural Dynamics and Earthquake Engineering, Rethymno, Greece*.

[84] MathWorks, I.(2005). *MATLAB: the language of technical computing. Desktop tools and development environment, version 8.3* vol. 9: MathWorks.

[85] Zolfaghari, M. R.(2014). Development of a synthetically generated earthquake catalogue towards assessment of probabilistic seismic hazard for Tehran. *Natural Hazards.* 76, 497-514.

[86] Cornell, C. A., &Krawinkler, H.(2000). Progress and challenges in seismic performance assessment. *PEER Center News.* 3, 1-3.

[87] Bozorgnia, Y., &Bertero, V. V.(2004). Earthquake engineering: from engineering seismology to performance-based engineering: CRC press.

[88] Lagaros, N. D., & Fragiadakis, M.(2007). Fragility assessment of steel frames using neural networks. *Earthquake Spectra.* 23, 735-752.

[89] Papadrakakis, M., Papadopoulos, V., Lagaros, N. D., Oliver, J., Huespe, A. E., &Sánchez, P.(2008). Vulnerability analysis of large concrete dams using the continuum strong discontinuity approach and neural networks. *Structural Safety.* 30, 217-235.

[90] Möller, B., & Beer, M., *Fuzzy randomness: uncertainty in civil engineering and computational mechanics*: Springer Science & Business Media, 2013.

[91] Jain, A. K., Murty, M. N., &Flynn, P. J.(1999). Data clustering: a review. *ACM computing surveys (CSUR).* 31, 264-323.

[92] Bezdek, J. C.(2013). Pattern recognition with fuzzy objective function algorithms: *Springer Science & Business Media*.

[93] Kennedy, J., Particle swarm optimization, in *Encyclopedia of Machine Learning*, ed: Springer, 2010, 760-766.

[94] Yang, F., Sun, T., &Zhang, C.(2009). An efficient hybrid data clustering method based on K-harmonic means and Particle Swarm Optimization. *Expert Systems with Applications.* 36, 9847-9852.

[95] Zadeh, L. A.(1965). Fuzzy sets. *Information and control.* 8, 338-353.

[96] Rao, S. S., &Berke, L.(1997). Analysis of uncertain structural systems using interval analysis. *AIAA journal.* 35, 727-735.

[97] Beer, M.(2009). Fuzzy probability theory, in *Encyclopedia of complexity and systems science*. Springer. 4047-4059.

[98] Ibarra, L., &Krawinkler, H.(2011). Variance of collapse capacity of SDOF systems under earthquake excitations. *Earthquake engineering & structural dynamics.* 40, 1299-1314.

[99] Foutch, D. A., &Yun, S.Y.(2002). Modeling of steel moment frames for seismic loads. *Journal of Constructional Steel Research.* 58, 529-564.

[100] Tesfamariam, S.(2008). Seismic risk assessment of reinforced concrete buildings using fuzzy based techniques.

[101] Mamdani, E. H.(1976). Advances in the linguistic synthesis of fuzzy controllers. *International Journal of Man-Machine Studies.* 8, 669-678.

APPENDIX

Appendix A: Theory of Fuzzy Inference System

Fuzzy logic which has been introduced by Zadeh (1965) is a modern and logical tool for converting qualitative knowledge into numerical reasoning. Accordingly, this approach makes it possible to combine descriptive knowledge with uncertainties caused by descriptive parameters and quantitative data and involve them in decision-making process to reach the ultimate results. The present study considers the modeling uncertainties, which are combined with aleatory uncertainties using probabilistic approaches, as being fuzzy in the first stage. Both epistemic and aleatory sources of uncertainty are then considered in the structure's collapse fragility curve using the fuzzy-random approach. In the second stage, related uncertainties of descriptive parameters (specifically, the construction quality uncertainty) are involved within the collapse fragility curve. The fuzzy logic and fuzzy inference method used in the present thesis for the incorporation of cognitive uncertainties associated with the material quality in the collapse fragility curve are explained in this section.

The fuzzy theory and fuzzy logic have been recently used in earthquake engineering involving seismicity estimation, structures' design and analysis, evaluation of existing buildings and after-earthquake conditions and crisis management. Studies on the risk models based on fuzzy logic, vulnerability due to earthquake, seismic hazard determination, decision-making in crisis management of earthquake, interpretation of seismic design guidelines, structure's non-linear design and analysis and evaluation of earthquake records using fuzzy logic are amongst the applications of this approach in earthquake engineering [100].

An appropriate approach for definition and presentation of one set is using the concept of characteristic function. Assuming that A is a subset of source set *X*, the characteristic function A is defined as follows:

$$Chf_A(X) = f(x) = \begin{cases} 1, & x \in A \\ 0, & x \notin A \end{cases}$$

As it is seen, the range of characteristic function is a two-member set [101]. The fuzzy set is defined and expressed by extending the characteristic function's range. Thus, the fuzzy sets are defined using this extension of characteristic function in the form of interval [0, 1] and such sets are defined as membership functions. Assume that the reference set is the interval of [0,2000]; if A is in the form of "close to 1000", then the membership function of A can be expressed as followed:

$$\mu_A(X) = \begin{cases} {}^{x}/_{1000} & x \leq 1000 \\ {}^{2000-x}/_{1000} & x > 1000 \end{cases}$$

Accordingly, all the operators employed in traditional sets (e.g. union, intersection, multiplication, etc.), can be extended for fuzzy sets using same operators that operate on the membership functions of those two considered variables. Similarly, the conventional two-valued logic (true and false), founded on the traditional set theory, has been extended as fuzzy logic using fuzzy sets and their related operators and rules. Therefore, the final inference and result can be determined by fuzzy data.

Extension of Reasoning Deduction to Fuzzy Deduction

In conventional logic (two-valued), reasoning is conducted based on Modus Ponens, hypothetical deduction and Modus Tollens. These deductions are briefly defined as follows and extended into approximate reasoning based on fuzzy data.

In Modus Ponens, the premise "if A is true, then B is true," assumes that if A is asserted to be true, so B must be true.

H1: if the room temperature is low, then turn up the heater.

H2: the room temperature is low.

Conclusion: turn up the heater.

Generalized Modus Ponens (GMP) to fuzzy sets is defined as such: if two fuzzy premises "if x is A, then y is B" and "x is A'", are present, then the premise "y is B'" must be concluded. So that the closer A' to A, the closer B' to B. for instance:

H1: if the room temperature is low, then turn up the heater.

H2: the temperature is relatively low.

Conclusion: turn up the heater relatively.

In hypothetical deduction in two-valued logic, from the premises "if A is true, then B is true", "if B is true, then C is true" and "A is true", it can be concluded that "C must be true". For instance:

H1: if it is winter, then the room temperature will be low.

H2: if the room temperature is low, then turn up the heater.

H3: it is winter now.

Conclusion: turn up the heater.

Extension of hypothetical deduction into fuzzy hypothetical deduction will be as follows: if the premises "if x is A, then y is B" and "if y is B', then z is C'" and "x equals A" are present, the new premise "z is C" will be concluded. So that, the closer B' to B, the closer C' to C. For instance:

H1: if it is winter, then the room temperature will be low.

H2: if the room temperature is too low, then turn up the heater too much.

H3: it is winter now.

Conclusion: turn up the heater.

In Modus Tollens, from the premises "if A is asserted to be true, then B is true" and "B is not true" it can be concluded that "A is not true". For instance:

H1: if it is spring, then the trees will blossom.

H2: trees do not have blossoms now.

Conclusion: it is not spring now.

This deduction is expressed with fuzzy extension: if the premises "if x is asserted to be A, then y is B" and "y is not B" are present, the premise "x is not A'" will be concluded. So that, the more the difference of B and B', the more the difference of A and A'. For instance:

H1: if you stir sugar in water, then the sugar will be solved in water.

H2: sugar has not been solved in water completely.

Conclusion: you have not stirred the sugar in water completely.

In fact, the fuzzy reasoning is made of some available rules (there should be some rules available for flexible reasoning) as follows:

Step1: the hypothetical compatibility of rules for an assumed input is measured.

Step2: the result of each rule is inferred from the compatibility obtained in step1.

Step3: the final result is determined by combining the results of each rules and their compatibility with respect to the assumed input.

General methods for determining the output (having the fuzzy rules and assumed input data) are divided into Mamdani and Takagi-Sugeno-Kang (TSK) methods which will be explained in the following sections.

Mamdani Inference Method

This method is used when both default and result in available rules have been expressed in the form of fuzzy parts. For instance, if the following rules are present:

Rule1: if x is present in A_1 and y is present in B_1, then z will be present in C_1.

Rule2: if x is present in A_2 and y is present in B_2, then z will be present in C_2.

Where, A_1, A_2, B_1, B_2, C_1 and C_2 are fuzzy sets. Now assume that the assumed input is (x_0, y_0). Then the reasoning procedure is as follows:

Step1: the compatibility of each rule for the input (x_0, y_0) is obtained as follows:

The first compatibility: $W_1 = \text{MIN}(\mu_{A1}(x_0), \mu_{B1}(y_0))$

The second compatibility: $W_2 = \text{MIN}(\mu_{A2}(x_0), \mu_{B2}(y_0))$

Step2: the result of each rule is determined using the compatibility in step1 and fuzzy sets in the result part.

The first rule: $\mu_{C'1}(z) = \text{MIN}(W_1, \mu_{C1}(x_0), \mu_{C2}(y_0))$

The second rule: $\mu_{C'2}(z) = \text{MIN}(W_2, \mu_{C1}(x_0), \mu_{C2}(y_0))$

Step3: the final result is obtained after summing the result of each rule as follows:

$$\mu_c(z) = \max(\mu_{c1}(z), \mu_{c2}(z))$$

A non-fuzzy algorithm should be used to express the final result in the form of a specific number rather than a fuzzy set. The center of gravity method is usually used for expression of the final result. This algorithm is shown in the following equation:

$$z_0 = \frac{\int \mu_c(z) z dz}{\int \mu_c(z) dz}$$

When the output value is numerically expressed and only the inputs are fuzzy, the Takagi-Sugeno method is used for fuzzy inference. Given the numerical form of response levels and their estimation by fuzzy inference, the present study also uses this inference approach. In this method, the output value is expressed as a linear function of inputs.

$$\boldsymbol{IF}\left(\boldsymbol{X}_1\boldsymbol{is}\,\boldsymbol{A}_1\right)\boldsymbol{AND}\left(\boldsymbol{X}_2\ \boldsymbol{is}\,\boldsymbol{A}_2\right)\boldsymbol{AND}\ldots,\boldsymbol{THEN}\ \ \boldsymbol{y}=\boldsymbol{c}_0+\boldsymbol{c}_1\boldsymbol{x}_1+\boldsymbol{c}_2\boldsymbol{x}_2+\ldots.$$

The reasoning value by fuzzy logic in this method is obtained as follows:

$$t=\frac{\sum_{i=1}^{N}w_i z_i}{\sum_{i=1}^{N}w_i}$$

Where, w_i indicates the compatibility of deductions of *ith* rule.

Appendix B: Selected 100 Natural Earthquakes Based on Site Specification

Record No	Year	Earthquake[3]	MW	Mech.[1]	Station	GM Characteristics	Dist.[2] (km)
1	1994	Northridge	6.7	RN	Leona Valley #2	Far-Fault	37.2
2	1994	Northridge	6.7	RN	LA, Baldwin Hills	Far-Fault	29.9
3	1994	Northridge	6.7	RN	Lake Hughes #1	Far-Fault	89.67
4	1994	Northridge	6.7	RN	LA, Hollywood Stor FF	Far-Fault	114.62
5	1994	Northridge	6.7	RN	LA, Centinela St.	Far-Fault	31.53
6	1994	Northridge	6.7	RN	Anaheim-W Ball Rd	Far-Fault	68.62
7	1994	Northridge	6.7	RN	Bell Gardens-Jaboneria	Far-Fault	44.11
8	1989	Loma Prieta	6.9	RO	Hollister Diff Array	Far-Fault	24.8
9	1989	Loma Prieta	6.9	RO	WAHO	Far-Fault	17.5
10	1989	Loma Prieta	6.9	RO	Halls Valley	Far-Fault	30.5
11	1989	Loma Prieta	6.9	RO	Agnews State Hospital	Far-Fault	24.6
12	1989	Loma Prieta	6.9	RO	Anderson Dam (Downstream)	Far-Fault	4.4
13	1989	Loma Prieta	6.9	RO	Coyote Lake Dam (Downstream)	Far-Fault	20.8
14	1989	Loma Prieta	6.9	RO	Hollister—South & Pine	Far-Fault	27.93
15	1979	Imperial Valley	6.5	SS	Chihuahua	Far-Fault	8.4
16	1979	Imperial Valley	6.5	SS	Compuertas	Far-Fault	15.3
17	1979	Imperial Valley	6.5	SS	Plaster City	Far-Fault	31.1
18	1979	Imperial Valley	6.5	SS	El Centro Array #12	Far-Fault	18.85
19	1979	Imperial Valley	6.5	SS	El Centro Array #13	Far-Fault	22.83
20	1979	Imperial Valley	6.5	SS	Bonds Corner	Far-Fault	4.01
21	1979	Imperial Valley	6.5	SS	Brawley Airport	Far-Fault	10.57
22	1979	Imperial Valley	6.5	SS	Calexico Fire Station	Far-Fault	11.56
23	1987	Superstition Hills	6.7	SS	El Centro Imp. Co Cent	Far-Fault	18.5
24	1987	Superstition Hills	6.7	SS	Wildlife Liquefaction Array	Far-Fault	24.1
25	1987	Superstition Hills	6.7	SS	Parachute Test Site	Far-Fault	3.53
26	1987	Superstition Hills	6.7	SS	Plaster City	Far-Fault	22.5

27	1987	Superstition Hills	6.7	SS	Brawley Airport	Far-Fault	29.91
28	1987	Superstition Hills	6.7	SS	Calipatria Fire Station	Far-Fault	27.21
29	1987	Superstition Hills	6.7	SS	Kornbloom Road	Far-Fault	18.79
30	1987	Superstition Hills	6.7	SS	Poe Road	Far-Fault	11.67
31	1987	Superstition Hills	6.7	SS	Salton Sea Wildlife Refuge	Far-Fault	26.11
32	1987	Superstition Hills	6.7	SS	Superstition Mtn Camera	Far-Fault	6.56
33	1987	Superstition Hills	6.7	SS	Westmorland Fire Sta	Far-Fault	13.47
34	1971	San Fernando	6.6	RN	San Onofre — So Cal Edison	Far-Fault	126.78
35	1971	San Fernando	6.6	RN	Castaic — Old Ridge Route	Far-Fault	22.63
36	1971	San Fernando	6.6	RN	Cedar Springs, Allen Ranch	Far-Fault	89.72
37	1971	San Fernando	6.6	RN	Lake Hughes #1	Far-Fault	27.4
38	1971	San Fernando	6.6	RN	Santa Anita Dam	Far-Fault	31.41
39	1983	Coalinga	6.4	RN	Parkfield — Cholame 2WA	Far-Fault	44.72
40	1983	Coalinga	6.4	RN	Parkfield — Cholame 5W	Far-Fault	48.7
41	1983	Coalinga	6.4	RN	Parkfield — Fault Zone 1	Far-Fault	41.99
42	1983	Coalinga	6.4	RN	Parkfield — Fault Zone 14	Far-Fault	29.48
43	1983	Coalinga	6.4	RN	Parkfield — Gold Hill 3W	Far-Fault	39.12
44	1983	Coalinga	6.4	RN	Parkfield — Stone Corral 3E	Far-Fault	34
45	1983	Coalinga	6.4	RN	Pleasant Valley P.P. — yard	Far-Fault	8.41
46	1983	Coalinga	6.4	RN	Parkfield — Fault Zone 4	Far-Fault	34.59
47	1983	Coalinga	6.4	RN	Parkfield — Vineyard Cany 2W	Far-Fault	30.35
48	1984	Coalinga	6.4	RN	Slack Canyon	Far-Fault	27.46
49	1987	Whittier Narrows	6	RO	Alhambra— Fremont School	Far-Fault	14.66
50	1987	Whittier Narrows	6	RO	LA—Hollywood Stor FF	Far-Fault	24.08
51	1987	Whittier Narrows	6	RO	Altadena—Eaton Canyon	Far-Fault	19.52
52	1987	Whittier Narrows	6	RO	Beverly Hills— 12520 Mulhol	Far-Fault	29.9

53	1987	Whittier Narrows	6	RO	Brea Dam (Downstream)	Far-Fault	23.99
54	1987	Whittier Narrows	6	RO	Glendale—Las Palmas	Far-Fault	22.82
55	1987	Whittier Narrows	6	RO	Riverside Airport	Far-Fault	55.48
56	1986	Chalfant Valley	5.9	SS	Benton	Far-Fault	21.92
57	1986	Chalfant Valley	5.9	SS	Bishop—LADWP South St	Far-Fault	17.17
58	1986	Chalfant Valley	5.9	SS	Bishop—Paradise Lodge	Far-Fault	18.31
59	1986	Chalfant Valley	5.9	SS	Lake Crowley—Shehorn Res.	Far-Fault	22.08
60	1986	Chalfant Valley	5.9		Zack Brothers Ranch	Far-Fault	7.58
61	1979	Coyote Lake	5.7	SS	Gilroy Array #1	Far-Fault	10.67
62	1979	Coyote Lake	5.7	SS	Coyote Lake Dam (SW Abut)	Far-Fault	6.13
63	1979	Coyote Lake	5.7	SS	Gilroy Array #2	Far-Fault	9.02
64	1979	Coyote Lake	5.7	SS	Gilroy Array #6	Far-Fault	3.11
65	1979	Coyote Lake	5.7	SS	San Juan Bautista	Far-Fault	19.7
66	1979	Coyote Lake	5.7	SS	Halls Valley	Far-Fault	33.83
67	1979	Coyote Lake	5.7	SS	SJB Overpass, Bent 3 g.l.	Far-Fault	20.67
68	1979	Coyote Lake	5.7	SS	Overpass, Bent 5 g.l.	Far-Fault	20.67
69	1979	Coyote Lake	5.7	SS	Gilroy Array #3	Far-Fault	7.42
70	1979	Coyote Lake	5.7	SS	Gilroy Array #4	Far-Fault	5.7
71	1992	Cape Mendocino	7.1	RN	Cape Mendocino	Far-Fault	6.96
72	1992	Cape Mendocino	7.1	RN	Eureka—Myrtle & West	Far-Fault	41.97
73	1992	Cape Mendocino	7.1	RN	Fortuna—Fortuna Blvd	Far-Fault	19.95
74	1992	Cape Mendocino	7.1	RN	Petrolia	Far-Fault	8.18
75	1992	Cape Mendocino	7.1	RN	Rio Dell Overpass—FF	Far-Fault	14.33
76	1992	Cape Mendocino	7.1	RN	Shelter Cove Airport	Far-Fault	28.78
77	1981	Westmorland	5.8	SS	Brawley Airport	Far-Fault	15.57
78	1981	Westmorland	5.8	SS	Niland Fire Station	Far-Fault	15.45
79	1981	Westmorland	5.8	SS	Parachute Test Site	Far-Fault	16.81
80	1981	Westmorland	5.8	SS	Superstition Mtn Camera	Far-Fault	19.5
81	1981	Westmorland	5.8	SS	Westmorland Fire Sta	Far-Fault	6.87
82	1981	Westmorland	5.8	SS	Salton Sea Wildlife Ref	Far-Fault	8.15

83	1992	Landers	7.3	SS	Desert Hot Springs	Far-Fault	21.98
84	1992	Landers	7.3	SS	Amboy	Far-Fault	69.17
85	1992	Landers	7.3	SS	Lucerne	Far-Fault	3.71
86	1992	Landers	7.3	SS	Hemet Fire Station	Far-Fault	68.72
87	1992	Landers	7.3	SS	Indio—Coachella Canal	Far-Fault	54.34
88	1992	Landers	7.3	SS	Joshua Tree	Far-Fault	11.34
89	1992	Landers	7.3	SS	Morongo Valley	Far-Fault	17.58
90	1992	Landers	7.3	SS	North Palm Springs	Far-Fault	27.01
91	1992	Landers	7.3	SS	Palm Springs Airport	Far-Fault	36.27
92	1992	Landers	7.3	SS	Puerta La Cruz	Far-Fault	94.53
93	1992	Landers	7.3	SS	Riverside Airport	Far-Fault	96.05
94	1992	Landers	7.3	SS	Arcadia—Campus Dr	Far-Fault	135.26
95	1979	Landers	7.3	SS	Baldwin Park—N Holly	Far-Fault	131.95
96	1992	Big Bear	6.4	SS	Desert Hot Spr. (New Fire Stn.)	Far-Fault	40.1
97	1952	Kern county	7.5	TH/REV	Taft	Far-Fault	36.2
98	1952	Kern county	7.5	TH/REV	SantaBarbara Courthouse	Far-Fault	45
99	1986	N. Palm Springs	6.2	SS	Temecula	Far-Fault	95
100	1986	N. Palm Springs	6.2	SS	Anza Tule Canyon	Far-Fault	74

1. Faulting Mechanism = TH: Thrust; REV: Reverse; SS: Strike-slip; OB: Oblique; RN (Reverse-Normal), RO (Reverse-Oblique), NO (Normal-Oblique).

2. Closest distance to fault rupture (i.e., r_{jb})

3. Data Source: PEER (http://peer.berkeley.edu/smcat).